

**Kode/ Nama Rumpun Ilmu : 451/Teknik Elektro**  
**Bidang Fokus : Teknologi konservasi energi**

**LAPORAN**  
**WORDL CLASS RESEARCH**



**PENGEMBANGAN METODE *MAXIMUM POWER POINT TRACKING***  
**(MPPT) DAN PENGENDALI *DC-DC BOOST CONVERTER* BERBASIS**  
***FIELD PROGRAMMABLE GATE ARRAY (FPGA)* PADA SISTEM**  
***PHOTOVOLTAIC***

**Oleh:**

**Ketua: Tole Sutikno, S.T., M.T., Ph.D., MIET**

**NIDN 0512067501**

**Anggota:**

**1. Anton Yudhana, S.T., M.T., Ph.D.**

**NIDN 0508087601**

**2. Mochammad Facta, S.T., M.T., Ph.D.**

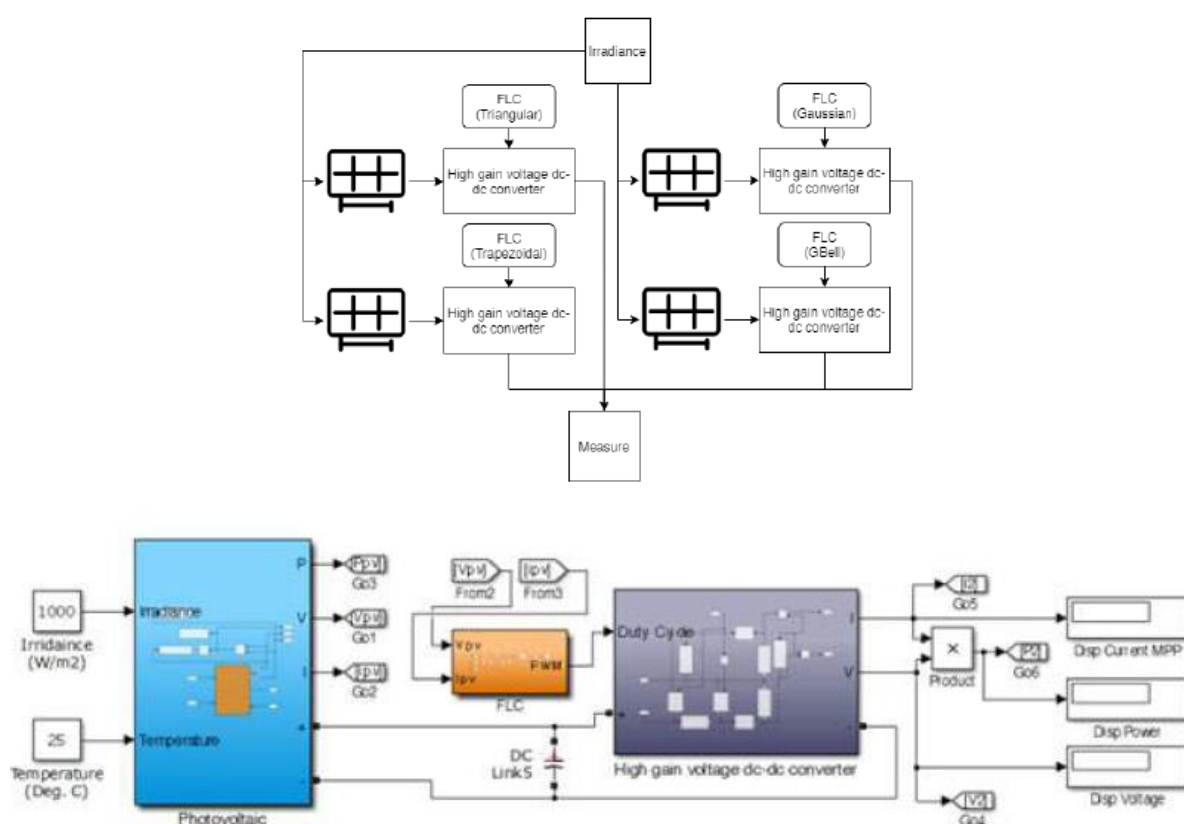
**NIDN 0016067104**

**UNIVERSITAS AHMAD DAHLAN**  
**DESEMBER 2021**

## LAPORAN AKHIR PENELITIAN

**C. HASIL PELAKSANAAN PENELITIAN:** Tuliskan secara ringkas hasil pelaksanaan penelitian yang telah dicapai sesuai tahun pelaksanaan penelitian. Penyajian meliputi data, hasil analisis, dan capaian luaran (wajib dan atau tambahan). Seluruh hasil atau capaian yang dilaporkan harus berkaitan dengan tahapan pelaksanaan penelitian sebagaimana direncanakan pada proposal. Penyajian data dapat berupa gambar, tabel, grafik, dan sejenisnya, serta analisis didukung dengan sumber pustaka primer yang relevan dan terkini.

Penelitian pada tahun ketiga dilaksanakan dengan membangun simulasi untuk mengevaluasi teknik MPPT berbasis metode Fuzzy. Selanjutnya, perangkat keras dibangun untuk mengimplementasikan metode yang telah dibuat. Tujuan utama simulasi adalah mengoptimalkan pelacakan MPP berbasis metode Fuzzy. Metode Fuzzy memiliki berbagai jenis inferensi dengan keunggulan dan kekurangan masing-masing. Oleh sebab itu, diperlukan evaluasi sebelum mengimplementasikan ke perangkat keras yang akan dibangun. Simulasi bangun menggunakan aplikasi MATLAB/Simulink. Berbagai parameter, seperti variasi kondisi iradiansi dan frekuensi switching, diujikan untuk mengetahui kinerja Fuzzy yang paling kokoh. Blok diagram dan simulasi yang dibangun ditunjukkan pada gambar berikut.



Pengujian dilakukan dengan membandingkan performa dari fungsi keanggotaan yang meliputi Triangular, Trapesium, Gaussian, dan GBell. Frekuensi switching konverter bervariasi untuk setiap fungsi keanggotaan. Frekuensi switching yang digunakan adalah 5 kHz, 10 kHz, dan 20 kHz. Selanjutnya variabel penyinaran juga divariasikan pada setiap frekuensi switching. Variasi penyinaran adalah 1000 W/m<sup>2</sup>, 800 W/m<sup>2</sup>, 600 W/m<sup>2</sup>, dan 400 W/m<sup>2</sup>.

Tabel-tabel berikut masing-masing adalah nilai untuk  $P_{out}$ ,  $V_{out}$ ,  $I_{out}$ , osilasi dan kecepatan pelacakan dari hasil pengujian yang diperoleh. Pada tabel-tabel tersebut, nilai-nilai blok warna menunjukkan perbedaan nilai antara Trapesium dan GBell. Warna hijau mewakili nilai yang lebih baik daripada biru.

$P_{out}$  saat frekuensi switching dan iradiansi divariasikan

Membership Function	Switching Frequency											
	5 kHz				10 kHz				20 kHz			
	1000	800	600	400	1000	800	600	400	1000	800	600	400
	Irradiance											
	Watt (W)											
Triangular	122.52	76.55	44.25	19.02	130.50	88.010	46.43	22.74	155.30	115.80	60.86	25.44
Trapezoidal	162.75	104.52	58.98	26.27	221.60	145.20	82.05	36.62	229.50	166.00	105.70	54.90
Gaussian	162.75	104.52	58.98	26.27	171.70	135.10	82.05	36.41	219.30	129.30	68.80	33.57
GBell	162.75	104.52	58.98	26.27	221.60	82.20	82.05	36.62	229.80	172.90	106.20	51.76

Vout saat frekuensi switching dan iradiansi divariasikan

Membership Function	Switching Frequency											
	5 kHz				10 kHz				20 kHz			
	1000	800	600	400	1000	800	600	400	1000	800	600	400
	Irradiance											
	Volt (V)											
Triangular	138.55	110.85	84.15	56.50	144.50	118.70	86.19	60.32	157.20	136.10	98.68	63.80
Trapezoidal	161.55	129.33	97.16	64.83	188.30	152.40	114.60	76.55	191.60	163.00	130.10	93.12
Gaussian	161.55	129.33	97.16	64.83	187.90	147.00	114.60	76.32	187.30	143.90	104.90	73.28
GBell	161.55	129.33	97.16	64.83	188.30	152.40	114.60	76.55	191.80	166.30	130.40	91.00

Iout saat frekuensi switching dan iradiansi divariasikan

Membership Function	Switching Frequency											
	5 kHz				10 kHz				20 kHz			
	1000	800	600	400	1000	800	600	400	1000	800	600	400
	Irradiance											
	Ampere (I)											
Triangular	0.8843	0.6906	0.5258	0.3532	0.9030	0.7417	0.5387	0.3770	0.9853	0.8506	0.6108	0.3987
Trapezoidal	1.0086	0.8082	0.6070	0.4052	1.1770	0.9527	0.7161	0.4784	1.1980	1.0190	0.8130	0.5820
Gaussian	1.0086	0.8082	0.6070	0.4052	1.1750	0.9189	0.7161	0.4770	1.1710	0.8991	0.6557	0.4580
GBell	1.0086	0.8082	0.6070	0.4052	1.1770	0.9527	0.7161	0.4784	1.1980	1.0400	0.8149	0.5688

Kecepatan pelacakan saat frekuensi switching dan iradiansi divariasikan

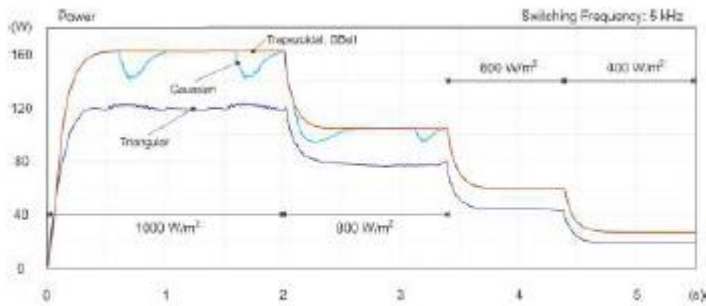
Membership Function	Switching Frequency											
	5 kHz				10 kHz				20 kHz			
	1000	800	600	400	1000	800	600	400	1000	800	600	400
	Irradiance											
	Second (s)											
Triangular	0.40	0.40	0.27	0.22	0.40	0.39	0.28	0.25	0.40	0.25	0.18	0.15
Trapezoidal	0.35	0.35	0.27	0.22	0.35	0.35	0.28	0.25	0.27	0.25	0.18	0.15
Gaussian	0.35	0.35	0.27	0.22	0.35	0.35	0.28	0.25	0.27	0.25	0.18	0.15
GBell	0.35	0.35	0.27	0.22	0.35	0.35	0.28	0.25	0.27	0.25	0.18	0.15

Perbandingan Trapezoidal dan GBell saat frekuensi switching 20 kHz

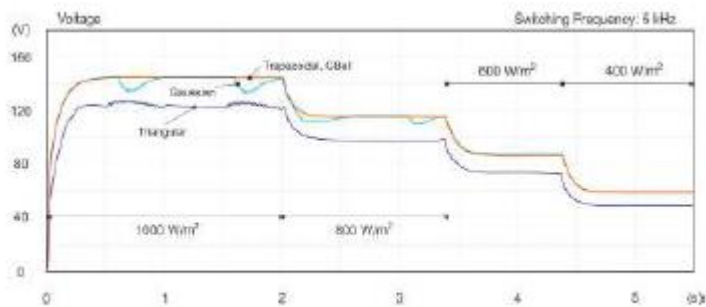
Membership Function	Switching Frequency 20 kHz															
	$P_{out}$				$V_{out}$				$I_{out}$				Oscillation			
	1000	800	600	1000	800	600	1000	800	600	1000	800	600	1000	800	600	
	Watt (W)															
	Volt (V)															
	Ampere (I)															
	Volt (V)															
Trapezoidal	229.50	166.00	105.70	191.60	163.00	130.10	1.1980	1.0190	0.8130	0.653	0.392	0.378				
GBell	229.80	172.90	106.20	191.80	166.30	130.40	1.1980	1.0400	0.8149	0.392	0.231	0.188				

Gambar-gambar berikut menunjukkan kemiringan  $P_{out}$ ,  $V_{out}$ , dan  $I_{out}$  dari empat fungsi keanggotaan yang diuji dengan frekuensi switching masing-masing 5 kHz. Terlihat bahwa Trapezium, Gaussian, dan GBell menghasilkan output yang lebih besar daripada Triangular. Selanjutnya, kecepatan pelacakan ketiga fungsi keanggotaan lebih cepat dalam mencapai MPP. Hal ini ditunjukkan pada Tabel diatas dimana Trapezium, Gaussian, dan GBell

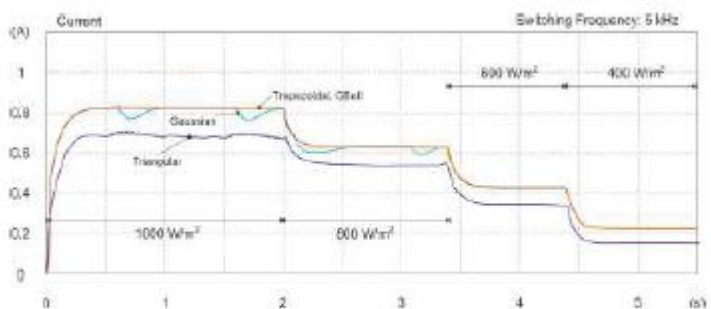
memiliki kecepatan pelacakan yang sama. Namun, ditunjukkan pada Tabel perbandingan osilasi, Gaussian memiliki osilasi yang lebih signifikan daripada tiga keanggotaan lainnya. Dalam pengujian ini, Trapezium dan GBell menghasilkan output, osilasi, dan kecepatan pelacakan yang serupa.



**$P_{out}$  with a switching frequency of 5 kHz.**

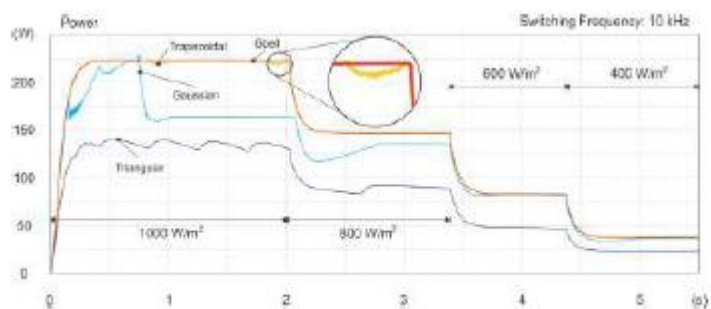


**$V_{out}$  with a switching frequency of 5 kHz.**

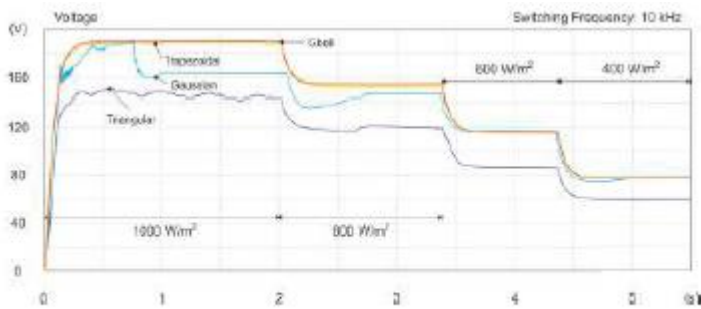


**$I_{out}$  with a switching frequency of 5 kHz.**

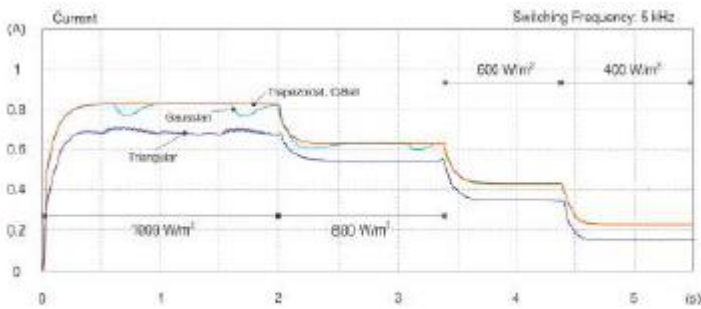
Performa trapesium dan GBell sedikit berbeda dalam pengujian dengan frekuensi switching 10 kHz. Gambar-gambar berikut menunjukkan slope  $P_{out}$ ,  $V_{out}$ , dan  $I_{out}$  untuk pengujian dengan frekuensi switching masing-masing 10 kHz. Hal ini ditunjukkan dari hasil yang diperoleh pada Tabel perbandingan osilasi, Trapezoid mengalami osilasi periodik sebesar 1,625% pada penyinaran 1000 W/m<sup>2</sup> pada kondisi tunak. Namun, nilai output, osilasi, dan kecepatan pelacakan masih lebih unggul daripada Gaussian dan Triangular.



**$P_{out}$  with a switching frequency of 10 kHz.**

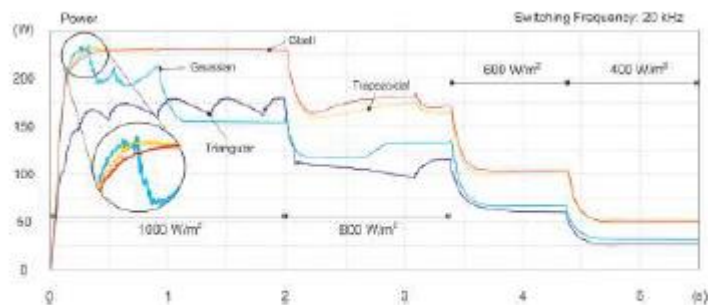


**$V_{out}$  with a switching frequency of 10 kHz.**

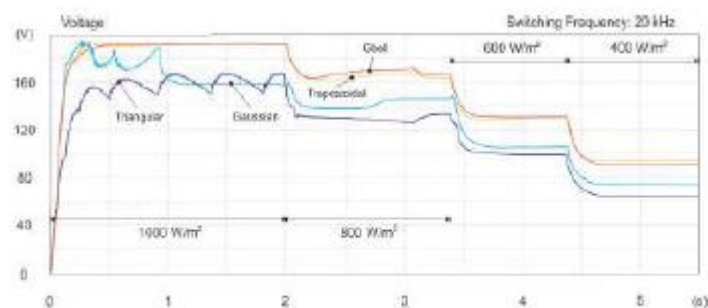


**$I_{out}$  with a switching frequency of 10 kHz.**

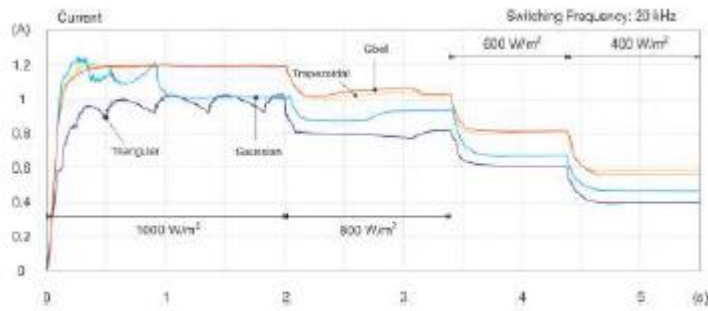
Pada pengujian dengan frekuensi switching 20 kHz, performansi Trapezoid dan Gbell mengalami penurunan. Osilasi dari kedua tingkat keanggotaan ini meningkat secara keseluruhan, pada penyinaran tinggi dan rendah. Pada tingkat radiasi rendah,  $V_{out}$ , maka  $P_{out}$ , dihasilkan dengan Gbell yang lebih rendah daripada Trapesium. Namun, osilasi yang dihasilkan masih dalam kisaran yang dapat diterima.  $V_{out}$  dan  $P_{out}$  yang dihasilkan oleh Gbell lebih tinggi dari Trapesium. Output  $P_{out}$ ;  $V_{out}$ , dan  $I_{out}$  dengan frekuensi switching 20 kHz ditunjukkan pada Gambar-gambar berikut.



**$P_{out}$  with a switching frequency of 20 kHz.**



**$V_{out}$  with a switching frequency of 20 kHz.**

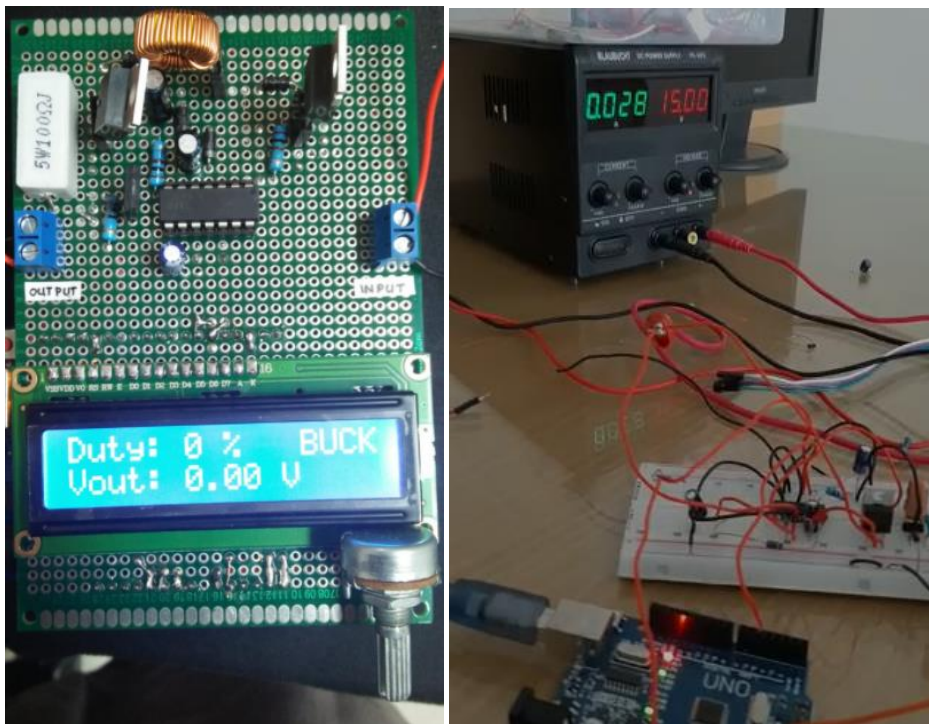


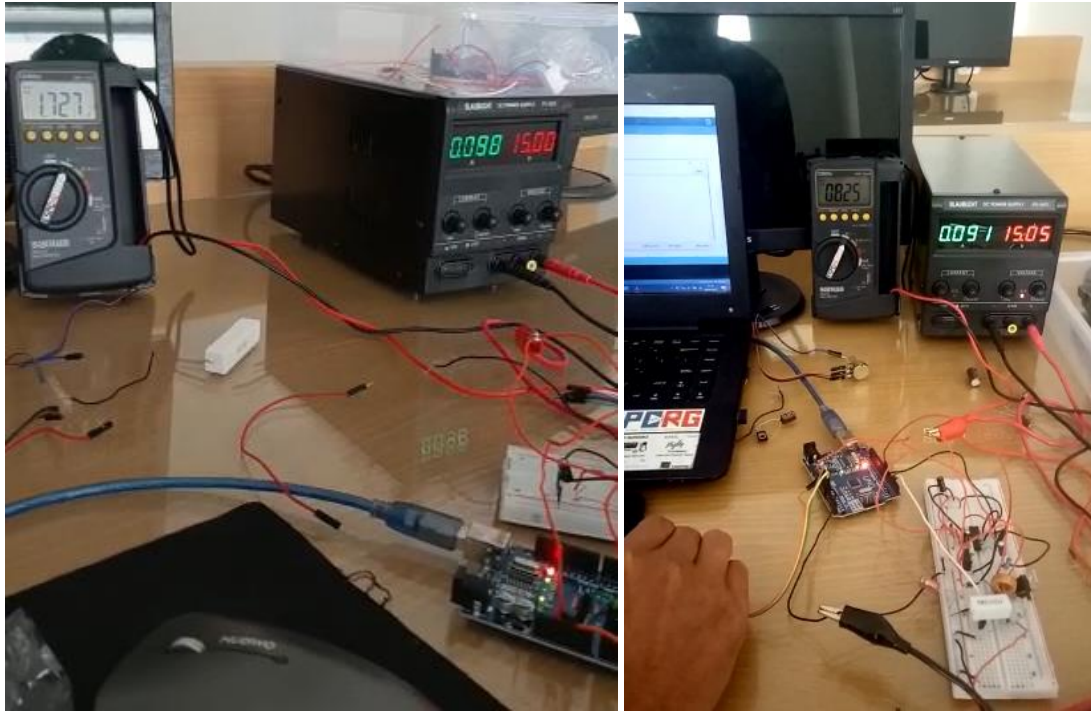
$I_{out}$  with a switching frequency of 20 kHz.

Berdasarkan pengujian yang dilakukan dengan memvariasikan iradiasi dan frekuensi switching, terlihat bahwa GBell mengungguli jenis fungsi keanggotaan fuzzy lainnya dalam hal optimasi output konverter, osilasi, dan kecepatan pelacakan.

Perbandingan head-to-head kinerja antara Trapesium dan GBell ditunjukkan pada Tabel dibawah. Variabel yang dibandingkan adalah  $P_{out}$ ,  $V_{out}$ ,  $I_{out}$ , dan osilasi pada frekuensi switching 20 kHz dan variasi penyinaran antara 1000  $W/m^2$  hingga 600  $W/m^2$ . Berdasarkan hasil, GBell mengungguli Trapesium dalam hal kinerja.

Selanjutnya, perangkat keras dibangun untuk mengimplementasikan simulasi yang telah dibuat. Berikut hasil pembuatan perangkat keras beserta dokumentasi pengujiannya.





**D. STATUS LUARAN:** Tuliskan jenis, identitas dan status ketercapaian setiap luaran wajib dan luaran tambahan (jika ada) yang dijanjikan. Jenis luaran dapat berupa publikasi, perolehan kekayaan intelektual, hasil pengujian atau luaran lainnya yang telah dijanjikan pada proposal. Uraian status luaran harus didukung dengan bukti kemajuan ketercapaian luaran sesuai dengan luaran yang dijanjikan. Lengkapi isian jenis luaran yang dijanjikan serta mengunggah bukti dokumen ketercapaian luaran wajib dan luaran tambahan melalui Simlitabmas.

Luaran yang telah tercapai adalah luaran wajib berupa publikasi di jurnal internasional bereputasi Q1 dan luaran tambahan berupa publikasi di jurnal internasional Q2. Status paper adalah telah dipublikasi (published). Nama jurnal untuk luaran wajib adalah IEEE ACCESS dengan URL website adalah <https://ieeaccess.ieee.org/> dengan judul paper “Evaluation of Fuzzy Membership Function Effects for Maximum Power Point Tracking Technique of Photovoltaic System”, sedangkan jurnal untuk luaran tambahan adalah IJECE dengan URL website <http://ijece.iaescore.com/index.php/IJECE> dengan judul paper “Internet of things-based photovoltaics parameter monitoring system using NodeMCU ESP8266”.

Bukti artikel diterima adalah sebagai berikut



**IEEE Access** <onbehalf@manuscriptcentral.com>  
 kepada tole, esperg, giovanni.pau, saya, a.elkhateb

Inggris    Indonesia    [Terjemahkan pesan](#)

27-Jul-2021

Dear Dr. Sutikno:

Your manuscript entitled "Evaluation of Fuzzy Membership Function Effects for Maximum Power Point Tracking Technique of Photovoltaic System" has been accepted for publication. Your article will be posted Early Access on IEEE *Xplore* within 2-3 business days. We ask that you make changes to your manuscript based on those comments, before uploading final files.

However, NO CHANGES to the author list or the references will be permitted.

Finally, please improve the English grammar and check spelling, as it is only lightly edited before publication.

Once you have updated your article accordingly, please send all final versions of your files through the "Awaiting Final Files" queue in your Author Center on ScholarOne Manuscript Central. Your article will be posted Early Access on IEEE *Xplore* within 2-3 business days. Within 7-10 business days you will receive your page proofs of the final version of your article. Once you approve the proofs, the final version will replace the Early Access version on IEEE *Xplore*.

When submitting final files, you must submit all of the items in the list below. All files intended for publication need to be submitted during this step, even if some files will delay the publication of your article, or result in certain files not being published.

- 1) Manuscript in MS Word or LaTeX with all author biographies and photos included.
- 2) A PDF of the final manuscript in double column, single-spaced format named "FINAL Article.pdf".
- 3) A Graphical Abstract (GA) which provides a concise, visual summary of the findings of your article. The GA should be a figure or image from the accepted article. The ideal article, the video will automatically become the GA and you will need to supply a still image to act as an overlay. For more information on the GA, please visit <https://ieeaccess.org>
- 4) Video(s) included in peer review (if any)
- 5) A Word file that indicates: a) the file name(s) of the GA and overlay (if applicable), b) a caption for the GA that should not exceed 60 words.



Innovative Tech ID <lfriyan220@gmail.com>

## [IJECE 2021 Batch #2] Your paper #1570725224 ("Internet of Things-Based Photovoltaics Parameter Monitoring System Using NodeMCU ESP8266")

1 pesan

**IJECE Editor (ijece@iaesjournal.com)** <ijece=iaesjournal.com@edas.info>

24 Agustus 2021 23.41

Balas Ke: Ijece Editor <ijece@iaesjournal.com>

Kepada: Tole Sutikno <thsutikno@ieee.org>, Hendril Satrian Purnama <Lfriyan220@gmail.com>, Anggit Pamungkas <anggitpamungkas17@gmail.com>, Abdul Fadil <fadil@mti.uad.ac.id>, Ibrahim M Alsofyani <alsofyani@ajou.ac.kr>, Mohd Hatta Jopri <hatta@utem.edu.my>

- Similarity score of camera-ready paper must be less than 25%. Single author is PROHIBITED !!
- Please Strictly use & follow to the template Manuscripts: <http://iaescore.com/gfa/ijece.docx>
- Number of minimum references for original research paper is 25 references (and minimum 20 recent journal articles).
- Number of minimum references for review paper is 50 references (and minimum 40 recent journal articles).

Dear Dr. Tole Sutikno,

Congratulations!! Your paper #1570725224 ("Internet of Things-Based Photovoltaics Parameter Monitoring System Using NodeMCU ESP8266") for the International Journal of Electrical and Computer Engineering (Submission Period: Apr-Aug 2021) has been ACCEPTED with minor revisions. The IJECE, ISSN 2088-8708, e-ISSN 2722-2578 (<http://ijece.iaescore.com>) is a SCOPUS indexed Journal, SNIP: 1.144; SJR: 0.368; CiteScore: 1.63; SJR & CiteScore Q2 on both of the Electrical & Electronics Engineering, and Computer Science). This journal is open to submission from scholars and experts in the wide areas of electrical, electronics, instrumentation, control, robotics, telecommunication, computer engineering, computer science, information system, information technology and informatics from the global world. The aim of this journal is to publish high-quality articles dedicated to all aspects of the latest outstanding developments in the field of electrical engineering. Its scope encompasses the applications of Telecommunication and Information Technology, Applied Computing and Computer, Instrumentation and Control, Electrical (Power), and Electronics Engineering.

Please make the necessary changes based on reviewers' comments and suggestions. The reviews are below or can be found at <https://edas.info/showPaper.php?m=1570725224>. Please prepare your final camera ready paper (in MS Word file format) adheres every detail of the guide of authors (<http://iaescore.com/gfa/ijece.docx>), and check it for spelling/grammatical mistakes. Please explain more your proposed method/approach/platform/algorithm... clearly. Smoothly method explanation are the one of main reasons to judge article quality and your article potentially receives a high citation number. The goal of your camera ready paper is to describe NOVEL TECHNICAL RESULTS.

For original research paper, there are four (4) types of novel technical results:

- 1) An algorithm;
  - 2) A system construct: such as hardware design, software system, protocol, etc.,. The main goal of your revised paper is to ensure that the next person who designs a system like yours doesn't make the same mistakes and takes advantage of some of your best solutions. So make sure that the hard problems (and their solutions) are discussed and the non-obvious mistakes (and how to avoid them) are discussed;
  - 3) A performance evaluation: obtained through analyses, simulation or measurements; or
  - 4) A theory: consisting of a collection of theorems.
- Your final camera ready paper should focus on:
- 1) Describing the results in sufficient details to establish their validity;
  - 2) Identifying the novel aspects of the results, i.e., what new knowledge is reported and what makes it non-obvious; and

Adapun luaran wajib dan tambahan untuk tanggungan luaran tahun sebelumnya berupa artikel di jurnal internasional bereputasi Q1 dan Q3. Status artikel adalah telah *submit* dan telah mengirim respon jawaban ke *reviewer*. Nama jurnal untuk tanggungan luaran wajib adalah IEEE ACCESS dengan URL website <https://ieeaccess.ieee.org/> dengan judul paper "A review of recent advances on hybrid energy storage system for solar photovoltaics power generation", sedangkan jurnal untuk luaran tambahan adalah Distributed Generation &



Alternative Energy Journal dengan URL website <https://www.journal.riverpublishers.com/index.php/DGAEJ/> dengan judul paper “A New FL-MPPT High Voltage DC-DC Converter for PV Solar Application”.

Bukti artikel telah melalui tahapan *review* adalah sebagai berikut

**E. PERAN MITRA:** Tuliskan realisasi kerjasama dan kontribusi Mitra baik *in-kind* maupun *in-cash* (untuk Penelitian Terapan, Penelitian Pengembangan, PTUPT, PPUPT serta KRUPPT). Bukti pendukung realisasi kerjasama dan realisasi kontribusi mitra dilaporkan sesuai dengan kondisi yang sebenarnya. Bukti dokumen realisasi kerjasama dengan Mitra diunggah melalui Simlitabmas.

.....  
.....  
.....  
.....  
.....

**IEEE Access - Decision on Manuscript ID Access-2021-28524**

IEEE Access <onbehalfof@manuscriptcentral.com> 11 September 2021 11.16  
Balas Ke: eleskp@nus.edu.sg  
Kepada: tole@ee.uad.ac.id, esperg@ee.uad.ac.id  
Cc: eleskp@nus.edu.sg, tole@ee.uad.ac.id, esperg@ee.uad.ac.id, watra24arsadiando@gmail.com, areceic@yahoo.com, eyudhana@ee.uad.ac.id, mochfacta@gmail.com

11-Sep-2021

Dear Dr. Sutikno:

I am writing to you in regards to manuscript # Access-2021-28524 entitled "Advances on hybrid energy storage system for solar photovoltaic power generation" which you submitted to IEEE Access.

Please note that IEEE Access has a binary peer review process. Therefore, in order to uphold quality to IEEE standards, an article is rejected even if it requires minor edits.

Your manuscript has not been recommended for publication in IEEE Access in its current form; however, we do encourage you to address the concerns and criticisms of the reviewers detailed at the bottom of this letter and resubmit your article once you have updated it accordingly.

Please revise your manuscript based on reviewers' feedback and resubmit; elaborate on your points and clarify with references, examples, data, etc. If you do not agree with the reviewers' views, then include your arguments in the updated manuscript. Also, note that if a reviewer suggested references, you should only add ones that will make your article better and more complete. Recommending references to specific publications is not appropriate for reviewers and you should report excessive cases to [ieeeaccessEIC@ieee.org](mailto:ieeeaccessEIC@ieee.org).

We highly recommend that you review the grammar one more time before resubmitting. IEEE offers a 3rd party service for language polishing, which you may utilize for a fee: <https://www.aje.com/c/ieee> (use the URL to claim a 10% discount).

Please be advised that authors are only permitted to resubmit their article ONCE. If the updated manuscript is determined not to have addressed all of the previous reviewers' concerns, the article may be rejected and no further resubmissions will be allowed.

When resubmitting, please submit as a new manuscript via our submission site (<https://mc.manuscriptcentral.com/ieee-access>) and include the following 3 files:

- 1) A document containing your response to reviewers from the previous peer review. The "response to reviewers" document (template attached) should have the following regarding each comment: a) Reviewer's concern, b) your response to the concern, c) your action to remedy the concern. The document should be uploaded with your manuscript files as a "Supplemental File for Review."
- 2) Your updated manuscript with all your individual changes highlighted, including grammatical changes (e.g. preferably with the yellow highlight tool within the pdf file). This file should be uploaded with your manuscript files as a "Supplemental File for Review".
- 3) A clean copy of the final manuscript (without highlighted changes) should be submitted as the "Formatted (Double Column) Main File – PDF Document Only."

We sincerely hope you will update your manuscript and resubmit soon. Please contact me if you have any questions.

For more information on successfully publishing within IEEE Access, please see [https://youtu.be/502WPjDhY\\_0](https://youtu.be/502WPjDhY_0)

Thank you for your interest in IEEE Access.

Sincerely,

Dr. S. K. Panda  
Associate Editor, IEEE Access  
[eleskp@nus.edu.sg](mailto:eleskp@nus.edu.sg)

---

## [DGAEJ] Editor Decision

---

Rajvant Nijjar via River Publishers <journals@riverpublishers.com>

25 Oktober 2021 14.42

Balas Ke: Rajvant Nijjar <rajvant@ivees.co.uk>

Kepada: Tole Sutikno <tole@ee.uad.ac.id>, Arsyad Subrata <arsyadcahya@gmail.com>, Awang Jusoh <awang@fke.utm.my>, "Prof. Sanjeevikumar Padmanaban" <sanjeev@btech.au.dk>

Tole Sutikno, Arsyad Subrata, Awang Jusoh, Prof. Sanjeevikumar Padmanaban:

We have reached a decision regarding your submission to Distributed Generation & Alternative Energy Journal, "A New FL-MPPT High Voltage DC-DC Converter for PV Solar Application".

Our decision is to: Resubmit for Review

Rajvant Nijjar  
iVEES, UK  
[rajvant@ivees.co.uk](mailto:rajvant@ivees.co.uk)

**F. KENDALA PELAKSANAAN PENELITIAN:** Tuliskan kesulitan atau hambatan yang dihadapi selama melakukan penelitian dan mencapai luaran yang dijanjikan, termasuk penjelasan jika pelaksanaan penelitian dan luaran penelitian tidak sesuai dengan yang direncanakan atau dijanjikan.

Penelitian sempat terhenti sementara akibat pandemi Covid-19. Akibat pandemi ini, penelitian yang dilaksanakan di area kampus tidak dilaksanakan untuk sementara.

**G. RENCANA TAHAPAN SELANJUTNYA:** Tuliskan dan uraikan rencana penelitian di tahun berikutnya berdasarkan indikator luaran yang telah dicapai, rencana realisasi luaran wajib yang dijanjikan dan tambahan (jika ada) di tahun berikutnya serta *roadmap* penelitian keseluruhan. Pada bagian ini diperbolehkan untuk melengkapi penjelasan dari setiap tahapan dalam metoda yang akan direncanakan termasuk jadwal berkaitan dengan strategi untuk mencapai luaran seperti yang telah dijanjikan dalam proposal. Jika diperlukan, penjelasan dapat juga dilengkapi dengan gambar, tabel, diagram, serta pustaka yang relevan. Jika laporan kemajuan merupakan laporan pelaksanaan tahun terakhir, pada bagian ini dapat dituliskan rencana penyelesaian target yang belum tercapai.

.....  
.....  
.....  
.....  
.....

**H. DAFTAR PUSTAKA:** Penyusunan Daftar Pustaka berdasarkan sistem nomor sesuai dengan urutan pengutipan. Hanya pustaka yang disitasi pada laporan kemajuan yang dicantumkan dalam Daftar Pustaka.

1. S. Messalti, A. Harrag, and A. Loukriz, "A new variable step size neural networks MPPT controller: Review, simulation and hardware implementation," *Renew. Sustain. Energy Rev.*, vol. 68, pp. 221233, Feb. 2017
2. A. Jusoh, R. Alik, T. K. Guan, and T. Sutikno, "MPPT for PV system based on variable step size P&O algorithm," *Telkonnika*, vol. 15, no. 1, p. 79, 2017.
3. A. Jusoh, T. Sutikno, T. K. Guan, and S. Mekhilef, "A review on favourable maximum power point tracking systems in solar energy application," *Telkonnika*, vol. 12, no. 1, p. 6, Mar. 2014.
4. P. A. Dahono, "New step-up DC-DC converters for PV power generation systems," in *Proc. Int. Seminar Intell. Technol. Appl. (ISITIA)*, Aug. 2017, pp. 187192.

Received July 3, 2021, accepted July 27, 2021, date of publication August 3, 2021, date of current version August 10, 2021.

Digital Object Identifier 10.1109/ACCESS.2021.3102050

# Evaluation of Fuzzy Membership Function Effects for Maximum Power Point Tracking Technique of Photovoltaic System

TOLE SUTIKNO<sup>1,2</sup>, (Member, IEEE), ARSYAD CAHYA SUBRATA<sup>1,2</sup>,  
AND AHMAD ELKHATEB<sup>3</sup>, (Senior Member, IEEE)

<sup>1</sup>Department of Electrical Engineering, Faculty of Industrial Technology, Universitas Ahmad Dahlan, Yogyakarta 55191, Indonesia

<sup>2</sup>Embedded Systems and Power Electronics Research Group, Yogyakarta 55191, Indonesia

<sup>3</sup>School of Electronics Engineering and Computer Science, Queen's University, Belfast BT9 5AH, U.K.

Corresponding author: Tole Sutikno (tole@ee.uad.ac.id)

This work was supported by the Ministry of Education, Culture, Research, and Technology (formerly Ministry of Research and Technology/National Agency for Research and Innovation), Indonesia, through a World Class Research (WCR) Scheme under Contract WCR-001/SKPP.ATJ/LPPM UAD/VI2020.

**ABSTRACT** The photovoltaic generation system (PGS) is considered a potential renewable energy harvesting system. However, the low conversion efficiency of PGS and maximum power point tracking (MPPT) technique are the main challenges that must be solved. In addition, the switching frequency of the converters employed also affects the MPPT system performance. A high gain voltage DC-DC converter is proposed to replace conventional power converter and fuzzy logic controller (FLC) is applied in the MPPT for optimizing solar energy harvesting system. Nevertheless, evaluation of suitable fuzzy membership function is needed for optimal MPPT technique of photovoltaic system. In this paper, FLC of MPPT for photovoltaic application system was built using various membership functions in MATLAB/Simulink environment. The switching frequency of the high gain voltage DC-DC converter is varied to test the robustness of the performance of each FLC membership function. The results showed that the FLC-based MPPT technique for high gain voltage DC-DC converter with GBell membership function type has the capability to track the maximum power point (MPP) accurately and to achieve optimum power conversion. Furthermore, GBell membership showed having stable and consistent performance at various switching frequencies.

**INDEX TERMS** Maximum power point tracking, fuzzy logic controller, membership function, high gain voltage DC-DC converter.

## I. INTRODUCTION

The demand for photovoltaic generation systems (PGSs) shows a graph of significant improvement. The need to meet global issues to reduce the harmful effects of conventional power plants has led to an increase in the demand for PGSs. As it is well known, traditional power plants, which usually use coal as fuel, have negative effects such as the greenhouse effect, pollution, and solid and liquid waste. The development of necessary material processing technology for making photovoltaic (PV) itself has made it increasingly produced and easily available.

However, PGSs that work by harvesting solar energy have a low power conversion. This is because the performance of

The associate editor coordinating the review of this manuscript and approving it for publication was Giovanni Pau<sup>1</sup>.

PV depends on ambient weather conditions such as irradiation and changing temperature [1]–[3]. Under these varying weather conditions, the maximum power point (MPP) received by PV also varies. This is what causes the low PV power conversion efficiency. The maximum power of PV must be extracted to ensure high power conversion efficiency [4]–[6]. The way to increase the power conversion efficiency of PV is by considering the best converter topology possible. Another way is by optimizing the techniques that have been developed by many researchers to track MPP which is commonly known as maximum power point tracking (MPPT) [7]–[45]. Apart from increasing the power conversion efficiency, the MPPT technique can also increase the lifetime of the PV module [8].

There are various MPPT methods. Conventional methods are unstable due to dynamic response and steady-state, thus

causing oscillations around the MPP. Another method that is often used because of its reliability is the fuzzy logic controller (FLC) [22]–[27]. The FLC method is suitable to be applied to PV MPPT because it can handle non-linear systems produced by the PV itself due to changing weather conditions [28]. In addition, FLC is also popular because it does not require knowledge of the PV system model [29]–[31].

However, FLC has some disadvantages. One of the shortcomings of FLC is the problem of efficiency which depends on the performance of the system design [16], [41]–[43]. The inherent weakness of FLC is more towards the design of the algorithm development itself, *i.e.* subset, membership function, and rules. Therefore, the development of the FLC algorithm needs to be optimized from the basics in order to provide optimal results. This basic optimization is conducted by choosing the form of membership function that best suits needs. In this research, FLC was employed to assist the high-gain voltage DC-DC converter topology. The test is conducted by varying the irradiation and switching frequency of the converter. Furthermore, various membership functions are discussed and evaluated to find the most suitable type. The final result of this study aims to improve the MPPT technique using FLC with basic optimization by adjusting the membership function according to the topology and switching frequency of the converter used. Designing a membership function is important in an FLC-based control system. Each type of membership function will produce different performance results. Therefore, choosing the most suitable membership function for the system being built is an important thing to consider.

## II. HIGH GAIN DC-DC CONVERTER

The converter used in this study was previously initiated by Dahono [46]. It is based on a modified DC-DC buck-boost converter modifications made to produce a converter that has a high gain voltage. Figure 1 shows the high gain voltage DC-DC converter. The resulting voltage ratio is

$$\frac{V_o}{E_d} = \frac{1}{1 - \alpha} \quad (1)$$

where  $\alpha$  is a transistor  $Q$  duty factor.

This converter switching device can be operated to reduce the ripple content of the switching device in a two-phase converter. The RMS value of voltage ripple and the output voltage ripple for the duty cycle of more than half of this converter are shown in (2) and (3), respectively.

$$\tilde{V}_o = \frac{\bar{i}_o}{Cf_s} \frac{\alpha(1 - 2\alpha)}{2\sqrt{3}(1 - \alpha)} \quad (2)$$

$$\tilde{V}_o = \frac{\bar{i}_o}{Cf_s} \frac{(2\alpha - 1)}{2\sqrt{3}} \quad (3)$$

where  $f_s$  is minimum switching of the converter.

## III. MAXIMUM POWER POINT TRACKING

There are numerous methods used in the MPPT which have their advantages and disadvantages. However, a

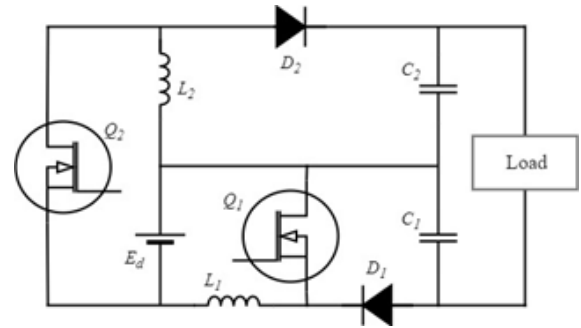


FIGURE 1. High gain voltage DC-DC converter.

capable method of optimally tracking MPP is preferred because it ensures maximum power extraction, reliability and efficiency [20], [21]. Conventional methods such as Perturb and Observe (P&O), Incremental Conductance (IncCond), and Hill Climbing (HC) are widely used even to commercial products because of their simplicity. Nevertheless, these methods are unstable due to dynamic response and steady-state, thus causing oscillations around the MPP.

Various studies on MPPT based on the FLC method have been carried out and compared with other algorithms, as well as tested through varying the irradiation. These algorithms are built to regulate the duty cycle of the DC-DC converter. Using a boost converter, FLC has better tracking speed and drift avoidance than the P&O, IncCond, and HC methods on dynamic response and steady state (no oscillations) [32]–[34]. Other study conducted by Bendib *et al.* [31] that implemented FLC with a buck converter yielded a similar result. Khateb *et al.* [35] used a SEPIC type converter which was tested with simulation and experimental works. The result obtained is that FLC produces better tracking speed than P&O in both tests. Even the combination of converters, such as buck-boost [36] and boost-SEPIC [37], [38] shows that FLC performance is also superior. Other researches were conducted to find the most reliable but easy to develop FLC performance based on algorithmic design. Hajjighorbani *et al.* [39] evaluated a subset of FLC applied to PV MPPT shown that FLC with many subsets produces better efficiency. However, the more subsets that are used, the more the computational burden will be due to the increasing number of rule-bases. Ali *et al.* [40] compared the effect of the FLC membership function but this study was not determined for the PV MPPT purpose.

## IV. FUZZY LOGIC CONTROLLER

FLC is based on a statement in the form of a set that is differentiated from other sets based on the degree of membership. In set theory, objects are members, which are denoted by “1”, and not members, “0”, of a set with crisp membership limits. In the fuzzy set theory, the member of the degree of an object in the set is possible to express the gradual transition of membership in the interval between “0” and “1”. The fuzzy set,  $F$ , in  $X$  is expressed as an ordered pair of the element  $x$ .

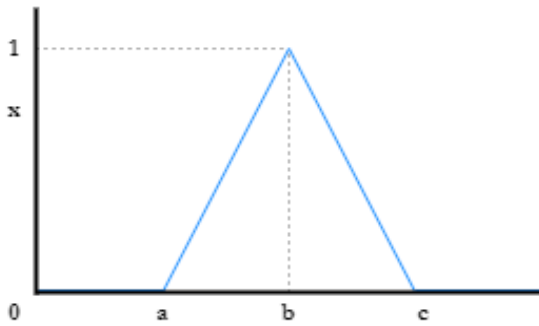


FIGURE 2. Triangular membership function.

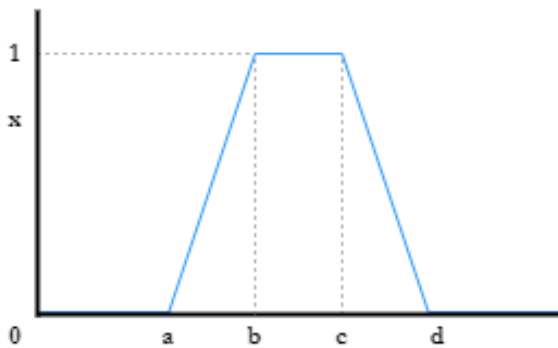


FIGURE 3. Trapezoidal membership function.

The fuzzy set has the membership degrees as

$$F = \{(x, \mu_F(x)) \mid x \in X\} \tag{4}$$

where  $\mu_F(x)$  is the degree of membership  $x$  (between 0 and 1).

In the MPPT technique, FLC is used to find MPP with input in the form of error ( $E$ ) and change of error ( $\Delta E$ ), while the output is in the form of PWM feed to control the converter duty cycle. The two inputs are obtained as

$$\text{Error, } E(k) = \frac{\Delta P}{\Delta V} = \frac{P(k) - P(k-1)}{V(k) - V(k-1)} \tag{5}$$

$$\text{Change Error, } \Delta E(k) = E(k) - E(k-1) \tag{6}$$

where  $(k)$  is the sample time,  $P(k)$  is the power,  $V(k)$  is the PV voltage.  $P(k-1)$  and  $V(k-1)$  are the previous PV power and voltage, respectively.  $E(k)$  indicates the operating load point that is located to the left or right, while  $\Delta E(k)$  in the direction of motion of the point.

In the FLC system design, there are three main components, namely fuzzification, inference, and defuzzification. In this work, the fuzzy Mamdani (min-max) model is employed.

**A. FUZZIFICATION AND MEMBERSHIP FUNCTION**

Fuzzification input in the form of crisp is then converted into fuzzy numbers into linguistic values. The inputs are then grouped into a membership function. Types of membership

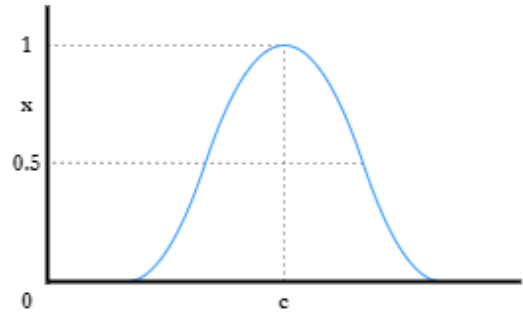


FIGURE 4. Gaussian membership function.

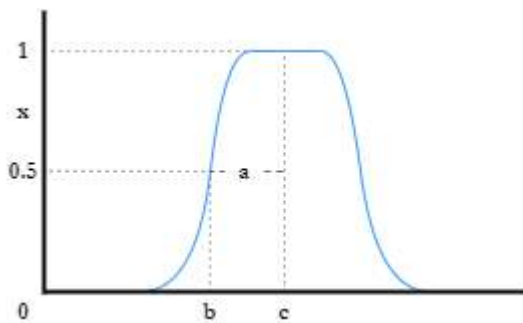


FIGURE 5. GBell membership function.

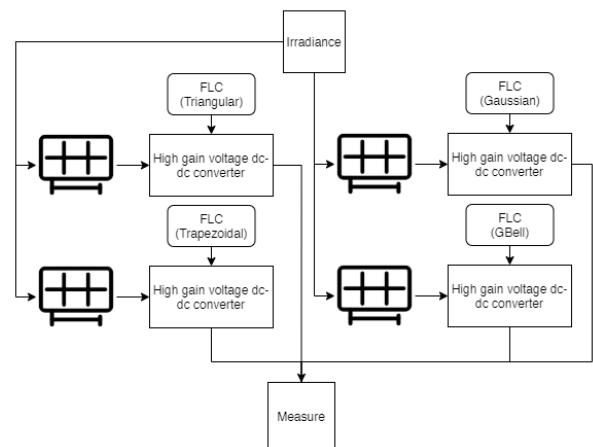


FIGURE 6. Block diagram of the system.

functions to be observed in this work are Triangular, Trapezoidal, Gaussian, and Generalized Bell (GBell). In this paper, the membership function is built with a symmetrical focused with 50% overlaps. Figure 2 to Figure 5 show the forms of the Triangular, Trapezoidal, Gaussian, and GBell membership function used, respectively. The mathematical equations for them are displayed sequentially in (7), (9), (11), and (12), respectively.

A Triangular curve as shown in Figure 2 is a combination of two linear lines, and it is determined by three parameters ( $a, b, c$ ). The  $x$  coordinates of the three angles of the Triangular membership function are determined by parameters

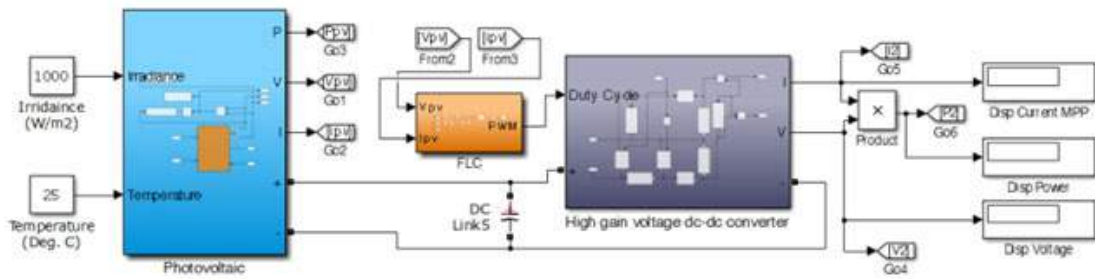


FIGURE 7. The developed system.

(a, b, c) with  $a < b < c$ . The Triangular curve is based on (7).

$$\text{triangle}(x; a, b, c) = \begin{cases} 0 & \text{for } x \leq a \\ \frac{x-a}{b-a} & \text{for } a \leq x \leq b \\ \frac{c-x}{c-b} & \text{for } b \leq x \leq c \\ 0 & \text{for } x \geq c \end{cases} \quad (7)$$

where the parameters a, b, and c give the location of fuzzy membership function.

Using the min-max, (7) can be reformulated as (8).

$$\text{triangle}(x; a, b, c) = \max\left(\min\left(\frac{x-a}{b-a}, \frac{c-x}{c-b}, 0\right)\right) \quad (8)$$

Trapezoidal curve as shown in Figure 3 has a shape resembling a Triangular curve, but there is a membership value of 1 at several points. The difference from Triangular is that the Trapezoidal membership function has a flat top so it is not fuzzy. Trapezoidal membership function is built with four parameters (a, b, c, d). Then the Trapezoidal membership function is (9).

$$\text{trap}(x; a, b, c, d) = \begin{cases} 0 & \text{for } x \leq a \\ \frac{x-a}{b-a} & \text{for } a \leq x \leq b \\ 1 & \text{for } b \leq x \leq c \\ \frac{d-x}{d-c} & \text{for } c \leq x \leq d \\ 0 & \text{for } x \geq d \end{cases} \quad (9)$$

where the parameters a, b, c and d give the location of fuzzy membership function.

Similar to Triangular, Trapezoidal membership function in (9) can be reformulated with the min-max as (10).

$$\text{trap}(x; a, b, c, d) = \max\left(\min\left(\frac{x-a}{b-a}, 1, \frac{d-x}{d-c}, 0\right)\right) \quad (10)$$

Unlike Triangular membership function which has sharp peak, Gaussian as shown in Figure 4 has soft peak. Then the Gaussian membership function is (11).

$$\text{gauss}(x; \sigma, c) = e^{-\frac{(x-c)^2}{2\sigma^2}} \quad (11)$$

where x is the crisp variable.

TABLE 1. Fuzzy rule base.

		E				
		NB	NS	Z	PS	PB
ΔE	NB	NB	NB	Z	PB	PB
	NS	NS	NS	Z	PS	PS
	Z	Z	Z	Z	Z	Z
	PS	PS	PS	Z	NS	NS
	PB	PB	PB	Z	NB	NB

GBell membership function as shown in Figure 5 is generalized Cauchy distribution used in probability theory. Then the GBell membership function is (12).

$$\text{bell}(x; a, b, c) = \frac{1}{1 + \left|\frac{x-c}{a}\right|^{2m}} \quad (12)$$

where m defines the width of the flat top of the bell function.

**B. INFERENCE**

In this process, the grouped fuzzy input is calculated into the rule-base to determine the output. This rule-base serves to define the desired relationship rules between input and output variables. The number of rules depends on the number of input membership functions used. In this study, each input has five membership functions, 25 rules are obtained accordingly as shown in Table 1.

**C. DEFUZZIFICATION**

In the defuzzification process, fuzzy numbers are converted into crisp as the final output of the FLC. The defuzzification process is based on the center of gravity obtained by (13). The FLC output obtained is used to control the duty cycle (D) of the high gain voltage DC-DC converter.

$$D = \frac{\sum x_i \times \mu_i}{\sum \mu_i} \quad (13)$$

where D and x are the duty cycle and the output triangle value, respectively.

**V. EXPERIMENTAL SETUP**

In this work, the FLC algorithm is utilized on the MPPT technique for PV systems feed to a high gain voltage

**TABLE 2. Parameters of the Trina Solar TSM-250PA05.08.**

PV Parameters	Value
<b>Module data</b>	
Maximum Power (W)	249.86
Cells per module ( $N_{cell}$ )	60
Open circuit voltage $V_{oc}$ (V)	37.6
Short-circuit current $I_{sc}$ (A)	8.55
Voltage at maximum power point $V_{mp}$ (V)	31
Current at maximum power point $I_{mp}$ (A)	8.06
Temperature coefficient of $V_{oc}$ ( $\%/^{\circ}C$ )	-0.35
Temperature coefficient of $I_{sc}$ ( $\%/^{\circ}C$ )	0.06
<b>Module parameters</b>	
Light-generated current $I_L$ (A)	8.5795
Diode saturation current $I_D$ (A)	2.0381e-10
Diode ideality factor	0.99766
Shunt resistance $R_{sh}$ ( $\Omega$ )	301.8149
Series resistance $R_s$ ( $\Omega$ )	0.247

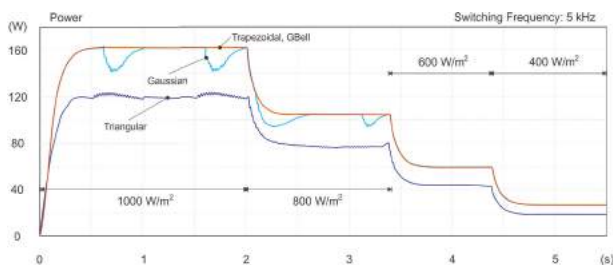


**FIGURE 8.  $P_{out}$  with a switching frequency of 5 kHz.**

DC-DC converter. The block diagram of the system is shown in Figure 6. Figure 7 shows a system consisting of a PV module, high gain voltage DC-DC converter with an MPPT controller connected to a load that has been created using MATLAB/Simulink. The PV model used is Trina Solar TSM-250PA05.08 with the specifications shown in Table 2.

**VI. RESULTS AND DISCUSSION**

In this work, the FLC algorithm has been successfully built on the MPPT technique for PV systems feed to a high gain voltage DC-DC converter. The resulting slope of each system created is then observed, and several vital parameters are recorded. The parameters measured are  $V_{out}$ ,  $I_{out}$ ,  $P_{out}$ , oscillation and tracking speed.

The testing is done by comparing the performance of membership functions including Triangular, Trapezoidal, Gaussian, and GBell. The switching frequency of the converter is varied for each membership function. The switching frequencies used are 5 kHz, 10 kHz, and 20 kHz. Furthermore, the irradiation variable is also varied at each switching frequency. The irradiation variations are 1000  $W/m^2$ , 800  $W/m^2$ , 600  $W/m^2$ , and 400  $W/m^2$ .

Tables 3 to 7 are the values for  $P_{out}$ ,  $V_{out}$ ,  $I_{out}$ , an oscillation and a tracking speed of the test results obtained, respectively. In Tables 3, 4, 5 and 6, the color-blocked values show the difference in values between Trapezoidal and GBell. The color green represents a better value than blue.

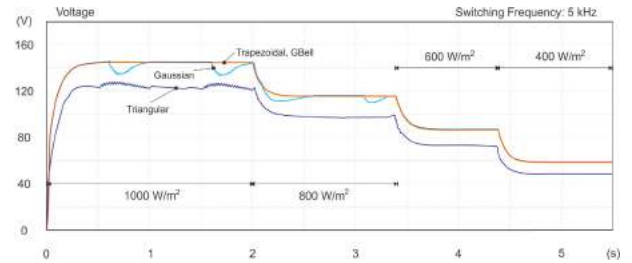


**FIGURE 9.  $V_{out}$  with a switching frequency of 5 kHz.**

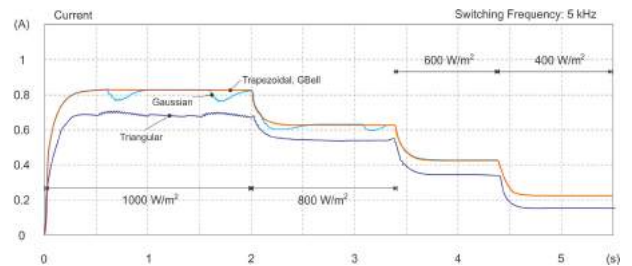


**FIGURE 10.  $I_{out}$  with a switching frequency of 5 kHz.**

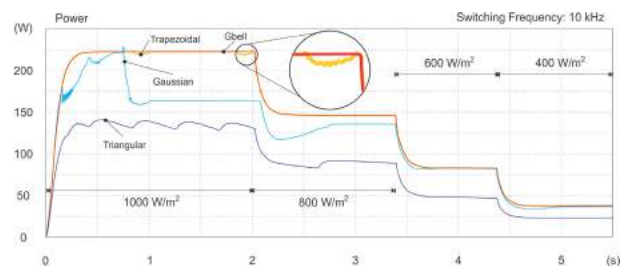


**FIGURE 11.  $P_{out}$  with a switching frequency of 10 kHz.**

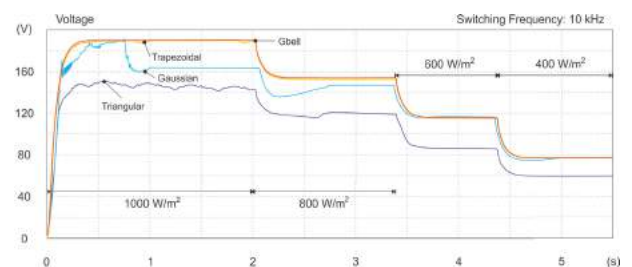


**FIGURE 12.  $V_{out}$  with a switching frequency of 10 kHz.**

Figures 8 to 10 show the  $P_{out}$ ,  $V_{out}$ , and  $I_{out}$  slope of the four membership functions that were tested with a switching frequency of 5 kHz, respectively. It appears that Trapezoidal, Gaussian, and GBell produce a larger output than the Triangular. Furthermore, the tracking speed of the three membership functions is faster in reaching MPP. This is shown in Table 7 where Trapezoidal, Gaussian, and GBell have the same tracking speed. However, shown in Table 6, Gaussian has more significant oscillations than the other three memberships. In this test, the Trapezoidal and GBell produce similar output, oscillations, and tracking speeds.



TABLE 3.  $P_{out}$  at the switching frequency and irradiance are varied.

Membership Function	Switching Frequency											
	5 kHz				10 kHz				20 kHz			
	1000	800	600	400	1000	800	600	400	1000	800	600	400
	Irradiance											
	Watt (W)											
Triangular	122.52	76.55	44.25	19.02	130.50	88.010	46.43	22.74	155.30	115.80	60.86	25.44
Trapezoidal	162.75	104.52	58.98	26.27	221.60	145.20	82.05	36.62	229.50	166.00	105.70	54.90
Gaussian	162.75	104.52	58.98	26.27	171.70	135.10	82.05	36.41	219.30	129.30	68.80	33.57
GBell	162.75	104.52	58.98	26.27	221.60	82.20	82.05	36.62	229.80	172.90	106.20	51.76

TABLE 4.  $V_{out}$  at the switching frequency and irradiance are varied.

Membership Function	Switching Frequency											
	5 kHz				10 kHz				20 kHz			
	1000	800	600	400	1000	800	600	400	1000	800	600	400
	Irradiance											
	Volt (V)											
Triangular	138.55	110.85	84.15	56.50	144.50	118.70	86.19	60.32	157.20	136.10	98.68	63.80
Trapezoidal	161.55	129.33	97.16	64.83	188.30	152.40	114.60	76.55	191.60	163.00	130.10	93.12
Gaussian	161.55	129.33	97.16	64.83	187.90	147.00	114.60	76.32	187.30	143.90	104.90	73.28
GBell	161.55	129.33	97.16	64.83	188.30	152.40	114.60	76.55	191.80	166.30	130.40	91.00

TABLE 5.  $I_{out}$  at the switching frequency and irradiance are varied.

Membership Function	Switching Frequency											
	5 kHz				10 kHz				20 kHz			
	1000	800	600	400	1000	800	600	400	1000	800	600	400
	Irradiance											
	Ampere (I)											
Triangular	0.8843	0.6906	0.5258	0.3532	0.9030	0.7417	0.5387	0.3770	0.9853	0.8506	0.6108	0.3987
Trapezoidal	1.0086	0.8082	0.6070	0.4052	1.1770	0.9527	0.7161	0.4784	1.1980	1.0190	0.8130	0.5820
Gaussian	1.0086	0.8082	0.6070	0.4052	1.1750	0.9189	0.7161	0.4770	1.1710	0.8991	0.6557	0.4580
GBell	1.0086	0.8082	0.6070	0.4052	1.1770	0.9527	0.7161	0.4784	1.1980	1.0400	0.8149	0.5688

TABLE 6. Oscillation at the switching frequency and irradiance are varied.

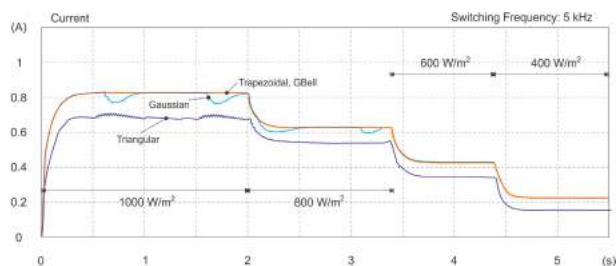
Membership Function	Switching Frequency											
	5 kHz				10 kHz				20 kHz			
	1000	800	600	400	1000	800	600	400	1000	800	600	400
	Irradiance											
	Volt (V)											
Triangular	1.816	1.550	0.384	0.321	7.279	3.815	0.258	0.164	12.680	1.036	0.657	0.314
Trapezoidal	0.184	0.171	0.169	0.166	1.625	0.076	0.016	0.013	0.653	0.392	0.378	0.364
Gaussian	13.820	12.460	0.169	0.166	12.500	8.952	0.116	0.113	11.990	8.348	0.291	0.089
GBell	0.184	0.171	0.169	0.166	0.049	0.046	0.016	0.013	0.392	0.231	0.188	0.077

TABLE 7. Tracking speed at the switching frequency and irradiance are varied.

Membership Function	Switching Frequency											
	5 kHz				10 kHz				20 kHz			
	1000	800	600	400	1000	800	600	400	1000	800	600	400
	Irradiance											
	Second (s)											
Triangular	0.40	0.40	0.27	0.22	0.40	0.39	0.28	0.25	0.40	0.25	0.18	0.15
Trapezoidal	0.35	0.35	0.27	0.22	0.35	0.35	0.28	0.25	0.27	0.25	0.18	0.15
Gaussian	0.35	0.35	0.27	0.22	0.35	0.35	0.28	0.25	0.27	0.25	0.18	0.15
GBell	0.35	0.35	0.27	0.22	0.35	0.35	0.28	0.25	0.27	0.25	0.18	0.15

**TABLE 8.** Comparison between trapezoidal and GBell at switching frequency 20 kHz.

Membership Function	Switching Frequency 20 kHz											
	$P_{out}$			$V_{out}$			$I_{out}$			Oscillation		
	1000	800	600	1000	800	600	1000	800	600	1000	800	600
	Watt (W)			Volt (V)			Ampere (I)			Volt (V)		
Trapezoidal	229.50	166.00	105.70	191.60	163.00	130.10	1.1980	1.0190	0.8130	0.653	0.392	0.378
GBell	229.80	172.90	106.20	191.80	166.30	130.40	1.1980	1.0400	0.8149	0.392	0.231	0.188



**FIGURE 13.**  $I_{out}$  with a switching frequency of 10 kHz.

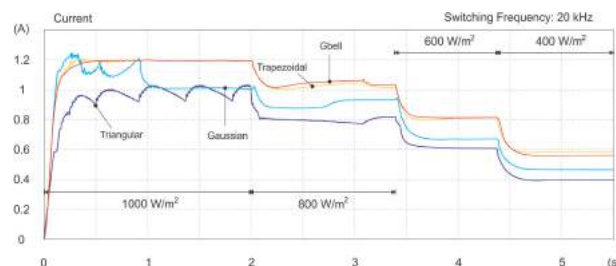


**FIGURE 16.**  $I_{out}$  with a switching frequency of 20 kHz.

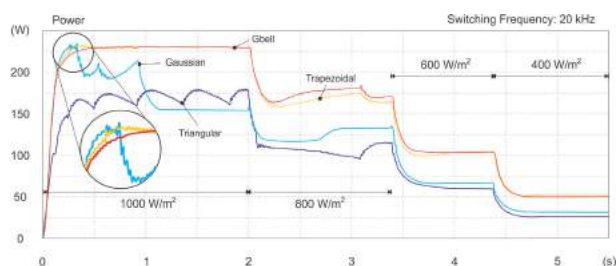


**FIGURE 14.**  $P_{out}$  with a switching frequency of 20 kHz.

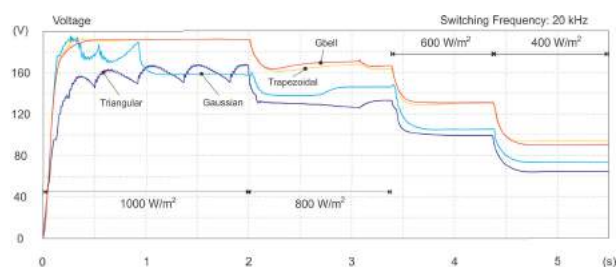


**FIGURE 15.**  $V_{out}$  with a switching frequency of 20 kHz.

Trapezoidal and GBell performance is slightly different in tests with a switching frequency of 10 kHz. Figures 11 to 13 show the slope  $P_{out}$ ,  $V_{out}$ , and  $I_{out}$  for testing with a switching frequency of 10 kHz, respectively. It is shown from the result obtained in Table 6, the Trapezoidal experiences periodic oscillations of 1.625% at 1000 W/m<sup>2</sup> irradiation at a steady-state condition. However, the output value, oscillation, and tracking speed are still superior to Gaussian and Triangular.

In the test with a switching frequency of 20 kHz, the performance of Trapezoidal and GBell are decreased. The oscillations of these two membership levels increase overall, at high and low irradiation. At low irradiation levels,  $V_{out}$ , hence  $P_{out}$ , are generated with a lower GBell than Trapezoidal. However, the resulting oscillations are still within an acceptable range.

The  $V_{out}$  and  $P_{out}$  produced by GBell are higher than Trapezoidal. The output of  $P_{out}$ ,  $V_{out}$ , and  $I_{out}$  with a switching frequency of 20 kHz are shown in Figures 14 to 16.

Based on the tests carried out by varying the irradiation and switching frequency, it is seen that GBell outperforms other fuzzy membership function types in terms of converter output optimization, oscillation, and tracking speed.

A head-to-head comparison of performance between Trapezoidal and GBell is shown in Table 8. The variables compared are  $P_{out}$ ,  $V_{out}$ ,  $I_{out}$ , and oscillation at 20 kHz switching frequency and irradiation variation between 1000 W/m<sup>2</sup> to 600W/m<sup>2</sup>. Based on the result, GBell outperforms the Trapezoidal in terms of performance.

The shape of the fuzzy membership function has an impact on the optimization results. However, the best shape of fuzzy membership function in one case may not necessarily show similar performance in other cases. Previous research evaluated fuzzy MF to control induction motor drive by Zhao and Bose [47]. The evaluation results show that Triangular provides superior performance than other membership function forms (Trapezoidal, Gaussian, Bell-shaped, Sigmoid, and Polynomial) in terms of reducing overshoot, undershoot, speed in response, recovery, and steady-state accuracy. The evaluation also shows that the Trapezoidal performance is close to the Triangular. The contrast result is shown in this study, where fuzzy membership function is evaluated for MPP tracking using a high gain voltage DC-DC converter. The GBell shape provides the most superior performance among other membership functions. Trapezoidal arrives as the second alternative.

**VII. CONCLUSION**

This paper discussed the different membership function effects, namely Triangular, Trapezoidal, Gaussian, and GBell which are utilized to construct fuzzy logic controller (FLC) for maximum power point tracking (MPPT) of solar photovoltaic (PV). The proposed high gain voltage

DC-DC converter is employed to the building system. Several parameters were observed by changing the switching frequency and irradiation variables. The results obtained indicate that the application of GBell and Trapezoidal outperform Triangular and Gaussian membership functions. Furthermore, these two membership function types (*i.e.* GBell and Trapezoidal) have comparable results during operation at 5 kHz or 10 kHz switching frequencies. In addition, GBell shows superior performance over Trapezoidal when the switching frequency is increased to 20 kHz.

## REFERENCES

- [1] S. Messalti, A. Harrag, and A. Loukriz, "A new variable step size neural networks MPPT controller: Review, simulation and hardware implementation," *Renew. Sustain. Energy Rev.*, vol. 68, pp. 221–233, Feb. 2017.
- [2] A. K. Podder, N. K. Roy, and H. R. Pota, "MPPT methods for solar PV systems: A critical review based on tracking nature," *IET Renew. Power Gener.*, vol. 13, no. 10, pp. 1615–1632, Jul. 2019.
- [3] T. Abderrahim, T. Abdelwahed, and M. Radouane, "Improved strategy of an MPPT based on the sliding mode control for a PV system," *Int. J. Electr. Comput. Eng.*, vol. 10, no. 3, p. 3074, Jun. 2020.
- [4] K. Sundareswaran, S. Peddapati, and S. Palani, "Application of random search method for maximum power point tracking in partially shaded photovoltaic systems," *IET Renew. Power Gener.*, vol. 8, no. 6, pp. 670–678, 2014.
- [5] N. Bizon, "Global maximum power point tracking (GMPPT) of photovoltaic array using the extremum seeking control (ESC): A review and a new GMPPT ESC scheme," *Renew. Sustain. Energy Rev.*, vol. 57, pp. 524–539, May 2016.
- [6] A. Kheldoun, R. Bradai, R. Boukenoui, and A. Mellit, "A new golden section method-based maximum power point tracking algorithm for photovoltaic systems," *Energy Convers. Manage.*, vol. 111, pp. 125–136, Mar. 2016.
- [7] E. Koutroulis, K. Kalaitzakis, and N. C. Voulgaris, "Development of a microcontroller-based, photovoltaic maximum power point tracking control system," *IEEE Trans. Power Electron.*, vol. 16, no. 1, pp. 46–54, Jan. 2001.
- [8] J. Appelbaum, "The operation of loads powered by separate sources or by a common source of solar cells," *IEEE Trans. Energy Convers.*, vol. 4, no. 3, pp. 351–357, Sep. 1989.
- [9] J. H. R. Enslin and D. B. Snyman, "Combined low-cost, high-efficient inverter, peak power tracker and regulator for PV applications," *IEEE Trans. Power Electron.*, vol. 6, no. 1, pp. 73–82, Jan. 1991.
- [10] J. H. R. Enslin, M. S. Wolf, D. B. Snyman, and W. Swiegers, "Integrated photovoltaic maximum power point tracking converter," *IEEE Trans. Ind. Electron.*, vol. 44, no. 6, pp. 769–773, Dec. 1997.
- [11] S. J. Chiang, K. T. Chang, and C. Y. Yen, "Residential photovoltaic energy storage system," *IEEE Trans. Ind. Electron.*, vol. 45, no. 3, pp. 385–394, Jun. 1998.
- [12] T.-F. Wu, C.-H. Chang, and Y.-J. Wu, "Single-stage converters for PV lighting systems with MPPT and energy backup," *IEEE Trans. Aerosp. Electron. Syst.*, vol. 35, no. 4, pp. 1306–1317, Oct. 1999.
- [13] N. Kasa, T. Lida, and H. Iwamoto, "Maximum power point tracking with capacitor identifier for photovoltaic power system," *IEE Proc., Electr. Power Appl.*, vol. 147, no. 6, pp. 497–502, Nov. 2000.
- [14] F. Giraud and Z. M. Salameh, "Analysis of the effects of a passing cloud on a grid-interactive photovoltaic system with battery storage using neural networks," *IEEE Trans. Energy Convers.*, vol. 14, no. 4, pp. 1572–1577, Dec. 1999.
- [15] Y.-C. Kuo, T.-J. Liang, and J.-F. Chen, "Novel maximum-power-point-tracking controller for photovoltaic energy conversion system," *IEEE Trans. Ind. Electron.*, vol. 48, no. 3, pp. 594–601, Jun. 2001.
- [16] M. Seyedmahmoudian, B. Horan, T. K. Soon, R. Rahmani, A. M. Than, S. Mekhilef, and A. Stojcevski, "State of the art artificial intelligence-based MPPT techniques for mitigating partial shading effects on PV systems—A review," *Renew. Sustain. Energy Rev.*, vol. 64, pp. 435–455, Oct. 2016.
- [17] A. Mohapatra, B. Nayak, P. Das, and K. B. Mohanty, "A review on MPPT techniques of PV system under partial shading condition," *Renew. Sustain. Energy Rev.*, vol. 80, pp. 854–867, Dec. 2017.
- [18] A. Jusoh, R. Alik, T. K. Guan, and T. Sutikno, "MPPT for PV system based on variable step size P&O algorithm," *Telkonnika*, vol. 15, no. 1, p. 79, 2017.
- [19] A. Jusoh, T. Sutikno, T. K. Guan, and S. Mekhilef, "A review on favourable maximum power point tracking systems in solar energy application," *Telkonnika*, vol. 12, no. 1, p. 6, Mar. 2014.
- [20] B. Yang, T. Zhu, J. Wang, H. Shu, T. Yu, X. Zhang, W. Yao, and L. Sun, "Comprehensive overview of maximum power point tracking algorithms of PV systems under partial shading condition," *J. Cleaner Prod.*, vol. 268, Sep. 2020, Art. no. 121983.
- [21] B. Subudhi and R. Pradhan, "A comparative study on maximum power point tracking techniques for photovoltaic power systems," *IEEE Trans. Sustain. Energy*, vol. 4, no. 1, pp. 89–98, Jan. 2013.
- [22] C. R. Algarín, J. T. Giraldo, and O. R. Álvarez, "Fuzzy logic based MPPT controller for a PV system," *Energies*, vol. 10, no. 12, p. 2036, Dec. 2017.
- [23] A. Youssef, M. E. Telbany, and A. Zekry, "Reconfigurable generic FPGA implementation of fuzzy logic controller for MPPT of PV systems," *Renew. Sustain. Energy Rev.*, vol. 82, pp. 1313–1319, Feb. 2018.
- [24] H. Rezk, M. Aly, M. Al-Dhaifallah, and M. Shoyama, "Design and hardware implementation of new adaptive fuzzy logic-based MPPT control method for photovoltaic applications," *IEEE Access*, vol. 7, pp. 106427–106438, 2019.
- [25] B. N. Alajmi, K. H. Ahmed, S. J. Finney, and B. W. Williams, "A maximum power point tracking technique for partially shaded photovoltaic systems in microgrids," *IEEE Trans. Ind. Electron.*, vol. 60, no. 4, pp. 1596–1606, Apr. 2013.
- [26] M. Rakhshan, N. Vafamand, M.-H. Khooban, and F. Blaabjerg, "Maximum power point tracking control of photovoltaic systems: A polynomial fuzzy model-based approach," *IEEE J. Emerg. Sel. Topics Power Electron.*, vol. 6, no. 1, pp. 292–299, Mar. 2018.
- [27] A. El Khateb, N. A. Rahim, J. Selvaraj, and M. N. Uddin, "Fuzzy-logic-controller-based SEPIC converter for maximum power point tracking," *IEEE Trans. Ind. Appl.*, vol. 50, no. 4, pp. 2349–2358, Jul./Aug. 2014.
- [28] S. Tang, Y. Sun, Y. Chen, Y. Zhao, Y. Yang, and W. Szeto, "An enhanced MPPT method combining fractional-order and fuzzy logic control," *IEEE J. Photovolt.*, vol. 7, no. 2, pp. 640–650, Mar. 2017.
- [29] U. Yilmaz, A. Kircay, and S. Borekci, "PV system fuzzy logic MPPT method and PI control as a charge controller," *Renew. Sustain. Energy Rev.*, vol. 81, pp. 994–1001, Jan. 2018.
- [30] Z. Sun and Z. Yang, "Improved maximum power point tracking algorithm with cuk converter for PV systems," *J. Eng.*, vol. 2017, no. 13, pp. 1676–1681, Jan. 2017.
- [31] B. Bendiba, F. Krim, H. Belmili, M. F. Almi, and S. Boulouma, "Advanced fuzzy MPPT controller for a stand-alone PV system," *Energy Proc.*, vol. 50, pp. 383–392, Jun. 2014.
- [32] H. Rezk and A. M. Eltamaly, "A comprehensive comparison of different MPPT techniques for photovoltaic systems," *Solar Energy*, vol. 112, pp. 1–11, Feb. 2015.
- [33] R. Boukenoui, H. Salhi, R. Bradai, and A. Mellit, "A new intelligent MPPT method for stand-alone photovoltaic systems operating under fast transient variations of shading patterns," *Sol. Energy*, vol. 124, pp. 124–142, Feb. 2016.
- [34] Y.-T. Chen, Y.-C. Jhang, and R.-H. Liang, "A fuzzy-logic based auto-scaling variable step-size MPPT method for PV systems," *Sol. Energy*, vol. 126, pp. 53–63, Mar. 2016.
- [35] A. H. E. Khateb, N. A. Rahim, and J. Selvaraj, "Fuzzy logic control approach of a maximum power point employing SEPIC converter for standalone photovoltaic system," *Proc. Environ. Sci.*, vol. 17, pp. 529–536, 2013.
- [36] M. Kermadi and E. M. Berkouk, "Artificial intelligence-based maximum power point tracking controllers for photovoltaic systems: Comparative study," *Renew. Sustain. Energy Rev.*, vol. 69, pp. 369–386, Mar. 2017.
- [37] M. B. Kalashani and M. Farsadi, "New structure for photovoltaic systems with maximum power point tracking ability," *Int. J. Power Electron. Drive Syst.*, vol. 4, no. 4, p. 489, Dec. 2014.
- [38] T. H. Kwan and X. Wu, "Maximum power point tracking using a variable antecedent fuzzy logic controller," *Sol. Energy*, vol. 137, pp. 189–200, Nov. 2016.
- [39] S. Hajjighorbani, M. A. M. Radzi, M. Z. A. A. Kadir, S. Shafie, R. Khanaki, and M. R. Maghami, "Evaluation of fuzzy logic subsets effects on maximum power point tracking for photovoltaic system," *Int. J. Photoenergy*, vol. 2014, Sep. 2014, Art. no. 719126.

- [40] O. A. M. Ali, A. Y. Ali, and B. S. Sumait, "Comparison between the effects of different types of membership functions on fuzzy logic controller performance," *Int. J.*, vol. 76, pp. 76–83, Mar. 2015.
- [41] C.-S. Chiu, "T-S fuzzy maximum power point tracking control of solar power generation systems," *IEEE Trans. Energy Convers.*, vol. 25, no. 4, pp. 1123–1132, Dec. 2010.
- [42] J. P. Ram, T. S. Babu, and N. Rajasekar, "A comprehensive review on solar PV maximum power point tracking techniques," *Renew. Sustain. Energy Rev.*, vol. 67, pp. 826–847, Jan. 2017.
- [43] E. Kandemir, N. S. Cetin, and S. Borekci, "A comprehensive overview of maximum power extraction methods for PV systems," *Renew. Sustain. Energy Rev.*, vol. 78, pp. 93–112, Oct. 2017.
- [44] W. I. Hameed, A. L. Saleh, B. A. Sawadi, Y. I. A. Al-Yasir, and R. A. Abd-Alhameed, "Maximum power point tracking for photovoltaic system by using fuzzy neural network," *Inventions*, vol. 4, no. 3, p. 33, Jun. 2019.
- [45] S. H. Hanzaei, S. A. Gorji, and M. Ektesabi, "A scheme-based review of MPPT techniques with respect to input variables including solar irradiance and PV arrays' temperature," *IEEE Access*, vol. 8, pp. 182229–182239, 2020.
- [46] P. A. Dahono, "New step-up DC-DC converters for PV power generation systems," in *Proc. Int. Seminar Intell. Technol. Appl. (ISITIA)*, Aug. 2017, pp. 187–192.
- [47] J. Zhao and B. K. Bose, "Evaluation of membership functions for fuzzy logic controlled induction motor drive," in *Proc. IEEE 28th Annu. Conf. Ind. Electron. Soc. (IECON)*, vol. 1. IEEE, 2002, pp. 229–234, doi: [10.1109/IECON.2002.1187512](https://doi.org/10.1109/IECON.2002.1187512).



**ARSYAD CAHYA SUBRATA** received the B.E. degree in electrical engineering from Universitas Ahmad Dahlan, Indonesia, in 2016, and the M.E. degree in electrical engineering from Universitas Diponegoro, Indonesia, in 2020. He is currently a Research Assistant at the Embedded Systems and Power Electronics Research Group (ESPERG), since 2018. His current research interests include artificial intelligent, digital control systems, renewable energy, and intelligent control systems.



**TOLE SUTIKNO** (Member, IEEE) received the B.E. degree from Universitas Diponegoro, in 1999, the M.E. degree from Universitas Gadjah Mada, in 2004, and the Ph.D. degree from Universiti Teknologi Malaysia, in 2016, all in electrical engineering. He has been an Associate Professor with Universitas Ahmad Dahlan (UAD), Yogyakarta, Indonesia, since 2008. He is currently a Lecturer with the Electrical Engineering Department, UAD. He has been the Editor-in-Chief of the *TELKOMNIKA*, since 2005, and the Leader of the Embedded Systems and Power Electronics Research Group, since 2016. His current research interests include digital design, industrial applications, industrial electronics, industrial informatics, power electronics, motor drives, renewable energy, FPGA applications, embedded systems, artificial intelligence, intelligent control, and information and digital technologies.



**AHMAD ELKHATEB** (Senior Member, IEEE) is currently a Lecturer of power electronics with the School of Electronics, Electrical Engineering and Computer Science, Queen's University, Belfast, U.K. His current research interests include power electronics, DC/DC converters, power generation, and grid integration. He is a fellow of Higher Education Academy, U.K.; a member of the ESPSRC Associate Review College; and an Associate Editor of *IEEE Access* and the *IET Power Electronics*.

...

See discussions, stats, and author profiles for this publication at: <https://www.researchgate.net/publication/353700379>

# Internet of things-based photovoltaics parameter monitoring system using NodeMCU ESP8266

Article in *International Journal of Electrical and Computer Engineering* · December 2021

DOI: 10.11591/ijece.v11i6.pp5578-5587

CITATIONS

0

READS

159

6 authors, including:



**Tole Sutikno**

Ahmad Dahlan University

351 PUBLICATIONS 2,043 CITATIONS

[SEE PROFILE](#)



**Hendril Satrian Purnama**

Ahmad Dahlan University

16 PUBLICATIONS 4 CITATIONS

[SEE PROFILE](#)



**Anggit Pamungkas**

Ahmad Dahlan University

2 PUBLICATIONS 3 CITATIONS

[SEE PROFILE](#)



**I.M. Alsofyani**

Ajou University

62 PUBLICATIONS 594 CITATIONS

[SEE PROFILE](#)

Some of the authors of this publication are also working on these related projects:



Publication [View project](#)



power electronics project [View project](#)

## Internet of things-based photovoltaics parameter monitoring system using NodeMCU ESP8266

Tole Sutikno<sup>1</sup>, Hendril Satrian Purnama<sup>2</sup>, Anggit Pamungkas<sup>3</sup>, Abdul Fadlil<sup>4</sup>,  
Ibrahim Mohd Alsofyani<sup>5</sup>, Mohd Hatta Jopri<sup>6</sup>

<sup>1,4</sup>Department of Electrical Engineering, Universitas Ahmad Dahlan, Yogyakarta, Indonesia

<sup>1,2,3</sup>Embedded Systems and Power Electronics Research Group, Yogyakarta, Indonesia

<sup>5</sup>Department of Electrical and Computer Engineering, Ajou University, Suwon, South Korea

<sup>6</sup>Faculty of Electrical and Electronic Engineering Technology, Universiti Teknikal Malaysia Melaka, Melaka, Malaysia

### Article Info

#### Article history:

Received May 8, 2021

Revised Jun 28, 2021

Accepted Jul 12, 2021

#### Keywords:

ESP8266

Internet of things

Online monitoring

Photovoltaic

ThingSpeak

### ABSTRACT

The use of the internet of things (IoT) in solar photovoltaic (PV) systems is a critical feature for remote monitoring, supervising, and performance evaluation. Furthermore, it improves the long-term viability, consistency, efficiency, and system maintenance of energy production. However, previous researchers' proposed PV monitoring systems are relatively complex and expensive. Furthermore, the existing systems do not have any backup data, which means that the acquired data could be lost if the network connection fails. This paper presents a simple and low-cost IoT-based PV parameter monitoring system, with additional backup data stored on a microSD card. A NodeMCU ESP8266 development board is chosen as the main controller because it is a system-on-chip (SOC) microcontroller with integrated Wi-Fi and low-power support, all in one chip to reduce the cost of the proposed system. The solar irradiance, ambient temperature, PV output voltage and PV output current, are measured with photo-diodes, DHT22, impedance dividers and ACS712. While, the PV output power is a product of the PV voltage and PV current. ThingSpeak, an open-source software, is used as a cloud database and data monitoring tool in the form of interactive graphics. The results showed that the system was designed to be highly accurate, reliable, simple to use, and low-cost.

This is an open access article under the [CC BY-SA](https://creativecommons.org/licenses/by-sa/4.0/) license.



### Corresponding Author:

Tole Sutikno

Department of Electrical Engineering, Faculty of Industrial Technology

Universitas Ahmad Dahlan (UAD)

4th UAD Campus, 6th Floor, South Ringroad St., Banguntapan, Bantul, Yogyakarta 55191, Indonesia

Email: tole@ee.uad.ac.id

## 1. INTRODUCTION

The demand for renewable energy sources is growing in tandem with global energy demand. This is due to the worsening environmental impact caused by the use of fossil fueled power plants, which cause a big air pollution and not environmentally friendly. On the other hand, there are several forms of renewable energy-based electricity generation, with technology that is constantly improving [1]-[11].

Solar energy has recently emerged as the most appealing renewable energy source for bridging the gap between consumption and production of electrical energy. This is due to the dramatic cost reductions and advancements in photovoltaic (PV) technology, which is still rapidly evolving [12]-[14]. In addition, solar energy is also the cleanest, environmentally friendly, and abundant type of energy compared to other energy

sources. Furthermore, the PV technology can be the most efficient source of energy with modern monitoring and control systems [5], [6], [15]-[23].

The data collected during the operation of a PV system is very interesting, not only for determining whether the design goals were met, but also for improving the PV system's design and operation, as well as a general assessment of the PV technology's potential [24]. Moreover, it is necessary to control the PV's parameters in order to optimize it. A PV monitoring system's goal is to provide accurate data on a variety of parameters, including energy potential, energy extracted, fault identification, historical generation analysis, and associated energy losses [14], [25]. The literature has detailed descriptions of the classification of PV monitoring systems based on internet technologies, the data acquisition system used, and the monitoring system methods [16], [26]-[29].

The internet of things (IoT) technology is able to monitor and control many smart devices remotely. Many IoT based online and remote monitoring systems has been developed by researcher [30]-[38] such as: i) object monitoring [31], [39]; ii) parking space monitoring and management [32]; iii) environmental monitoring [33], [36]; 4) electricity power consumption monitoring [35]; and 5) Body health monitoring [30], [37]. Most of the developed device is using NodeMCU ESP8266 for the main processor and Wi-Fi provider because of the low-cost and low-power consumption module [31], [39]-[42].

In the area of renewable energy generations, especially on PV power generation systems, much research's that has been done to design and develop PV parameter monitoring systems, both offline and online are available in the literature [14], [43]-[51]. Due to the sensitivity of PV panels to environmental factors, data such as solar radiation, ambient temperature, weather, and electrical data are used to assess the condition of the PV station. This is why it's crucial to keep track the performance of a PV system at all times [52], [53].

Presently, the PV parameter monitoring system that has been developed by many researchers is still relatively complex and requires high production costs for small-to-medium scale PV applications, this is due to the use of a pyranometer sensor (as a measure of solar irradiance), the use of an expensive controller and also use of high paid monitoring software such as LABVIEW [54]. Besides this, the existing system also does not provide an offline data backup/storage feature, if the system's network fails, this may result in data loss [55].

In this paper, an IoT based PV parameter monitoring system is designed with low production costs for small-scale PV-based power generation applications (in this case for energy independent home applications). To achieve this goal, many costly components such as sensors and controllers are replaced with sensors and controllers that perform the same role but cost less and are readily available. Furthermore, instead of using special software that needs high service costs, such as LABVIEW, the monitoring software used was open-source and free IoT software. In addition, to prepare for any network failures, a MicroSD card-based offline data backup system is introduced.

## 2. RESEARCH SYSTEM DESIGN

IoT technology is used in the proposed system to track parameter data from PV via internet connection, including both environmental data (metrology) and electrical data (I and V). The microcontroller is used in an IoT-based PV monitoring system to capture, process, store, and analyse data from sensors based on the calculated parameters in the system. The microcontroller will send the data to the cloud server through a WiFi gateway after it has been processed.

### 2.1. The proposed IoT PV monitoring system

Figure 1 depicts a block diagram of the entire proposed system, which includes PV data in the form of environmental parameters collected from temperature and light sensors (to estimate the solar irradiance). The electrical parameters of PV, such as current and voltage, are obtained from the appropriate sensors. With the IoT protocol, the microcontroller collects, processes, data from sensors. Then the data transmit and store into offline data backup systems and cloud servers, respectively. The web-based and open-source software serves as a cloud database and visual data viewer can be accessed via Smartphone or personal computer (PC) via a web server.

### 2.2. Internet of things for PV monitoring system

The IoT allows smart microgrids to exchange information with more users and improves communication through a variety of infrastructures [3]. IoT plays a significant role in human everyday life by allowing the integration of many physical devices via the internet, where devices are intelligently linked, enabling new forms of communication between devices and humans, as well as between devices and the system itself, to share data, track, and manage devices from anywhere in the world using only an internet connection [54].

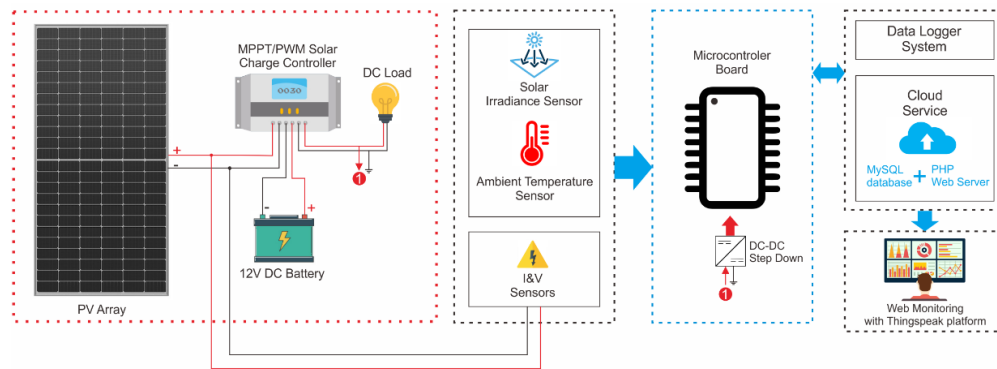


Figure 1. Block diagram of a proposed IoT-based PV monitoring system

IoT technology is used in the field of renewable energy, especially solar PV systems, to track important parameters affecting PV system output in real-time and online. The sensor and transducer provide these parameters, which are then sent to the microcontroller for analysis. Furthermore, PV plants and other power generation systems can be tracked using an IoT-based monitoring system to enhance analysis, quality, and system maintenance.

### 2.3. Display unit and cloud storage system

Continuous data acquisition necessitates graphic or visual data display capabilities, which can be accessed remotely and in real-time via a smartphone or PC. The application programming interface (API) that used for the display unit of the proposed system is an open-source IoT platform namely ThingSpeak. ThingSpeak enables the development of sensor logging applications, location tracking applications, and social networking things with customizable status updates. It allows users to collect, store, analyze, visualize and make decisions based on data that obtained from sensors.

## 3. EXPERIMENTAL SETUP

In this research, various sensors are used to measure various parameters of the PV system, such as solar irradiance (light intensity), ambient temperature, PV output current, PV output voltage, and PV output power. The acquired data from the sensor is transferred wirelessly to the cloud server using IoT protocol, then the data is displayed visually using ThingSpeak platform. The goal of the proposed system in this paper is to develop a simple, low-cost, and high-performance IoT solution for monitoring the electric and environmental data of PV solar farms, especially small-scale PV farms (on and off grid condition). It is essential to select sensor and controller hardware that is both low-cost and capable of providing highly accurate data acquisitions. The following are the low-cost sensors that can be used to quantify both environmental variation and electrical data:

- DHT22 is used to measure the temperature and humidity data.
- Photodiode sensor is used to measure the solar radiation intensity.
- ACS712 is used to measure the current produced by PV.
- Impedance divider sensor module is used to measure the voltage produced by PV.

Instead of DHT11, DHT22 is used to assess room temperature and humidity because it provides more precise data acquisition. Pyranometer sensor is replaced by a photodiode sensor due to measure the light intensity transmitted to the PV screen, resulting in lower device costs. The current sensor ACS712 and impedance divider are used to measure the generated power by PV.

The ESP8266 controller is chosen as the main processor of data acquisition systems because of its low-cost, low-power consumption and high-performance computational controller. In addition, the ESP8266 controller has many useful features, such as a built-in WiFi module, has a many general-purpose input/output (GPIO) ports, and a simple programming method. The open-source IoT platform ThingSpeak is used as a database and to visualise the acquired data with an interactive graph and dashboard in order to keep the system low-cost and easy to access and create. Besides, using non-open-source software such as LABVIEW cost would rise the cost due to costly software service payments. Furthermore, an offline backup data system comprised of RTC and MicroSD modules has been introduced to expand the database systems and serve as internal data storage systems that can be accessed when online data is unavailable.



**3.1. Hardware design**

Figure 2 shows the wiring diagram for the proposed system's main board. The key components of the device are the NodeMCU ESP8266, various sensors, the ADC module, the RTC, and the SD card module. Table 1 shows the complete data and usability of each device.

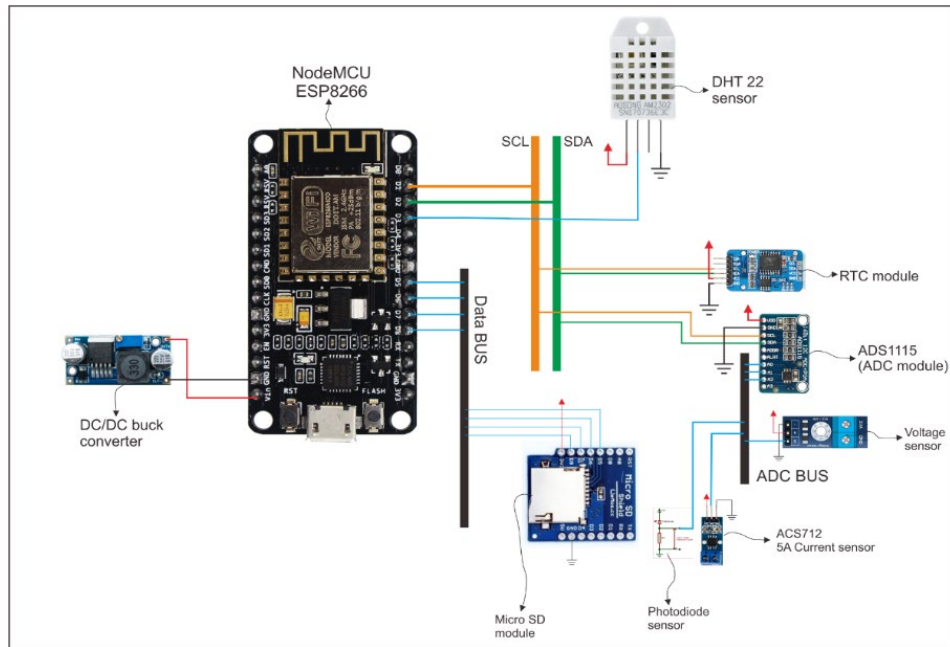


Figure 2. Schematic diagram of proposed system

Table 1. Research components

Component name	Function/usability
NodeMCU V3 ESP8266	Main controller
MicroSD Shield	Data logger storage
RTC module shield	Data logger time reference
INA219 Sensor	Voltage sensor
ACS712 5A Current Sensor	Current sensor
ADS1115	ADC 16bit reader
DHT22	Temperature sensor
Photodiode sensor	Solar irradiance level sensor
Solar Panel 50Wp	Power generator
PWM Solar Charge Controller	Charging controller
12V battery	Energy backup system
Inverter	System load

**3.1.1. Photovoltaic system**

In the proposed design system, the PV system consist of 50Wp monocrystalline PV panel, 10 A PWM solar charge controller, 12 V 7.2 Ah battery for energy backup, and 30W constant load.

**3.1.2. Sensing unit**

a) Current sensor

An ACS712 current sensor with a maximum operating range of 5 A was used in this study. Since this sensor can detect both AC and DC currents in a circuit, it can be used in a variety of applications. An Arduino, ESP8266, or another kind of microcontroller can be used to access this sensor. In principle, this sensor works with indirect sensing. The current flows through the onboard hall sensor circuit in its IC. The hall-effect sensor detects incoming current by generating a magnetic field. The hall effect sensor detects the magnetic field and produces a voltage proportional to it, which is then used to calculate the current.

b) Voltage sensor

The proposed system's voltage sensor is a voltage divider sensor that is used to read the value of the output voltage provided by the PV when the system is in service.

c) Temperature sensor

The DHT22 sensor is used in the PV monitoring system to measure temperature and humidity at the same time. It is a negative temperature coefficient (NTC) type thermistor that measures temperature and a humidity sensor that is resistant to changes in water content in the air, as well as a chip that performs some analogue to digital conversion (two-way single cable).

d) Irradiance sensor

The photodiode sensor was chosen as an irradiance sensor to replace the pyranometer sensor, which is rated as extremely costly, thereby raising the overall device cost. To obtain an accurate value, the photodiode sensor must be calibrated using an accurate solar irradiance sensor, such as a pyranometer.

### 3.1.3. NodeMCU ESP8266 based controller

NodeMCU is an open-source firmware and development kit that assists in the development of IoT-based application systems. NodeMCU was created to make it easier to use a sophisticated application programming interface (API) for IO hardware. APIs can help to reduce the amount of time spent configuring and manipulating hardware devices. The NodeMCU has the advantage of being programmable in a variety of programming languages and with an open-source IDE. The code for this study will be uploaded directly to the nodeMCU board using the Arduino IDE. Meanwhile, the ESP8266 is used as the WiFi integrated chip, and it is very small in size.

## 3.2. Software design

### 3.2.1. Thingspeak

ThingSpeak is an open-source internet of things (IoT) platform and API for storing and retrieving data from things that use HTTP over the Internet or a local area network (LAN). The internet of things (IoT) gives users access to a wide range of embedded devices and web services. Moreover, it is capable of collecting, storing, analyzing, visualizing, and acting on data from sensors or actuators such as Arduino, NodeMCU, Raspberry Pi, BeagleBone, and other hardware. ThingSpeak, for example, allows sensor logging and location tracking applications.

Additionally, it is a data collector that gathers data from nodeMCU devices and then loads it into the software environment for historical data analysis. A channel, which contains a data field, a position field, and a status field, is the most important part of the ThingSpeak operation. ThingSpeak features includes: (i) open API, (ii) real-time data collection, (iii) geolocation data, (iv) data processing, (v) data visualizations, (vi) device status messages, and (vii) plugins are the key features of ThingSpeak.

### 3.2.2. Monitoring algorithm

Figure 3 shows a flowchart of an IoT-based PV device monitoring algorithm. The proposed monitoring system start with the library definitions, variable parameters, and board setup. Then the system will check the availability of WiFi connectivity. If the connection is accessible, the controller will start to open and read the SD card folder file. Furthermore, if the system successfully reads the SD card folder file, the operation will proceed to read all of the system's sensors before reading the time reference from the RTC module. As a final point, the collected data will be written and stored into the SD card module. In addition, using the built-in WiFi gateway on the NodeMCU, the collected data will be sent to a cloud server. Until the device is deactivated, all procedures will be replicated.

## 4. RESULTS AND DISCUSSION

Figure 4 depicts an experimental system in which the PV is used as a power generator and the laptop is used to view graphic data obtained via the ThingSpeak platform. The electrical measurement device is used to verify the accuracy of the electric sensor, the breadboard is used to attach the sensor to the mainboard, the box contains the mainboard and the PWM solar charge controller, and the 12 V battery serves as an energy backup system.

Figure 5 shows the graphical data obtained from the ThingSpeak platform. Moreover, Figures 5(a) to (e) depict the PV parameter measurements, which include solar irradiation level, ambient temperature, PV output voltage and current, as well as the PV output power. The monitoring device's channel placement is shown in Figure 5(f). The linear relationship between solar irradiation, PV output current, and PV output power values indicates that the sensor readings and data collecting system are working appropriately. In around 30 seconds, the sensor collects, analyses, transmits, and stores the data into cloud server. Meanwhile, Table 2 tabulates the costs comparison of several key controllers used in the IoT-based PV monitoring system. This is to show that the proposed system's development costs are the lowest compare to others.

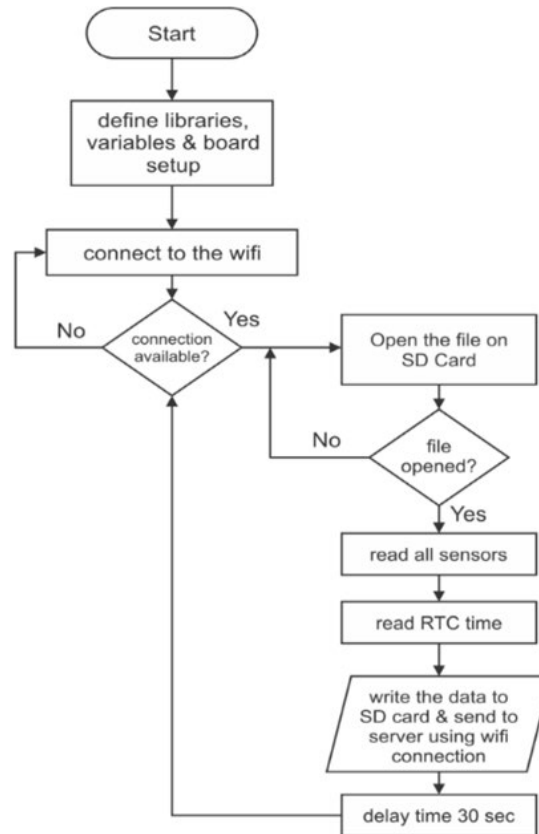


Figure 3. Flowchart of the proposed system

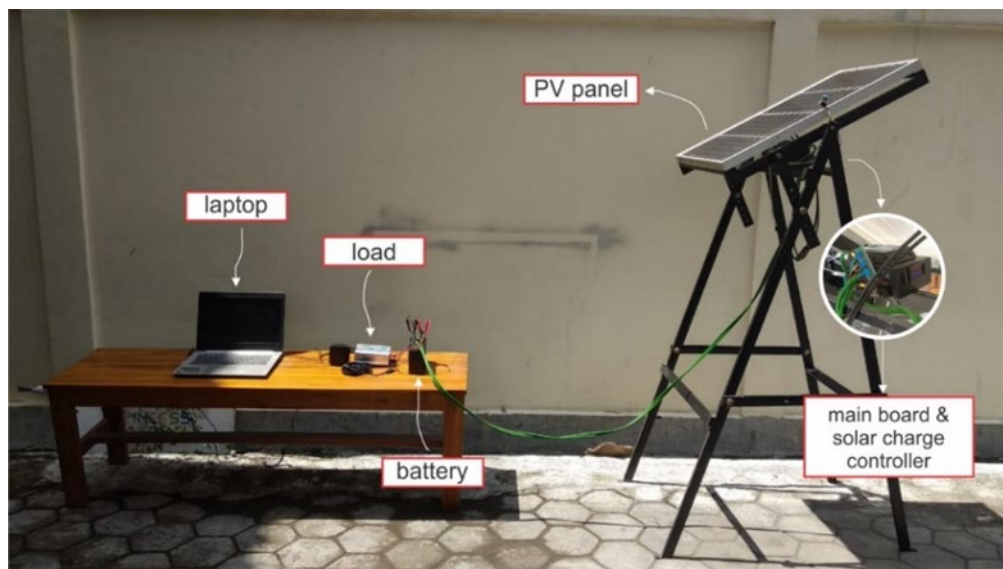


Figure 4. Experimental setup of the proposed system

In comparison to the other controllers, the Raspberry Pi [10] and BeagleBone Black [9] have the most efficient computational efficiency, but they are also the most costly and complex to programme. The cheapest controller is the PIC 16F877 [20], but it has the lowest computational efficiency and requires an external WiFi module to connect to the internet. Due to their easy programming and relatively high performance for many applications, the Arduino MEGA2560 and Arduino UNO R3 [4], [19] have become popular controllers.



Figure 5. Captured visual data from ThingSpeak platform; (a) ambient temperature; (b) PV voltage out; (c) PV current out; (d) PV power out; (e) solar irradiance level; (f) channel location

Table 2. Comparison of the controller for IOT monitoring systems

Paper	Main Controller	Characteristic of the Controller	Cost (\$)*	Built-in WiFi?
[45]	BeagleBone black	Very High computation Need external ADC	73,98	No
[16]	Arduino Mega2560	High power consumption Low computation Integrated ADCs	34,00	No
[55]	Arduino UNO R3	Low power consumption Low computation Integrated ADCs	22,00	No
[56]	PIC 16F877	Low power consumption Low computation Integrate ADCs	5,50	No
[46]	Raspberry Pi 3	Low power consumption High computation Need external ADC	42,99	Yes
[54]	ESP32	High power consumption Average level computation Integrated ADCs	10,99	Yes
Proposed	ESP8266	Low power consumption Average level computation Integrated ADCs Low power consumption	6,49	Yes

\*Estimated cost of the main controller (amazon.com)

However, they still have a low computational level as compared to other controllers on the market, and they need an additional WiFi module for IoT applications. The ESP board series [18] was chosen for this proposed system due to its low cost and ability to perform reasonably high-level computation. In addition, the ESP board series has a built-in WiFi module and consumes very little electricity.

## 5. CONCLUSION

An IoT-based PV parameter monitoring system was introduced in this paper. The parameters such as solar irradiance, ambient temperature, PV output voltage, PV output current, and PV output power are all measured by the system. Moreover, solar irradiance, ambient temperature, PV output voltage, and PV output current are measured using photodiode, DHT22, impedance divider, and ACS712, respectively. Besides, PV output power is obtained from the product of PV voltage and PV current. The main controller of the system is the NodeMCU V3 ESP8266, which also has the ability to create a WiFi enabled gateway. As a result, the calculated parameters can be transferred wirelessly from the sensor to the cloud without the need for an external WiFi module. Finally, the acquired parameters are tracked on the Cloud server using ThingSpeak.

The selected components for the proposed system are low-cost and readily available on the market. The reliability of each components also a factor to consider. Finally, laboratory experiments are used to verify the proposed system. The outcome clearly show that the proposed system offers accurate result in monitoring the PV parameters. It is important to test the proposed system under a variety of environmental conditions over a prolonged period of time for future work.

## ACKNOWLEDGEMENTS

We would like to thank Universitas Ahmad Dahlan (UAD) for funding this research under Leading Research Scheme (PUPS), contract No: PUPS-015/SP3/LPPM-UAD/2020; and Embedded System and Power Electronics Research Group (ESPERG) for providing the excellent support and cooperation to produce the work described in this paper.

## REFERENCES

- [1] B. I. Yassine and A. Boumediene, "Renewable energies evaluation and linking to smart grid," *International Journal of Power Electronics and Drive Systems (IJPEDS)*, vol. 11, no. 1. pp. 107-118, 2020, doi: 10.11591/ijpeds.v11.i1.pp107-118.
- [2] C. U. Cassiani Ortiz, J. E. Candelo-Becerra, and F. E. Hoyos Velasco, "Electricity market strategies applied to microgrid development," *International Journal of Power Electronics and Drive Systems (IJPEDS)*, vol. 11, no. 1. pp. 530-546, 2020, doi: 10.11591/ijpeds.v11.i1.pp530-546.
- [3] Y. M. Esmail, A. H. Kasem Alaboudy, M. S. Hassan, and G. M. Dousoky, "Mitigating power quality disturbances in smart grid using FACTS," *Indonesian Journal of Electrical Engineering and Computer Science (IJECS)*, vol. 22, no. 3. pp. 1223-1235, 2021, doi: 10.11591/ijeecs.v22.i3.pp1223-1235.
- [4] N. Pati, B. Panda, and B. Panda, "Stability analysis of photovoltaic system under grid faults," *International Journal of Power Electronics and Drive Systems (IJPEDS)*, vol. 11, no. 2. pp. 931-941, 2020, doi: 10.11591/ijpeds.v11.i2.pp931-941.
- [5] M. Q. Taha, "Advantages and recent advances of smart energy grid," *Bulletin of Electrical Engineering and Informatics (BEEI)*, vol. 9, no. 5. pp. 1739-1746, 2020, doi: 10.11591/eei.v9i5.2358.
- [6] B. Rajapandian and G. T. Sundarrajan, "Evaluation of dc-dc converter using renewable energy sources," *International Journal of Power Electronics and Drive Systems (IJPEDS)*, vol. 11, no. 4. pp. 1918-1925, 2020, doi: 10.11591/ijpeds.v11.i4.pp1918-1925.
- [7] M. A. A. Sufyan, M. Zuhair, and M. Rihan, "An investigation on the application and challenges for wide area monitoring and control in smart grid," *Bulletin of Electrical Engineering and Informatics (BEEI)*, vol. 10, no. 2, pp. 580-587, 2021, doi: 10.11591/eei.v10i2.2767.
- [8] P. Sharma, S. R. Salkuti, and S.-C. Kim, "Energy audit: Types, scope, methodology and report structure," *Indonesian Journal of Electrical Engineering and Computer Science (IJECS)*, vol. 22, no. 1. pp. 45-52, 2021, doi: 10.11591/ijeecs.v21.i4.pp45-52.
- [9] A. Lekbich, A. Belfqih, C. Zedak, J. Boukherouaa, and F. Elmariami, "Implementation of a decentralized real-time management system for electrical distribution networks using the internet of things in smart grids," *Bulletin of Electrical Engineering and Informatics (BEEI)*, vol. 10, no. 3, pp. 1142-1153, 2021, doi: 10.11591/eei.v10i3.2436.
- [10] P. K. Panda, A. Sahoo, A. Samal, D. P. Mishra, and S. R. Salkuti, "Voltage control of ac hybrid microgrid," *International Journal of Power Electronics and Drive Systems (IJPEDS)*, vol. 12, no. 2. pp. 793-802, 2021, doi: 10.11591/ijpeds.v12.i2.pp793-802.
- [11] H. Azoug, H. Belmili, and F. Bouazza, "Grid-connected control of pv-wind hybrid energy system," *International Journal of Power Electronics and Drive Systems (IJPEDS)*, vol. 12, no. 2. pp. 1228-1238, 2021, doi: 10.11591/ijpeds.v12.i2.pp1228-1238.

- [12] M. Datta, T. Senjyu, A. Yona, and T. Funabashi, "Photovoltaic output power fluctuations smoothing by selecting optimal capacity of battery for a photovoltaic-diesel hybrid system," *Electric Power Components and Systems*, vol. 39, no. 7, pp. 621–644, 2011, doi: 10.1080/15325008.2010.536809.
- [13] T. Rout, A. Chowdhury, M. K. Maharana, and S. Samal, "Analysis of energy management system for photovoltaic system with battery and supercapacitor using fuzzy logic controller," 2018 Technologies for Smart-City Energy Security and Power (ICSESP), no. 2, 2018, pp. 1-4, doi: 10.1109/ICSESP.2018.8376737.
- [14] S. R. Madeti and S. N. Singh, "Monitoring system for photovoltaic plants: A review," *Renewable and Sustainable Energy Reviews*, vol. 67, pp. 1180-1207, 2017, doi: 10.1016/j.rser.2016.09.088.
- [15] M. M. Abdullahi et al., "A review of building integrated photovoltaic: Case study of tropical climatic regions," *International Journal of Power Electronics and Drive Systems (IJPEDS)*, vol. 12, no. 1, pp. 474-488, 2021, doi: 10.11591/ijped.v12.i1.pp474-488.
- [16] M. M. Rahman, J. Selvaraj, N. A. Rahim, and M. Hasanuzzaman, "Global modern monitoring systems for PV based power generation: A review," *Renewable and Sustainable Energy Reviews*, vol. 82, Part 3, pp. 4142-4158, 2018, doi: 10.1016/j.rser.2017.10.111.
- [17] E. H. Chahid, M. I. Oumhand, M. Feddaoui, M. Erritali, and A. Malaoui, "Effect of measurement factors on photovoltaic cell parameters extracting," *International Journal of Electrical and Computer Engineering (IJECE)*, vol. 7, no. 1, pp. 50-57, 2017, doi: 10.11591/ijece.v7i1.pp50-57.
- [18] A. Halim, A. Fudholi, S. Phillips, and K. Sopian, "Review on optimised configuration of hybrid solar-PV diesel system for off-grid rural electrification," *International Journal of Power Electronics and Drive Systems (IJPEDS)*, vol. 9, no. 3, pp. 1374-1380, 2018, doi: 10.11591/ijped.v9n3.pp1374-1380.
- [19] O. A. Ahmad, H. Sayed, K. A. Jalal, D. Y. Mahmood, and W. H. Habeeb, "Design and implementation of an indoor solar emulator based low-cost autonomous data logger for PV system monitoring," *International Journal of Power Electronics and Drive Systems (IJPEDS)*, vol. 10, no. 3, pp. 1645-1654, 2019, doi: 10.11591/ijped.v10.i3.1645-1654.
- [20] A. A. Sneineh and W. A. Salah, "Design and implementation of an automatically aligned solar tracking system," *International Journal of Power Electronics and Drive Systems (IJPEDS)*, vol. 10, no. 4, pp. 2055-2064, 2019, doi: 10.11591/ijped.v10.i4.2055-2064.
- [21] A. Amir, A. Amir, H. S. Che, A. Elkhateb, and N. A. Rahim, "Comparative analysis of high voltage gain DC-DC converter topologies for photovoltaic systems," *Renewable Energy*, vol. 136, pp. 1147-1163, 2019, doi: 10.1016/j.renene.2018.09.089.
- [22] S. Gorai, D. Sattianadan, V. Shanmugasundaram, S. Vidyasagar, G. R. Prudhvi Kumar, and M. Sudhakaran, "Investigation of voltage regulation in grid connected PV system," *Indonesian Journal of Electrical Engineering and Computer Science (IJECS)*, vol. 19, no. 3, pp. 1131-1139, 2020, doi: 10.11591/ijeecs.v19.i3.pp1131-1139.
- [23] K. L. Shenoy, C. G. Nayak, and R. P. Mandi, "Effect of partial shading in grid connected solar pv system with fl controller," *International Journal of Power Electronics and Drive Systems (IJPEDS)*, vol. 12, no. 1, pp. 431-440, 2021, doi: 10.11591/ijped.v12.i1.pp431-440.
- [24] M. Torres, F. J. Muoz, J. V. Muoz, and C. Rus, "Online monitoring system for stand-alone photovoltaic applications-analysis of system performance from monitored data," *Journal of Solar Energy Engineering*, vol. 134, no. 3, pp. 1-8, 2012, doi: 10.1115/1.4005448.
- [25] S. Adhya, J. Das, A. Jana, and H. Saha, "An IoT Based Smart Solar Photovoltaic Remote Monitoring and Control unit," 2016 2nd International Conference on Control, Instrumentation, Energy & Communication (CIEC), 2016, pp. 432-436, doi: 10.1109/CIEC.2016.7513793.
- [26] B. Khadidja, B. S. Amine, and B. Noureddine, "Control and supervision of a solar electric system," *International Journal of Power Electronics and Drive Systems (IJPEDS)*, vol. 10, no. 4, pp. 2096-2100, 2019, doi: 10.11591/ijped.v10.i4.2096-2100.
- [27] M. Z. M. Nasir, S. Salimin, B. Chan, and S. A. Jumaat, "Prototype development of smart parking system powered by solar photovoltaic," *Indonesian Journal of Electrical Engineering and Computer Science (IJECS)*, vol. 18, no. 3, pp. 1229-1235, 2020, doi: 10.11591/ijeecs.v18.i3.pp1229-1235.
- [28] S. Z. Islam, M. L. Othman, N. Mariun, H. Hizam, and N. Ayuni, "Feasibility analysis of standalone pv powered battery using SEN for smart grid," *International Journal of Power Electronics and Drive Systems (IJPEDS)*, vol. 11, no. 2, pp. 667-676, 2020, doi: 10.11591/ijped.v11.i2.pp667-676.
- [29] R. N. Hasanah, A. B. Setyawan, E. Maulana, T. Nurwati, and Taufik, "Computer-based solar tracking system for PV energy yield improvement," *International Journal of Power Electronics and Drive Systems (IJPEDS)*, vol. 11, no. 2, pp. 743-751, 2020, doi: 10.11591/ijped.v11.i2.pp743-751.
- [30] M. W. Hasan, "Covid-19 fever symptom detection based on IoT cloud," *International Journal of Electrical and Computer Engineering (IJECE)*, vol. 11, no. 2, pp. 1823-1829, 2021, doi: 10.11591/ijece.v11i2.pp1823-1829.
- [31] H. Ouldzira, A. Mouhsen, H. Lagraini, M. Chhiba, A. Tabyaoui, and S. Amrane, "Remote monitoring of an object using a wireless sensor network based on NODEMCU ESP8266," *Indonesian Journal of Electrical Engineering and Computer Science (IJECS)*, vol. 16, no. 3, pp. 1154-1162, 2019, doi: 10.11591/ijeecs.v16.i3.pp1154-1162.
- [32] Z. Dzulkurnain, A. K. Mahamad, S. Saon, M. A. Ahmadon, and S. Yamaguchi, "Internet of things (IoT) based traffic management & routing solution for parking space," *Indonesian Journal of Electrical Engineering and Computer Science (IJECS)*, vol. 15, no. 1, pp. 336-345, 2019, doi: 10.11591/ijeecs.v15.i1.pp336-345.
- [33] A. A. Jaber, F. K. I. Al-Mousawi, and H. S. Jasem, "Internet of things based industrial environment monitoring and control: A design approach," *International Journal of Electrical and Computer Engineering (IJECE)*, vol. 9, no. 6, pp. 4657-4667, 2019, doi: 10.11591/ijece.v9i6.pp4657-4667.

- [34] A. H. Ali, A. H. Duhis, N. A. Lafta Alzurfi, and M. J. Mnati, "Smart monitoring system for pressure regulator based on IOT," *International Journal of Electrical and Computer Engineering (IJECE)*, vol. 9, no. 5, pp. 3450-3456, 2019, doi: 10.11591/ijece.v9i5.pp3450-3456.
- [35] K. Luechaphonthara and A. Vijayalakshmi, "IOT based application for monitoring electricity power consumption in home appliances," *International Journal of Electrical and Computer Engineering (IJECE)*, vol. 9, no. 6, pp. 4988-4992, 2019, doi: 10.11591/ijece.v9i6.pp4988-4992.
- [36] M. S. A. Mahmud, S. Buyamin, M. M. Mokji, and M. S. Z. Abidin, "Internet of things based smart environmental monitoring for mushroom cultivation," *Indonesian Journal of Electrical Engineering and Computer Science (IJECS)*, vol. 10, no. 3, pp. 847-852, 2018, doi: 10.11591/ijeecs.v10.i3.pp847-852.
- [37] M. Niswar, M. Nur, A. A. Ilham, and I. Mappangara, "A low cost wearable medical device for vital signs monitoring in low-resource settings," *International Journal of Electrical and Computer Engineering (IJECE)*, vol. 9, no. 4, pp. 2321-2327, 2019, doi: 10.11591/ijece.v9i4.pp2321-2327.
- [38] H. S. Kim, J. S. Seo, and J. Seo, "A daily activity monitoring system for internet of things-assisted living in home area networks," *International Journal of Electrical and Computer Engineering (IJECE)*, vol. 6, no. 1, pp. 399-405, 2016, doi: 10.11591/ijece.v6i1.9339.
- [39] P. Veerakumar, "Energy monitoring system to display on web page using ESP8266," *Indonesian Journal of Electrical Engineering and Computer Science (IJECS)*, vol. 9, no. 2, pp. 286-288, 2018, doi: 10.11591/ijeecs.v9.i2.pp286-288.
- [40] R. S. Rosli, M. H. Habaebi, and P. R. Islam, "On the analysis of received signal strength indicator from ESP8266," *Bulletin of Electrical Engineering and Informatics (BEEI)*, vol. 8, no. 3, pp. 933-940, 2019, doi: 10.11591/eei.v8i3.1511.
- [41] M. A. A. Aziz, M. F. Abas, M. K. A. Abu Bashri, N. M. Saad, and M. H. Ariff, "Evaluating IoT based passive water catchment monitoring system data acquisition and analysis," *Bulletin of Electrical Engineering and Informatics (BEEI)*, vol. 8, no. 4, pp. 1373-1382, 2019, doi: 10.11591/eei.v8i4.1583.
- [42] A. M. A. Jalil, R. Mohamad, N. M. Anas, M. Kassim, and S. I. Suliman, "Implementation of vehicle ventilation system using nodemcu ESP8266 for remote monitoring," *Bulletin of Electrical Engineering and Informatics (BEEI)*, vol. 10, no. 1, pp. 327-336, 2020, doi: 10.11591/eei.v10i1.2669.
- [43] A. S. Spanias, "Solar energy management as an Internet of Things (IoT) application," *2017 8th International Conference on Information, Intelligence, Systems & Applications (IISA)*, 2018, pp. 1-4, doi: 10.1109/IISA.2017.8316460.
- [44] M. Benganem and A. Maafi, "Data acquisition system for photovoltaic systems performance monitoring," *IEEE Transactions on Instrumentation and Measurement*, vol. 47, no. 1, pp. 30-33, 1998, doi: 10.1109/19.728784.
- [45] G. C. Ngo, J. K. I. Floriza, C. M. C. Creayla, F. C. C. Garcia, and E. Q. B. MacAbebe, "Real-time energy monitoring system for grid-tied Photovoltaic installations," *TENCON 2015 - 2015 IEEE Region 10 Conference*, 2016, pp. 1-4, doi: 10.1109/TENCON.2015.7372784.
- [46] R. I. S. Pereira, I. M. Dupont, P. C. M. Carvalho, and S. C. S. Jucá, "IoT embedded linux system based on Raspberry Pi applied to real-time cloud monitoring of a decentralized photovoltaic plant," *Measurement*, vol. 114, pp. 286-297, 2018, doi: 10.1016/j.measurement.2017.09.033.
- [47] Y. F. Li et al., "On-line monitoring system of PV array based on internet of things technology," *IOP Conference Series Earth and Environmental Science*, vol. 93, no. 1, 2017, Art. no. 012078, doi: 10.1088/1755-1315/93/1/012078.
- [48] U. Jan A. woyte M. R. D. M. S. M. Nils Reich, "Monitoring of photovoltaic System: Good practices and System Analysis," *Вестник Казнму*, vol. №3, p. 30, 2013.
- [49] H. Rezk, I. Tyukhov, M. Al-Dhaifallah, and A. Tikhonov, "Performance of data acquisition system for monitoring PV system parameters," *Measurement*, vol. 104, pp. 204-211, 2017, doi: 10.1016/j.measurement.2017.02.050.
- [50] B. Ando, S. Baglio, A. Pistorio, G. M. Tina, and C. Ventura, "Sentinella: Smart Monitoring of Photovoltaic Systems at Panel Level," *IEEE Transactions on Instrumentation and Measurement*, vol. 64, no. 8, pp. 2188-2199, 2015, doi: 10.1109/TIM.2014.2386931.
- [51] J. C. Franklin, M. Chandrasekar, and D. A. Mattius, "Development of Cost Effective Data Acquisition System to Evaluate the Performance of Solar Photovoltaic Thermal Systems," *Journal of Solar Energy Engineering*, vol. 143, no. 1, 2021, Art. no. 011003, doi: 10.1115/1.4047453.
- [52] A. Chouder, S. Silvestre, B. Taghezouit, and E. Karatepe, "Monitoring, modelling and simulation of PV systems using LabVIEW," *Solar Energy*, vol. 91, pp. 337-349, 2013, doi: 10.1016/j.solener.2012.09.016.
- [53] J. Han, I. Lee, and S. H. Kim, "User-friendly monitoring system for residential PV system based on low-cost power line communication," *IEEE Transactions on Consumer Electronics*, vol. 61, no. 2, pp. 175-180, 2015, doi: 10.1109/TCE.2015.7150571.
- [54] Y. Cheddadi, H. Cheddadi, F. Cheddadi, F. Errahimi, and N. Es-sbai, "Design and implementation of an intelligent low - cost IoT solution for energy monitoring of photovoltaic stations," *SN Applied Sciences*, vol. 2, 2020, Art. no. 1165, doi: 10.1007/s42452-020-2997-4.
- [55] A. Lopez-Vargas, M. Fuentes, and M. Vivar, "IoT Application for Real-Time Monitoring of Solar Home Systems Based on ArduinoTM with 3G Connectivity," *IEEE Sensors Journal*, vol. 19, no. 2, pp. 679-691, 2019, doi: 10.1109/JSEN.2018.2876635.
- [56] M. Benganem, "Measurement of meteorological data based on wireless data acquisition system monitoring," *Applied Energy*, vol. 86, no. 12, pp. 2651-2660, 2009, doi: 10.1016/j.apenergy.2009.03.026.

Date of publication xxxx 00, 0000, date of current version xxxx 00, 0000.

Digital Object Identifier 10.1109/ACCESS.2017.Doi Number

# A review of recent advances on hybrid energy storage system for solar photovoltaics power generation

Tole Sutikno<sup>1</sup>, Watra Arsadiando<sup>2</sup>, Aree Wangsupphaphol<sup>3</sup>, Anton Yudhana<sup>4</sup>, Mochammad Facta<sup>5</sup>

<sup>1,4</sup>Department of Electrical Engineering, Universitas Ahmad Dahlan, Yogyakarta, Indonesia

<sup>2</sup>Embedded System and Power Electronics Research Group (ESPERG), Yogyakarta, Indonesia

<sup>3</sup>Department of Electrical Engineering, Chulalongkorn University, Bangkok, Thailand

<sup>5</sup>Department of Electrical Engineering, Universitas Diponegoro, Semarang, Indonesia

Corresponding author: Tole Sutikno (tole@ee.uad.ac.id).

We would like to thank Ministry of Education, Culture, Research and Technology of Republic Indonesia, for funding this research under Word Class Research (WCR) grant, contract No: WCR-001/SKPP.ATJ/LPPM UAD/IV/2020; and Embedded System and Power Electronics Research Group (ESPERG) for supporting this research.

**ABSTRACT** The use of hybrid energy storage systems (HESS) in renewable energy sources (RES) of solar Photovoltaic (PV) power generation provides many advantages. These include increased balance between generation and demand, improvement in power quality, flattening PV intermittence, frequency, and voltage regulation in Microgrid (MG) operation. Ideally, HESS has one storage is dedicated for high energy storage (HES) and another storage for high power storage (HPS) purpose. HES is used to fulfill long-term energy demand, while HPS is used to handle power transients and fast load fluctuations. This paper examines HESS comprehensively for on-grid PV power generation and focuses on its ability to combine two storage technologies. This paper also analyzes the important aspects of HESS in on-grid PV power generation in the context of capacity sizing and power converter topology. Several capacity sizing methods of the HESS are reviewed, namely Analytical Method (AM), Statistical Method (SM), Search Based-Heuristic Method (SB-HM), Search Based-Mathematical Optimization Method (SB-MOM), Pinch Analysis Method (PAM), and the Ragone Plot Method (RPM). Power converter (PC) topologies of the HESS are classified into three types, namely passive, semi-active, and active. Performance comparison of the different HESS configurations for on-grid PV power generation in term of power quality, lifetime, intermittence and stability is compared. The various literature reviews available, future trends of configuration HESS are proposed.

**INDEX TERMS** Energy storage, hybrid energy storage system, photovoltaic, capacity sizing, power converter, power generation, microgrid

## I. INTRODUCTION

Renewable energy source (RES) is an alternative means of generating energy to reduce greenhouse gas emissions [1]. Preliminary studies on RES-based power generation such as solar photovoltaic (PV), wind, hydro, biomass, geothermal have been extensively conducted. However, in the last few decades, PV power generation has become one of the most prominent RES technologies because it is easy to install, has

low operating costs, and comprises mature technology [2]. PV and Microgrid (MG) power generation as a batch of load are proposed to be operated in grid-connected mode. A PV power generation connected to the MG needs an energy storage system (ESS), which contributes to its integration by flattening PV fluctuations, improvement power quality, contributing in frequency, *etc.* [3].



EES has been used for centuries and its experience continuous improvement. In the ESS structure, several energy storage technologies (ES) are used to store electrical energy [4]–[6]. Figure 1 shows ES technologies that is typically used for PV power generation in grid-connected mode. The classification of various electrical ES as well as their energy conversion processes and efficiencies are studied in [7]. In addition, its battery technology is considered competent storage that is economical, adequate for power balancing, and able to maintain the power grid [8]. In supporting large-scale energy storage applications, there are storage technologies such as compressed air energy storage (CAES) and pumped hydro energy storage (PHES)[9]. However, both these energy storages rely on environmental and geographic situations, which make their development challenging [10]. Furthermore, ESS Flywheel is based on electromechanical technology [11]–[13], with its stability and efficiency affected by mechanical parts. The ESS Supercapacitor (SC) technology is an example of electrostatic storage, with high recyclability and density [14]. Superconducting Magnetic energy storage (SMES) is an example of ESS that produces storage of electrical energy directly in a magnetic field obtained by current flow [15].

unit volume or mass, while power density is the rate of energy transfer per unit volume or mass. The energy and power densities of various ES technologies are shown and compared in Figure 1. ES technology such as batteries and fuel cells (FC) have high energy and low power densities, thereby creating power control challenges due to the slow dynamic response. Conversely, ES technology such as SC and flywheel have a high power density, hence it can supply high power demand but a decrease in the lifetime of the storage system [16]. However, of the several ES technologies, none has the ability to fulfill the power and energy densities simultaneously. Due to this limitation, it is necessary to enhance the performance of an advanced storage system known as a hybrid energy storage system (HESS). HESS is a two or more energy storage technology combined into one device to improve ESS performance [17], [18]. The HESS can be incorporated with PV power generation for optimal and safe MG operation. HESS modeling in MG depends on several interrelated factors, such as energy storage capacity sizing, energy management, power converter topology, and control strategies that need to be handled with care.

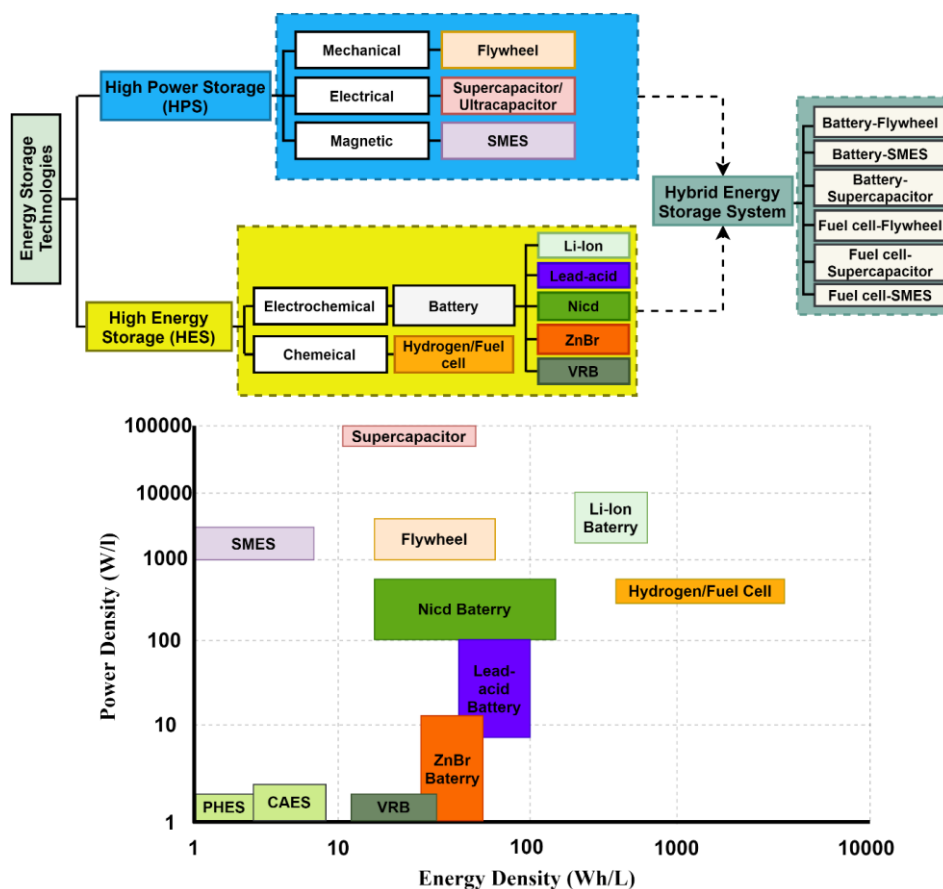


Figure 1. Classification of energy storage systems

In this type of ES technology there is energy density and power density. Energy density is the accumulated energy per

Various papers have investigated HESS related to PV power generation. From various literature, HESS is used for

PV power generation RES applications [19], [20], and Off-MG [21]–[24]. Capacity sizing, power converter topology, control strategies, and utilizations are examined in several papers. However, neither did discuss the on-grid HESS review in detail. In addition, studying and analysis of capacity calculating method and power converter topology on the HESS. In this paper, configuration HESS with type technology storage, capacity sizing, and power converter topology on-grid PV power generation the last five-year will be discussed in detail. The remaining sections are organized as follows: section II hybrid energy storage system (HESS), section III HESS capacity sizing, section IV HESS power converter (PC) topologies, section V HESS for on-grid PV power generation, and section VI conclusion and future trends.

Therefore, HPS needs to have a fast response time, high efficiency, and high life cycle [31]. Several ES technologies with HPS and HES are shown in Figure 1. The ideal technical characteristics of HESS include density energy, density power, response time, energy efficiency, ease of implementation, and durability. In short, HESS leverages HES and HPS to achieve the desired performance.

Density energy (Wh/L) and power (W/L) refer to the maximum energy and power available per unit volume. While response time is the length of time, the storage device releases power. Furthermore, energy efficiency refers to the level of utilizing chemical and electrical energy [32]. Ease of implementation describes the difficulty of installing and maintaining a new system to ensure it operates properly under optimal conditions. Furthermore, while durability is the expected life of the ESS [33]. The characteristics of the

TABLE I  
The characteristics of types of technology ESS based on HES and HPS

Types of technology ESS	Type		Capacity (MW)	Density		Response time	Energy efficiency (%)	Life time (year)	Maturity
	HES	HPS		Energy (Wh/L)	Power (W/L)				
Battery (NiCd) [34]–[39]	✓	✗	0-40	15-80	75-700	Fast (s)	60-80	5-20	Commercial
Battery (Li-Ion) [35][34][40], [41]	✓	✗	0-0.1	200-400	1300-10.000	Fast (s)	65-90	5-15	Commercial
Battery (Lead-acid) [34], [42]–[44]	✓	✗	40-60	50-85	0-20	Fast (s)	70-90	5-15	Mature
Battery (ZnBr) [34], [35], [45]	✓	✗	0.05-2	15-65	1-25	Very fast (< ms)	65-85	5-10	Developing
Battery (VRB) [35], [41], [46][47]	✓	✗	0.03-3	20-70	0.5-2	Fast (s)	60-75	5-20	-
Supercapacitor [34], [35], [41], [48], [49]	✗	✓	0.03	2.5-20	40.000-120.000	Very fast (< ms)	85-98	4-12	Developed
SMES [34], [35], [41], [50], [51]	✗	✓	0.1-10	0.5-5	2600	Very fast (< ms)	95-98	20+	Demonstration
Flywheel [34], [35], [41], [45], [52]–[56]	✗	✓	0-0.25	20-80	5000	Very fast (< ms)	93-95	15-20	Demonstration
Fuel cell/Hydrogen [34], [35], [41], [57]	✓	✗	0-50	600 (200 bar)	0.2-20	Good (<1s)	20-50	5-15	Developing
PHS/PHES [34], [35], [41], [45], [58], [59]	✗	✗	100-5000	0.2-2	0.1-0.2	Slow (min)	75-85	>25	Mature
CAES [34], [35], [45], [46]	✗	✗	5-400	2-6	0.2-0.6	Slow (min)	50-89	>50	Developing

## II. HYBRID ENERGY STORAGE SYSTEM

In MG, discharging/charging irregularities of the ESS can shorten the storage lifetime [25]. HESS is the right solution to solve PV and MG power generation challenges. Various studies have addressed the positive impact of HESS on PV and MG power generation [26]–[28]. Due to the existence of various ESSs with different characteristics, many possible HESS combinations are created depending on the hybridization process's purpose.

In HESS ideally, one storage is high-energy (HE) storage. High energy storage (HES) as ESS1 is used to meet energy demand in the long term [29], [30]. Another storage is storage that is dedicated to covering high-power (HP) applications. High power storage (HPS) as the ESS2 is used to handle power transients and fast load fluctuations.

types of technology ESS based on HES and HPS are shown in Table 1. [34]

HESS is determined by analyzing the HPS and HES characteristics of different ES technologies. The possible variations in the combination of HESS created are shown in Figure 1. The combination of the storage system FC-Battery, Battery-Flywheel, Battery-SC, Battery-SMES, and SC-Fuel cell is frequently used for RES [60]–[64]. Several other factors need to be considered in choosing the appropriate HESS combination, such as storage hybridization targets, space for HESS, and costs. There are various technical problems associated with the use of PV and MG power generation, such as intermittent properties, poor power quality, stability problems, unbalanced loads, frequency instability, and DC bus voltage [27], [65]–[70]. In this

section, various techniques from previously studies to solve the about problems are presented and evaluated.

### A. RES INTERMITTENCE IMPROVEMENT

Many studies have used the HESS (SC-battery) to flattening the RES fluctuations in PV and wind power [71]. ESS can be integrated to solve fluctuation in the power production source in PV and wind power generation, which comprises several frequency components with varying amplitudes. In this regard, HESS with a low and high-speed response has the ability to smoothen the process better than a single ESS [71]. Literature [72], presents flattening the fluctuation wind power short-term and long-term by using wavelet transformation algorithm in HESS capacity configuration. Battery-SC combination is used to consider the frequency distribution of wind power generation's output. Meanwhile, in [27], optimal fuzzy logic control with genetic algorithms was used in the SMES-Battery HESS to flattening PV and wind power generation fluctuations and fulfill grid demand. In [73], the HESS of the SMES-Fuel cell is precisely compensated for the fluctuation of PV power generation's output. HESS has two technologies, namely HPS and HES, with each compensating for low and high-frequency power fluctuations.

### B. Power Quality Enhancement

HESS is not only for managing power from RES rather it is also for sundry power quality purposes, such as for management frequency regulation, increased system stability, unbalanced load, and increased dc bus voltage regulation in MG [65], [66]. Furthermore, the benefits of HESS are investigated and presented.

#### 1) FREQUENCY REGULATION

Frequency management controls in the use of HESS are divided into two types, namely the off-grid system [74]–[76] and on-grid [77]–[79] systems. Furthermore, the high penetration of the RES power generation in the electric system has a negative impact on the inertia of the system [79][67]. Therefore, it has the endanger to compromise the system frequency, which leads to power outages and equipment damage [65], [66]. In ref [67] carried out research on the design of a new working structure for the Battery-Ultracapacitor HESS operation to keep the system frequency within allowable limits. Furthermore, frequency regulation in the electricity market proposed a strategy of efficient and coordinated operation. Battery storage technology plays a significant effect in regulating the frequency in off-grid MG systems. However, for frequency regulation, the battery experiences fast charging/discharging, reducing its life. Furthermore, the battery also needs to cope with sudden power changes in the main frequency control. This condition also accelerates the battery degradation process, therefore, to solve this problem, [74][75] proposed the SMES-Battery HESS. This process was carried out by combining SMES

and Battery, thereby enabling the successful regulation of the frequency and extending battery lifetime.

#### 2) UNBALANCED LOAD REGULATION

The supply of high-quality power to consumers is an essential issue for MG, which enables the handling of unbalanced and nonlinear conditions using HESS. Furthermore, the MG voltage quality is improved by applying the negative-sequence voltage control method. In ref [68] researched on the use of the Battery-SC HESS to improve MG performance under unbalanced loads. Utilization of HESS for MG demonstrates quick and appropriate voltage regulation unbalanced load conditions. Furthermore, Literature [80] proposes a coordination control strategy using HESS (Battery-SC ) for increasing power quality in MG unbalanced load situations.

#### 3) DC BUS VOLTAGE REGULATION

Problems associated with increasing the DC link voltage in MG. However, despite these problems, for a variety of reasons many prefer Standalone MG common bus DC. Besides that, Fast and accurate DC bus voltage regulation is one of the important problems in standalone MG [81]. HESS technology (Battery-SC) is used for DC link voltage restoration and is proposed in isolated systems with effective power-sharing between storage technology the battery and SC [82], [83]. In other studies, grid-connected mode the HESS (Battery-SC) was used for improved regulation of DC link [69], [84].

#### 4) PULSE LOAD REGULATION

While the average power is low, the pulse load requires high instantaneous force [85]–[87]. Distributional disturbances in power and thermal are created when one energy source is used supplying pulsed loads. In addition, various advantage can be achieved while energy and power density ES technology is integrated into the system. Such an advantage as deficient volume and weight on the system, the elimination of the problem of thermal, voltage deviation is reduced and frequency fluctuations [88], [89]. Literature [90] a control strategy in real-time proposed on HESS (Battery-SC) to the DC MG independently with high redundancy and load pulse. The ES Supercapacitor technology is used to supply pulse loads and support the grid during transient periods. Therefore, to prevent frequency fluctuation in the generator and improve system performance, this control method is used. Pulse loads have a significant negative impact on battery lifetime. This impact was analyzed in research carried out by [91], and two scenarios were applied to rate the battery lifetime. The first scenario, uses only battery storage technology to supply load power pulses. The next scenario, uses HESS (battery-SC) to supply the load pulse power. There is a substantial profit of 17.6% in the cost of the HESS (battery-SC) lifetime.

### C. Stability

In MG stability is usually divided into types 3, namely rotor angle, voltage, and frequency. The rotor angle stability is associated with the static state of the generator while maintaining synchronization during turbulence. This represents the firmness among the electromagnetic and the mechanical torques of the prime mover and rotor. Furthermore, frequency stability refers to the power grid maintaining a constant frequency under varying conditions. This stability is based on a balance between production, power dissipation, and load loss. Meanwhile, voltage stability is dependent on the constant voltage across all buses after the occurrence of turbulence. This stability equilibrates the load demand and the power supply per bus. It is divided into two in MG, namely in grid-connected and grid-islanded modes [66], [92]. HESS has the ability to overcome transient stability problems in MG applications [93], [94]. While the Battery-SMES HESS proposed in [70] is used to enhance the transient performance of PV power generation-based MG in several disturbances. The outcomes showed that HESS has an excellent performance in the timely management of transient MG disorders due to its ability to provide fast power injection in the early stages of full feeding. Based on the studies reviewed, it is concluded that ES technology's use increases the margin of MG stability. In addition, the increase is much better using HESS than a single ESS [95].

### D. Storage Lifetime Improvement

Electrochemical energy storages such as batteries and fuel cells have one major drawback, which is its low lifetime. Therefore, by avoiding excessive and frequent energy supplying and receiving of the battery, degradation is prevented with an increase in its lifetime [95]. The control strategy proposed by [95] contributes to the development of instantaneous power between storage technology SMES and battery. In the proposed control method, the discharge and charge of the battery function as SMES storage technology currents rather than directly accepting power fluctuations. The use of HESS battery lifetime is increased by reducing the involvement of the battery in fast charge and discharge cycles as proposed by [96], [97]. In ref [96], [97] researched on a power management strategy using a (lithium) battery with SC. These studies showed that to extend battery life, SC storage technology provides high-frequency demand, with a 19% increase in (lithium) battery lifetime. In [98], [99] stated Supercapacitor-Fuel Cell hybridization utilizing the Supercapacitor for instantaneous charging and discharging to increase the lifetime of Fuel Cell.

## III. HESS CAPACITY SIZING

In HESS, determining a suitable energy storage capacity is one of the most important attributes. Therefore, various methods have been proposed and developed to measure its capacity. Furthermore, several methods have been developed to determine the HESS capacity of particular storage

technology. In [100] carried out a research to analyze the various methods for battery sizing and applications of RES. The strategy in the HESS capacity sizing method is based on the objective function. Capacity sizing strategies for energy storage are classified into analytical methods (AM), statistical methods (SM), search-based methods (SBM), pinch analysis methods (PAM), and Ragone plot methods (RPM). The classification of the capacity sizing methods on HESS is shown in Figure 2. In this section, measurement strategies of HESS capacity sizing are evaluated.

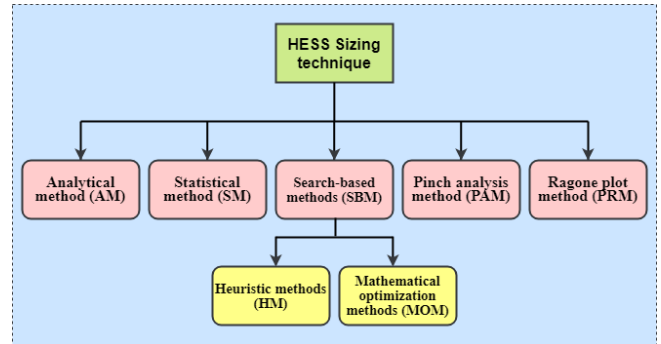


Figure 2. Classification of HESS capacity sizing methods

### A. Analytical method (AM)

Analytical method (AM) is the strategy often used in measuring HESS capacity. It is based on circuit analysis of power system configurations with various weather systems which need optimization against performance criteria. The basic principle of this method operation is as shown in the following equation.

$$P_{HESS} = P_{DG} - P_{load}$$

where,

$$\begin{aligned} P_{HESS} > 0 & \quad \text{charging} \\ P_{HESS} < 0 & \quad \text{discharging} \end{aligned}$$

This method shows that the HESS operation varies upon the change between the distribution generations (DG) output power and based on the load power rate. In (1),  $P_{HESS}$  is a clean power storage hybrid consisting of the first and second energy storage power.  $P_{DG}$  denotes the DG output power, and  $P_{Load}$  is the load power.  $P_{HESS}$  sends power to the load via the discharging process when  $P_{Load} > P_{DG}$  and HEES charge when  $P_{DG} > P_{Load}$ . The topology mentioned above is given in [101]. Meanwhile, in ref [102], a fuel cell-SC HESS was proposed where a high pass filter determines the power of the SC with different cut-off frequencies. Meanwhile, the power from the fuel cell and grid are obtained by subtracting the power of SC from  $P_{HESS}$ . The cut-off frequencies of an individual filter designate the operating period of each ESS technology and determine the required SC capacity. Furthermore, ref [103] researched by proposing a Fourier

transform-based method for measuring the Battery-SC HESS to maintain an isolated system's power balance. This strategy is for the lifetime cost object function from each type of ESS technology. In this method, the power grid variation generated from wind energy is divided into two components, namely frequency spectrum, and HPS, for rapid compensation.

### B. Statistical methods (SM)

Statistical methods (SM) provide more flexibility for determining energy storage capacity in several applications than analytical methods. In a research carried out by [101], a statistical method was proposed to measure the Battery-SC HESS capacity. Furthermore, output power controllers for each storage system with hysteresis-loop and frequency control are projected. Battery-SC HESS controller aims to maneuver the variety of solar-wind power for the smoothen output generation power. Statistical methods with Monte Carlo simulation were proposed in [104] to determine Battery-SC capacity in the HESS.

### C. Search-based methods (SBM)

Search-based methods (SBM) are further divided into heuristic methods (HM) and mathematical optimization methods (MOM). These methods are basically used because of the non-linearity function in the energy storage size problem. Several studies have been conducted for capacity sizing of HESS using the heuristic methods (HM). In ref [105] proposed a strengthening process for the particle swarm optimization (PSO) algorithm to prevent the HESS optimization problem from achieving a minimum cost. Furthermore, in [106] used a genetic algorithm to calculate the battery and supercapacitor's hybrid storage capacity. The results showed that adding a Supercapacitor to the system meaningfully rises the battery lifetime while reduces the total system cost.

### D. Pinch analysis method (PAM)

The pinch analysis method is a modest and flexible methodology for considering the minimum energy point in a radiator network utility system. It is a low burden computing tool used for RES in MG implementation [66]. A research carried out by [107] indicated that the general HESS capacity calculating method for island microgrids is based on the PAM and design space approach. The method incorporates the production variations, load, and discharge time of energy storage, therefore, the capacity curves of the HESS along with any time scales can be obtained by applying this method with the RES and its loads of information. The curves represent a practical set of storage capacities accordingly the timescales. Some are also researching the use of PAM in HESS applications [108], [109].

### E. Ragone theory method

The Ragone plot method (RPM) is deployed for performance categorizing of the energy storage technologies in which

makes up an HESS as is shown in ref [110] and [111]. In [110] stated that the enhancing of the energy storage life cycle is considered as an objective function, and the Ragone plot of the energy storage is added as a constraint. Thus, the common constraint between capability and capacity of energy storage is measured. HESS capacity and real-time control strategy are investigated separately. However, the control method is effected by the sizing due to the objective function and charge/discharge schemes. A greater study of the problem and a more precise solution is to consider capacity sizing and real-time control strategies simultaneously as in [112], [113].

The use of the correct method is based on a variety of various parameters i.e. data availability from the generation, load, and linearity or non-linearity problems. Furthermore, it is necessary to consider the dynamics between generation and load, combine HESS technology's dynamic characteristics, and determine different goals. From the existing parameters, different capacity sizing methods can be utilized.

## IV. HESS POWER CONVERTER (PC) TOPOLOGIES

The charging/discharging characteristics of devices from energy storage are significantly different and dependent on the energy storage technology to be utilized. HESS connected to the grid, or the load goes through different power converter topologies. Ideally, the power converter topology combines ESS1 and ESS2 [114]–[116]. In ref [17] carried out a research that completely reviewed the HESS power converter topology classified into three, namely passive, semi-active, and active, as shown in Figure 3. In this section, HESS power converter topology types are discussed.

### A. Passive HESS topology

The passive power converter (PC) topology consists of two storages with the same voltage connected to MG. Passive topology advantages are efficiency, simplicity, and cost-efficient [117]–[119]. The simplicity and cost-saving are due to low implementation and the absence of power electronics and control circuits [120]. However, the power distribution between ESS 1 and ESS 2 cannot be controlled. Passive topology PC is shown in Figure 3 (a). In a passive topology, a greater part of the voltage is determined from the internal resistance and the current characteristics due to the terminals' irregular voltages. Therefore, the potential for HESS in a passive topology is limited.

### B. Semi-active HESS topology

In semi-active topology, the PC is interfaced with one of the energy storages while the other is direct connection with the DC bus [121]. The application of the converter needs an extra space and costs incremental are inevitably. However, this topology class offers better control and delivery capabilities than the passive. Several semi-active HESS topologies have been reviewed in the study carried out by

[121]. The use of an additional converters in semi-active topology allows a better control of energy of the HESS [122]. Figure 3 (b) shows the semi-active topology in PC.

**C. Active HESS topology**

In [66], the active PC topology has two or more ESSs, and each storage unit interfacing with the system has an individual control of the power converter. This topology has a higher complexity, cost, and system losses than the passive

and semi-active ones. However, this topology class has certain advantages, such as controlling all energy storage forces [98]. Active parallel PC topology uses two converters to control the ESS1 and ESS2 power. Figure 3 (d) shows the topology of the parallel active power converter. Meanwhile, for the traditional parallel active topology, energy is converted through the main DC bus. However, the whole system is negatively affected by two multi-level converters.

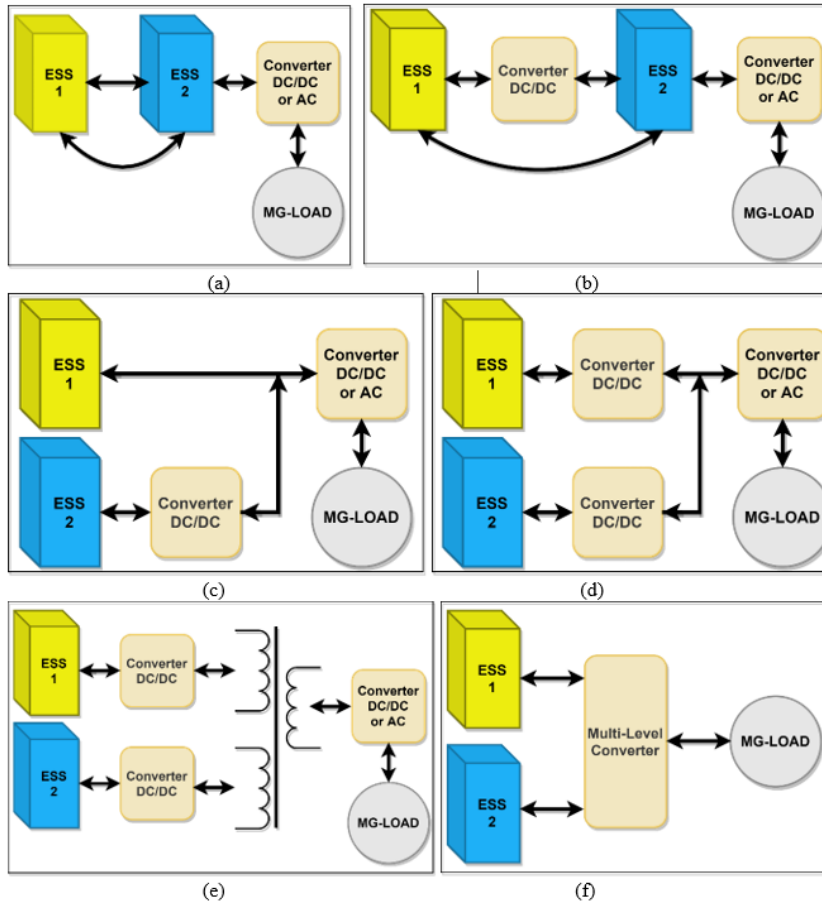


**Figure 3.** The classification of HESS power converter topologies (a) passive, (b) semi-active, (c) series active, (d) parallel active, (e) isolated active, and (f) multi-level active [66]

TABLE 2  
COMPARISON OF VARIOUS HESS PC TOPOLOGIES [91], [117], [121], [131]–[133]

Topology power converter	Efficiency	Flexibility	Range of control strategies adoption	DC bus voltage fluctuation	Fault tolerance	Control complexity	Space requirement	Cost	Recommendations
Passive	high	low	low	yes	no	low	less	low	Used in small capacity systems and cost as a determining factor
Semi-active	medium	medium	medium	yes when HPS is connected directly	only HPS	medium	higher than passive	medium	Used when compromising storage life extension at a small additional cost
Active	low	high	high	no	yes	high	high	high	Used to have a dynamic and more precise response to the large-scale system

In [123], the authors studied to solve the problem mentioned in the reconfigurable topology to decrease the DC bus capacitor in order to increase the efficiency during the energy exchange mode compared to basic active topologies. In several studies, multi-level converters were developed and used for power converters in HESS [124]–[127]. The use of multi-level converters tends to improve the system reliability and power quality. Furthermore, connecting many energy storages using a single power converter decreases the expenses and difficulty of control coordination. However, the capacitors and the switching power electronics switches used in the multi-level converter are large, and controls are more complex [66]. In [128]–[130] stated that various PC topology classes are used to connect HESS to MG.

HESS PC topology directly influences energy management strategies with a comparison of various topologies shown in Table 2. Although the passive PC topology has no direct control over storage power, it comprises a simple configuration and economical. Furthermore, for semi-active PC topology, the output power of one ESS cannot be controlled, and the other voltages need to be similar to the DC bus. The semi-active topology provides limited controllability at a lower cost. Meanwhile, for the active PC topology, the input or output power is from the two ESSs with a rational control strategy and low-cost efficiency. The active topology has flexibility ability, performance, and controllability the best. Despite the fact that flexibility, complexity, controllability, efficiency, and cost are all factors that influence the selection of a suitable PC [66], making an active topology is complicated and expensive.

## V. HESS FOR ON-GRID PV POWER GENERATION

Studies carried out by [18], [134], [135] stated that HESS has the ability to flattening the fluctuations of RES in the wind and solar PV power generation. Furthermore, HESS also controls the power output generated from the PV. In this section, the most popular of the HESS configurations for on-grid PV power generation are evaluated. Performance comparison of the different HESS configurations for on-grid PV in term of power quality, lifetime, intermittence and stability is compared in Table 3.

### A. Battery-Supercapacitor (SC) HESS for on-grid PV power generation

Hajiaghasi *et al.* [68] proposed HESS to enhance power quality under unbalanced load conditions for microgrid applications. According to the study, one of the important issues in microgrids is providing high-quality power to consumers. When an unbalanced load is present in the microgrid system, the voltage loses its symmetry and reduces the power quality. Hajiaghasi *et al.* [68] used the AM capacity sizing method to determine Battery (ESS1) and SC (ESS2) capacity. In Hajiaghasi's research, battery storage technology is used to support constant power changes due to

its high energy density. Meanwhile, SC supports rapid transient power changes due to high power density with an active PC parallel topology. The Battery-SC HESS configuration is shown in Figure 4. Hajiaghasi *et al.* [68] added a proportional resonance (PR) and fuzzy control to adjust the AC load voltage and DC bus voltage control. Performance goals generated using this configuration are increased system performance, good response to its dynamics under unbalanced load conditions, and extended battery lifetime.

Tummuru *et al.* [60] carried out research on the Battery (ESS1) and SC (ESS2) HESS for grid integrated PV systems. The study stated that due to the intermittent properties of PV and irregular load changes, the system experienced issues of power quality and MG stability. To deal with these issues, Tummuru *et al.* [60] used ES with high energy (battery) and power (SC) densities, with the AM capacity sizing method used to determine each storage technology's capacity. SC storage is used to handle sudden changes in power surges. Meanwhile, HESS interface with grid, active parallel PC topology was used by Tummuru *et al.* [60]. Furthermore, Tummuru *et al.* [60], also proposed an energy management system for HESS which achieved fast DC-link regulation, effective energy management, and increased battery lifetime.

Mohamed *et al.* [136] researched the Battery (ESS1) and SC (ESS2) HESS to minimize the effect of pulsed (short duration) loads. According to Mohamed *et al.* [136], the effect of pulsed (short duration) loads causes power quality and MG stability issues. Furthermore, this study used the Ragone plot capacity sizing method to determine the capacity of HESS. In SC storage is used to fulfill loads rapidly due to high power density. Meanwhile, the battery is used for relatively long-term buffer loads due to its high energy density. Active parallel PC topology is used by Mohamed *et al.* to determine the HESS interface to the grid. Furthermore, Mohamed *et al.* [136] developed a real-time energy management algorithm on HESS for AC/DC microgrids. The performance goal generated using this configuration is that pulsed loads show a better margin of stability. Furthermore, shifting the load to off-peak hours saves energy by 7% per year.

### B. Battery-Flywheel HESS for on-grid PV power generation

Barelli *et al.* [61], [137] carried out an analysis on the impact of power fluctuation on battery current (ESS1) and power exchange to the grid. This research indicated the possibilities of lifetime issues on battery and MG stability. Barelli *et al.* [61], [137] used the AM capacity sizing method to determine the capacity of the HESS. Flywheel energy storage (ESS2) serves as peak-shaving due to its high-power density. Therefore, the battery tends to avoid fast charging/discharging loads due to high energy density, which tends to affect the lifespan. Barelli *et al.* [61], [137] applied the active parallel PC topology to determine the grid's

interface. The Battery-Flywheel HESS configuration is shown in Figure 4. This configuration's performance goals are the more stable quality of power transferred to a grid and a significant battery increase for a longer lifetime.

**C. Fuel cell-SC HESS for on-grid PV power generation**

Kong *et al.* [138] proposed modeling for grid-connected HESS. According to the study, the intermittent properties of PV created inconsistencies in power quality and MG stability. However, in order to avoid existing issues, fuel cell (ESS1) and SC (ESS2) HESS were proposed. Kong *et al.* used the AM capacity sizing method to determine the capacity of the HESS. The study further chose Fuel cell storage technology and SC due to their high energy and

transient stability, and voltage fluctuation are some of the issues in on-grid PV power generation. HESS is used to stabilize the Microgrid under different faults and used the AM capacity sizing method to determine the HESS's capacity. The SMES storage is used to handle transient microgrid faults in a timely manner due to their high-power density. Meanwhile, battery storage is used to control long-term power fluctuations when the Microgrid operates normally. For interfaces to the grid, Chen *et al.* applied active parallel PC topology to the HESS configuration, as shown in Figure 4. The performance goals generated using this configuration increases in power quality, battery lifetime, and MG stability.

Bae *et al.* [139] carried out a research that examined the

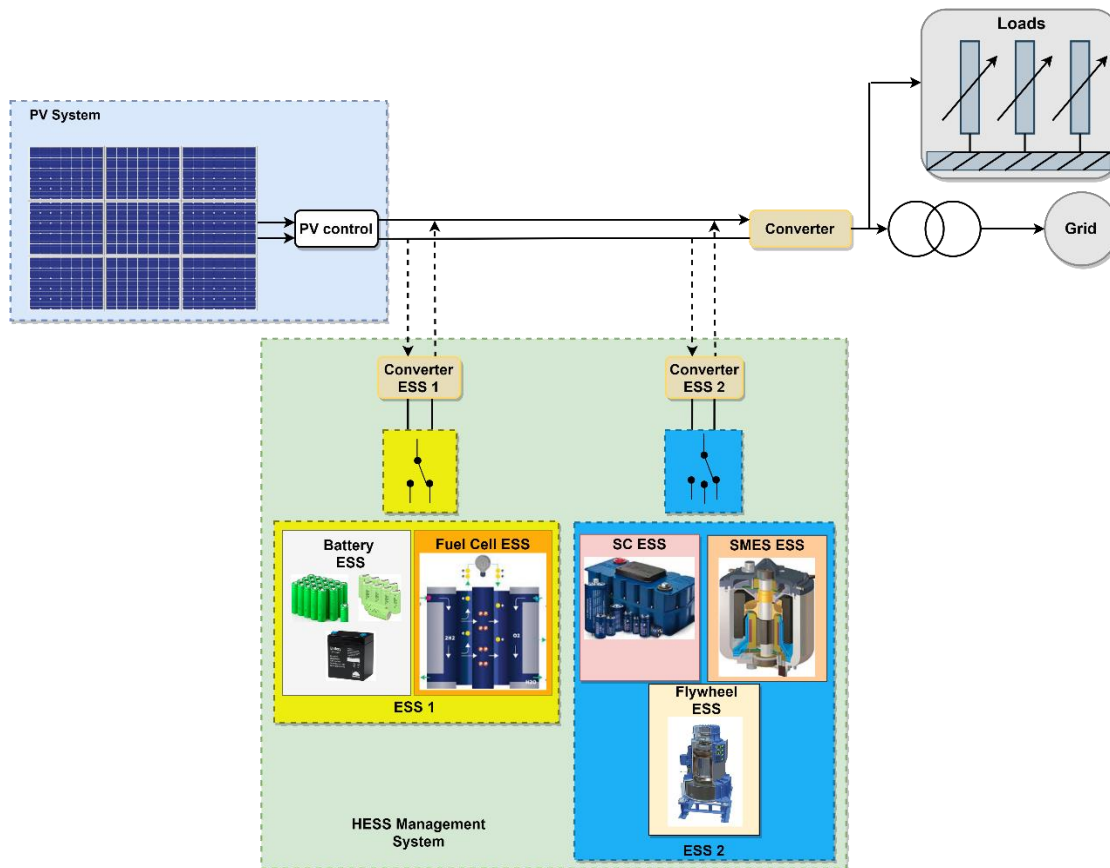


Figure 4. The configuration of active parallel HESS topology

power densities, respectively. Kong *et al.* [138] applied active parallel PC topology for interface to the grid and further proposed the formulation of a coordinated control strategy for HESS. Performance goals generated using this configuration increased power quality, improved intermittence, and MG stability. The Fuel cell-SC HESS configuration is shown in Figure 4.

**D. SMES-Battery HESS for on-grid PV power generation**

Chen *et al.* [70] carried out a research on the Battery (ESS1) and SMES (ESS2) HESS technologies in on-grid PV power generation. According to several studies, energy transfer,

Battery (ESS1) and SMES (ESS2) HESS in on-grid PV power generation. The various inconsistencies associated with this study are related to eliminating fluctuations in power output, stability, and quality. Furthermore, Bae *et al.* applied the AM capacity sizing method to determine the capacity of the HESS with SMES storage used to handle large and fast output power and demand due to its high-power density. Meanwhile, battery storage is used to handle normal responses to baseload and power generation. For interfaces to the grid, Bae *et al.* apply active parallel PC topology. Furthermore, the study focuses on the optimization



TABLE 3  
PERFORMANCE COMPARISON OF THE DIFFERENT HESS TYPES FOR ON-GRID PV

HEES Technology	Sizing Technique	Power converter (PC) topologies	Goal of Hybridization			
			Power Quality Improvement	Lifetime Improvement	Intermittence Improvement	stability Improvement
Battery-SC [68] [69] [84]	AM	Active (Parallel)	✓	✓	✓	✓
Battery-SC [136]	RPM	Active (Parallel)	✓	✗	✗	✓
Battery-Ultracapacitor [140]	SB-MOM	Active (Parallel)	✓	✗	✗	✓
Battery-Flywheel [61], [137]	AM	Active (Parallel)	✗	✓	✗	✓
SMES-Battery [70], [139]	AM	Active (Parallel)	✓	✓	✗	✓
Fuel cell-SC [138]	AM	Active (Parallel)	✓	✗	✓	✓

operation of HESS to achieve an effective energy management system. Performance goals generated using this configuration increased power quality, MG stability, and battery lifetime.

The combination of HESS supercapacitor (SC) technology with Battery is one of the most interesting solutions and also the most significantly developed [68], [69], [84], [136], [140]–[144]. Furthermore, the use of SC has high charge/discharge efficiency [145], [146] and increases battery lifetime.

## VI. Conclusion and future trends

In conclusion, this paper analyzed the implementation of HESS for on-grid PV power generation to fulfill a dynamic balance of power and energy. It focused on HESS by combining two storage technologies based on the characteristics of HPS and HES. HESS formed from storage technologies based on the characteristics of HPS and HES creates prospective six combinations, namely Battery-SC, Battery-Flywheel, Battery-SMES, Fuel cell-SC, Fuel cell-Flywheel, and Fuel cell-SMES. The storage technologies with high energy density are battery and fuel cell, while HES technology is used to fulfill energy demand over a long period. Meanwhile, storage technologies with high power density are SC, Flywheel, and SMES. HPS technology is used to handle power transients and fast load fluctuations, which comprises fast response times, high efficiency, and cycle life. This paper also provided a brief overview of the capacity sizing and power converter topology for HESS in PV power generation. Six methods were developed in determining the capacity of HESS, namely analytical method (AM), statistical method (SM), Search-based heuristic method (SB-HM), Search-based mathematical optimization methods (SB-MOM), pinch analysis method, and the Ragone theory method (RPM).

In on-grid PV power generation, the three greatest generally used for capacity calculating methods are AM, SB-MOM, and RPM. However, the AM capacity sizing method is often used in on-grid power generation the most popular because it is very easy to apply, simple, and effortless to be understood. Furthermore, various PC topologies used to interface the HESS to the grid are described in this paper. The PC topologies of HESS are divided into three, namely

passive, semi-active, and active. In the last five years, the active (parallel) topology is more popularly used in on-grid PV power generation. It is considered to have the flexible ability, the best performance, and the best controllability. However, this topology has high complexity, and it is expensive.

The most popular HESS configurations for on-grid PV power generation in term of power quality, lifetime, intermittence, and stability obtained the following configurations. Firstly, a Battery-SC configuration with AM capacity and active parallel PC is addressed to increase power quality, intermittence, MG stability, and lifetime. Secondly, the Fuel cell-SC configuration with AM capacity sizing and active parallel PC is addressed to increase power quality, MG stability, and intermittence. Thirdly, the Battery-SMES configuration with AM capacity sizing and active parallel PC is addressed to increase power quality, MG stability, and lifetime. Fourthly, the Battery-flywheel configuration with AM capacity sizing and active parallel PC is addressed to increase MG stability and lifetime. Battery-SC and Fuel cell-SC are the ideal combination for on-grid PV power generation based on HESS characteristics. Battery and fuel cell as HES are used to fulfill energy storage and demand over a long-term period. This is because they have the highest energy density compared to other storage technologies. Meanwhile, the supercapacitor (SC) technology is used to handle power transients and fast load fluctuations because it has the highest power density among other storage technologies. Furthermore, SC storage technology also has a fast response time, high efficiency, and high cycle life.

## REFERENCES

- [1] A. Demirbaş, "Global Renewable Energy Resources," *Energy Sources, Part A Recover. Util. Environ. Eff.*, vol. 28, no. 8, pp. 779–792, Jul. 2006, doi: 10.1080/00908310600718742.
- [2] W. Jing, C. H. Lai, W. S. H. H. Wong, and M. L. D. Wong, "A comprehensive study of battery-supercapacitor hybrid energy storage system for standalone PV power system in rural electrification," *Appl. Energy*, vol. 224, no. April, pp. 340–356, 2018, doi: 10.1016/j.apenergy.2018.04.106.
- [3] L. W. Chong, Y. W. Wong, R. K. R. K. R. K.

- Rajkumar, R. K. R. K. R. K. Rajkumar, and D. Isa, "Hybrid energy storage systems and control strategies for stand-alone renewable energy power systems," *Renew. Sustain. Energy Rev.*, vol. 66, pp. 174–189, 2016, doi: 10.1016/j.rser.2016.07.059.
- [4] T. M. I. I. Mahlia, T. J. Saktisahdan, A. Jannifar, M. H. Hasan, and H. S. C. C. Matseelar, "A review of available methods and development on energy storage; Technology update," *Renew. Sustain. Energy Rev.*, vol. 33, pp. 532–545, 2014, doi: 10.1016/j.rser.2014.01.068.
- [5] E. Chemali et al., "Electrochemical and Electrostatic Energy Storage and Management Systems for Electric Drive Vehicles : State-of-the-Art Review and Future Trends," *IEEE J. Emerg. Sel. Top. Power Electron.*, vol. 6777, no. c, pp. 1117–1134, 2016, doi: 10.1109/JESTPE.2016.2566583.
- [6] H. Zhang, J. Baeyens, G. Cáceres, J. Degrève, and Y. Lv, "Thermal energy storage : Recent developments and practical aspects," *Prog. Energy Combust. Sci.*, vol. 53, pp. 1–40, 2016, doi: 10.1016/j.peccs.2015.10.003.
- [7] A. Cansiz, "Electromechanical Energy Conversion," *Compr. Energy Syst.*, vol. 4–5, pp. 598–635, 2018, doi: 10.1016/B978-0-12-809597-3.00425-9.
- [8] G. J. May, A. Davidson, and B. Monahov, "Lead batteries for utility energy storage : A review," *J. Energy Storage*, vol. 15, pp. 145–157, 2018, doi: 10.1016/j.est.2017.11.008.
- [9] G. Venkataramani, P. Parankusam, V. Ramalingam, and J. Wang, "A review on compressed air energy storage – A pathway for smart grid and polygeneration," *Renew. Sustain. Energy Rev.*, vol. 62, pp. 895–907, 2016, doi: 10.1016/j.rser.2016.05.002.
- [10] S. Rehman, L. M. Al-Hadhrani, and M. M. Alam, "Pumped hydro energy storage system: A technological review," *Renew. Sustain. Energy Rev.*, vol. 44, pp. 586–598, 2015, doi: 10.1016/j.rser.2014.12.040.
- [11] S. M. Mousavi G, F. Faraji, A. Majazi, and K. Al-Haddad, "A comprehensive review of Flywheel Energy Storage System technology," *Renew. Sustain. Energy Rev.*, vol. 67, pp. 477–490, 2017, doi: 10.1016/j.rser.2016.09.060.
- [12] A. A. K. K. Arani, H. Karami, G. B. Gharehpetian, and M. S. A. A. Hejazi, "Review of Flywheel Energy Storage Systems structures and applications in power systems and microgrids," *Renew. Sustain. Energy Rev.*, vol. 69, no. November 2016, pp. 9–18, 2017, doi: 10.1016/j.rser.2016.11.166.
- [13] M. Ghanaatian and S. Lutfifard, "Control of Flywheel Energy Storage Systems in the Presence of Uncertainties," *IEEE Trans. Sustain. Energy*, vol. 10, no. 1, pp. 36–45, 2019, doi: 10.1109/TSST.2018.2822281.
- [14] L. Zhang, X. Hu, Z. Wang, F. Sun, and D. G. Dorrell, "A review of supercapacitor modeling, estimation, and applications: A control/management perspective," *Renew. Sustain. Energy Rev.*, vol. 81, pp. 1868–1878, 2018, doi: <https://doi.org/10.1016/j.rser.2017.05.283>.
- [15] W. Buckles and W. V. Hassenzahl, "Superconducting magnetic energy storage," *IEEE Power Eng. Rev.*, vol. 20, no. 5, pp. 16–20, 2000.
- [16] A. Etxeberria, I. Vechiu, H. Camblong, and J.-M. Vinassa, "Hybrid energy storage systems for renewable energy sources integration in microgrids: A review," in *2010 Conference Proceedings IPEC*, 2010, pp. 532–537.
- [17] T. Zimmermann, P. Keil, M. Hofmann, M. F. Horsche, S. Pichlmaier, and A. Jossen, "Review of system topologies for hybrid electrical energy storage systems," *J. Energy Storage*, vol. 8, pp. 78–90, 2016, doi: 10.1016/j.est.2016.09.006.
- [18] R. Hemmati and H. Saboori, "Emergence of hybrid energy storage systems in renewable energy and transport applications – A review," *Renew. Sustain. Energy Rev.*, vol. 65, pp. 11–23, 2016, doi: 10.1016/j.rser.2016.06.029.
- [19] T. Bocklisch, "Hybrid energy storage approach for renewable energy applications," *J. Energy Storage*, vol. 8, pp. 311–319, 2016, doi: <https://doi.org/10.1016/j.est.2016.01.004>.
- [20] S. Ahmad Hamidi, D. M. Ionel, and A. Nasiri, "Modeling and Management of Batteries and Ultracapacitors for Renewable Energy Support in Electric Power Systems—An Overview," *Electr. Power Components Syst.*, vol. 43, no. 12, pp. 1434–1452, Jul. 2015, doi: 10.1080/15325008.2015.1038757.
- [21] S. Nasri, B. S. Sami, and A. Cherif, "Power management strategy for hybrid autonomous power system using hydrogen storage," *Int. J. Hydrogen Energy*, vol. 41, no. 2, pp. 857–865, 2016, doi: 10.1016/j.ijhydene.2015.11.085.
- [22] S. Hajiaghasi, A. Salemnia, and M. Hamzeh, "Hybrid energy storage performance improvement in microgrid application," *9th Annu. Int. Power Electron. Drive Syst. Technol. Conf. PEDSTC 2018*, vol. 2018-Janua, pp. 392–397, 2018, doi: 10.1109/PEDSTC.2018.8343829.
- [23] F. Homayouni, R. Roshandel, and A. A. Hamidi, "Sizing and performance analysis of standalone hybrid photovoltaic/battery/hydrogen storage technology power generation systems based on the energy hub concept," *Int. J. Green Energy*, vol. 14, no. 2, pp. 121–134, 2017, doi: 10.1080/15435075.2016.1233423.
- [24] L. W. Chong, Y. W. Wong, R. K. Rajkumar, and D. Isa, "An optimal control strategy for standalone PV system with Battery-Supercapacitor Hybrid Energy Storage System," *J. Power Sources*, vol. 394, no. April, pp. 35–49, 2018, doi: 10.1016/j.jpowsour.2018.05.041.
- [25] V. A. Boicea, "Energy storage technologies: The past

- and the present,” *Proc. IEEE*, vol. 102, no. 11, pp. 1777–1794, 2014, doi: 10.1109/JPROC.2014.2359545.
- [26] R. K. Sharma and S. Mishra, “Dynamic power management and control of a PV PEM fuel-cell-based standalone ac/dc microgrid using hybrid energy storage,” *IEEE Trans. Ind. Appl.*, vol. 54, no. 1, pp. 526–538, 2017, doi: 10.1109/TIA.2017.2756032.
- [27] G. Wang, M. Ciobotaru, and V. G. Agelidis, “Power smoothing of large solar PV plant using hybrid energy storage,” *IEEE Trans. Sustain. Energy*, vol. 5, no. 3, pp. 834–842, 2014.
- [28] T. Alnejai, S. Drid, D. Mehdi, L. Chrifi-Alaoui, R. Belarbi, and A. Hamdouni, “Dynamic control and advanced load management of a stand-alone hybrid renewable power system for remote housing,” *Energy Convers. Manag.*, vol. 105, pp. 377–392, 2015, doi: 10.1016/j.enconman.2015.07.080.
- [29] Y. Y. Chia, L. H. Lee, N. Shafiabady, and D. Isa, “A load predictive energy management system for supercapacitor-battery hybrid energy storage system in solar application using the Support Vector Machine,” *Appl. Energy*, vol. 137, pp. 588–602, 2015, doi: 10.1016/j.apenergy.2014.09.026.
- [30] S. Wang et al., “Design and advanced control strategies of a hybrid energy storage system for the grid integration of wind power generations,” *IET Renew. Power Gener.*, vol. 9, no. 2, pp. 89–98, 2015, doi: 10.1049/iet-rpg.2013.0340.
- [31] T. Bocklisch, “Hybrid energy storage systems for renewable energy applications,” *Energy Procedia*, vol. 73, pp. 103–111, 2015, doi: 10.1016/j.egypro.2015.07.582.
- [32] J. Kang, F. Yan, P. Zhang, and C. Du, “A novel way to calculate energy efficiency for rechargeable batteries,” *J. Power Sources*, vol. 206, pp. 310–314, 2012.
- [33] S. M. Schoenung, “Characteristics and technologies for long-vs. short-term energy storage,” United States Dep. Energy, 2001.
- [34] T. Kousksou, P. Bruel, A. Jamil, T. El Rhafiki, and Y. Zeraouli, “Energy storage: Applications and challenges,” *Sol. Energy Mater. Sol. Cells*, vol. 120, no. PART A, pp. 59–80, 2014, doi: 10.1016/j.solmat.2013.08.015.
- [35] H. Zhao, Q. Wu, S. Hu, H. Xu, and C. N. Rasmussen, “Review of energy storage system for wind power integration support,” *Appl. Energy*, vol. 137, pp. 545–553, 2015, doi: 10.1016/j.apenergy.2014.04.103.
- [36] P. J. Hall and E. J. Bain, “Energy-storage technologies and electricity generation,” *Energy Policy*, vol. 36, no. 12, pp. 4352–4355, 2008.
- [37] K. C. Divya and J. Østergaard, “Battery energy storage technology for power systems—An overview,” *Electr. power Syst. Res.*, vol. 79, no. 4, pp. 511–520, 2009.
- [38] V. G. Lacerda, A. B. Mageste, I. J. B. Santos, L. H. M. Da Silva, and M. do C. H. Da Silva, “Separation of Cd and Ni from Ni–Cd batteries by an environmentally safe methodology employing aqueous two-phase systems,” *J. Power Sources*, vol. 193, no. 2, pp. 908–913, 2009.
- [39] R. Wagner, *Industrial Applications of Batteries: From Cars to Aerospace and Energy Storage*, no. Chapter 10. Elsevier, 2007.
- [40] A. G. Ritchie, “Recent developments and future prospects for lithium rechargeable batteries,” *J. Power Sources*, vol. 96, no. 1, pp. 1–4, 2001.
- [41] H. Chen, T. N. Cong, W. Yang, C. Tan, Y. Li, and Y. Ding, “Progress in electrical energy storage system: A critical review,” *Prog. Nat. Sci.*, vol. 19, no. 3, pp. 291–312, 2009, doi: 10.1016/j.pnsc.2008.07.014.
- [42] J. McDowall, “Integrating energy storage with wind power in weak electricity grids,” *J. Power Sources*, vol. 162, no. 2, pp. 959–964, 2006.
- [43] N.-K. C. Nair and N. Garimella, “Battery energy storage systems: Assessment for small-scale renewable energy integration,” *Energy Build.*, vol. 42, no. 11, pp. 2124–2130, 2010.
- [44] F. Díaz-González, A. Sumper, O. Gomis-Bellmunt, and R. Villafafila-Robles, “A review of energy storage technologies for wind power applications,” *Renew. Sustain. energy Rev.*, vol. 16, no. 4, pp. 2154–2171, 2012.
- [45] R. Amirante, E. Cassone, E. Distaso, and P. Tamburrano, “Overview on recent developments in energy storage: Mechanical, electrochemical and hydrogen technologies,” *Energy Convers. Manag.*, vol. 132, pp. 372–387, 2017, doi: 10.1016/j.enconman.2016.11.046.
- [46] M. Swierczynski, R. Teodorescu, C. N. Rasmussen, P. Rodriguez, and H. Vikelgaard, “Overview of the energy storage systems for wind power integration enhancement,” in *IEEE International Symposium on Industrial Electronics*, 2010, pp. 3749–3756, doi: 10.1109/ISIE.2010.5638061.
- [47] T. S. Babu, K. R. Vasudevan, V. K. Ramachandaramurthy, S. B. Sani, S. Chemud, and R. M. Lajim, “A Comprehensive Review of Hybrid Energy Storage Systems: Converter Topologies, Control Strategies and Future Prospects,” *IEEE Access*, vol. 8, pp. 148702–148721, 2020, doi: 10.1109/ACCESS.2020.3015919.
- [48] H. Gualous, D. Bouquain, A. Berthon, and J. M. Kauffmann, “Experimental study of supercapacitor serial resistance and capacitance variations with temperature,” *J. Power Sources*, vol. 123, no. 1, pp. 86–93, 2003.
- [49] F. Rafik, H. Gualous, R. Gallay, A. Crausaz, and A. Berthon, “Frequency, thermal and voltage supercapacitor characterization and modeling,” *J. Power Sources*, vol. 165, no. 2, pp. 928–934, 2007.
- [50] S. M. Said, H. S. Salama, B. Hartmann, and I. Vokony, “A robust SMES controller strategy for

- mitigating power and voltage fluctuations of grid-connected hybrid PV–wind generation systems,” *Electr. Eng.*, vol. 101, no. 3, pp. 1019–1032, 2019, doi: 10.1007/s00202-019-00848-z.
- [51] N. Koshizuka et al., “Progress of superconducting bearing technologies for flywheel energy storage systems,” *Phys. C Supercond.*, vol. 386, pp. 444–450, 2003.
- [52] H. Liu and J. Jiang, “Flywheel energy storage—An upswing technology for energy sustainability,” *Energy Build.*, vol. 39, no. 5, pp. 599–604, 2007.
- [53] A. Evans, V. Strezov, and T. J. Evans, “Assessment of utility energy storage options for increased renewable energy penetration,” *Renew. Sustain. Energy Rev.*, vol. 16, no. 6, pp. 4141–4147, 2012.
- [54] X. Luo, J. Wang, M. Dooner, and J. Clarke, “Overview of current development in electrical energy storage technologies and the application potential in power system operation,” *Appl. Energy*, vol. 137, pp. 511–536, 2015, doi: 10.1016/j.apenergy.2014.09.081.
- [55] B. Bolund, H. Bernhoff, and M. Leijon, “Flywheel energy and power storage systems,” *Renew. Sustain. Energy Rev.*, vol. 11, no. 2, pp. 235–258, 2007, doi: 10.1016/j.rser.2005.01.004.
- [56] I. Hadjipaschalis, A. Poullikkas, and V. Efthimiou, “Overview of current and future energy storage technologies for electric power applications,” *Renew. Sustain. Energy Rev.*, vol. 13, no. 6–7, pp. 1513–1522, 2009, doi: 10.1016/j.rser.2008.09.028.
- [57] A. Rabiee, H. Khorramdel, and J. Aghaei, “A review of energy storage systems in microgrids with wind turbines,” *Renew. Sustain. Energy Rev.*, vol. 18, pp. 316–326, 2013, doi: 10.1016/j.rser.2012.09.039.
- [58] P. Denholm and T. Holloway, “Improved accounting of emissions from utility energy storage system operation,” *Environmental Science and Technology*, vol. 39, no. 23, ACS Publications, pp. 9016–9022, 2005, doi: 10.1021/es0505898.
- [59] J. K. Kaldellis and D. Zafirakis, “Optimum energy storage techniques for the improvement of renewable energy sources-based electricity generation economic efficiency,” *Energy*, vol. 32, no. 12, pp. 2295–2305, 2007.
- [60] M. Mohammadi and M. Nafar, “Fuzzy sliding-mode based control (FSMC) approach of hybrid micro-grid in power distribution systems,” *Int. J. Electr. Power Energy Syst.*, vol. 51, pp. 232–242, 2013, doi: 10.1016/j.ijepes.2013.03.009.
- [61] L. Barelli et al., “Flywheel hybridization to improve battery life in energy storage systems coupled to RES plants,” *Energy*, vol. 173, pp. 937–950, 2019, doi: 10.1016/j.energy.2019.02.143.
- [62] A. Pareek, P. Singh, and P. N. Rao, “Analysis and Comparison of Charging Time between Battery and Supercapacitor for 300W Stand-Alone PV System,” *Proc. 2018 Int. Conf. Curr. Trends Towar. Converging Technol. ICCTCT 2018*, pp. 1–6, 2018, doi: 10.1109/ICCTCT.2018.8551164.
- [63] B. K. Kang, S. T. Kim, S. H. Bae, and J. W. Park, “Effect of a SMES in power distribution network with PV system and PBEVs,” *IEEE Trans. Appl. Supercond.*, vol. 23, no. 3, pp. 3–6, 2013, doi: 10.1109/TASC.2012.2230681.
- [64] D. N. Luta and A. K. Raji, “Energy management system for a hybrid hydrogen fuel cell-supercapacitor in an islanded microgrid,” *Proc. - 2019 South. African Univ. Power Eng. Conf. Mechatronics/Pattern Recognit. Assoc. South Africa, SAUPEC/RobMech/PRASA 2019*, pp. 611–615, 2019, doi: 10.1109/RoboMech.2019.8704834.
- [65] Y. Tahir, M. F. Nadeem, A. Ahmed, I. A. Khan, and F. Qamar, “A Review on Hybrid Energy Storage Systems in Microgrids,” *2020 3rd Int. Conf. Comput. Math. Eng. Technol. Idea to Innov. Build. Knowl. Econ. iCoMET 2020*, pp. 0–6, 2020, doi: 10.1109/iCoMET48670.2020.9073919.
- [66] S. Hajiaghasi, A. Salemnia, and M. Hamzeh, “Hybrid energy storage system for microgrids applications: A review,” *J. Energy Storage*, vol. 21, no. December 2018, pp. 543–570, 2019, doi: 10.1016/j.est.2018.12.017.
- [67] U. Akram and M. Khalid, “A coordinated frequency regulation framework based on hybrid battery-ultracapacitor energy storage technologies,” *IEEE Access*, vol. 6, pp. 7310–7320, 2017, doi: 10.1109/ACCESS.2017.2786283.
- [68] S. Hajiaghasi, A. Salemnia, and M. Hamzeh, “Hybrid Energy Storage For Microgrid Performance Improvement Under unbalanced load Conditions,” *J. Energy Manag. Technol.*, vol. 2, no. 1, pp. 30–39, 2018, doi: 10.22109/jemt.2018.109536.1065.
- [69] U. Manandhar et al., “Energy management and control for grid connected hybrid energy storage system under different operating modes,” *IEEE Trans. Smart Grid*, vol. 10, no. 2, pp. 1626–1636, 2017, doi: 10.1109/TSG.2017.2773643.
- [70] L. Chen et al., “SMES-battery energy storage system for the stabilization of a photovoltaic-based microgrid,” *IEEE Trans. Appl. Supercond.*, vol. 28, no. 4, pp. 1–7, 2018.
- [71] P. Zhao, J. Wang, and Y. Dai, “Capacity allocation of a hybrid energy storage system for power system peak shaving at high wind power penetration level,” *Renew. Energy*, vol. 75, pp. 541–549, 2015.
- [72] Q. Jiang and H. Hong, “Wavelet-based capacity configuration and coordinated control of hybrid energy storage system for smoothing out wind power fluctuations,” *IEEE Trans. Power Syst.*, vol. 28, no. 2, pp. 1363–1372, 2012.
- [73] Z. Zhang et al., “Characteristics of compensation for fluctuating output power of a solar power generator in a hybrid energy storage system using a Bi2223 SMES coil cooled by thermosiphon with liquid hydrogen,”

- IEEE Trans. Appl. Supercond., vol. 26, no. 4, pp. 1–5, 2016.
- [74] J. Li et al., “A novel use of the hybrid energy storage system for primary frequency control in a microgrid,” *Energy Procedia*, vol. 103, pp. 82–87, 2016.
- [75] J. Li, R. Xiong, Q. Yang, F. Liang, M. Zhang, and W. Yuan, “Design/test of a hybrid energy storage system for primary frequency control using a dynamic droop method in an isolated microgrid power system,” *Appl. Energy*, vol. 201, pp. 257–269, 2017.
- [76] P. S. Indu and M. V. Jayan, “Frequency regulation of an isolated hybrid power system with superconducting magnetic energy storage,” in 2015 International conference on power, instrumentation, control and computing (PICCC), 2015, pp. 1–6.
- [77] S. Tamura, “Economic analysis of hybrid battery energy storage systems applied to frequency control in power system,” *Electr. Eng. Japan*, vol. 195, no. 1, pp. 24–31, 2016.
- [78] Y. Kim and N. Chang, *Design and management of energy-efficient hybrid electrical energy storage systems*, vol. 9783319072. Springer, 2014.
- [79] F. Guo and R. Sharma, “Hybrid Energy Storage Systems integrating battery and Ultracapacitor for the PJM frequency regulation market,” in 2016 IEEE Power and Energy Society General Meeting (PESGM), 2016, pp. 1–4.
- [80] Y. Zhu, F. Zhuo, and F. Wang, “Coordination control of lithium battery-supercapacitor hybrid energy storage system in a microgrid under unbalanced load condition,” in 2014 16th European Conference on Power Electronics and Applications, 2014, pp. 1–10.
- [81] N. Mendis, K. M. Muttaqi, and S. Perera, “Management of low-and high-frequency power components in demand-generation fluctuations of a DFIG-based wind-dominated RAPS system using hybrid energy storage,” *IEEE Trans. Ind. Appl.*, vol. 50, no. 3, pp. 2258–2268, 2013.
- [82] U. Manandhar, N. R. Tummuru, S. K. Kollimalla, A. Ukil, G. H. Beng, and K. Chaudhari, “Validation of faster joint control strategy for battery-and supercapacitor-based energy storage system,” *IEEE Trans. Ind. Electron.*, vol. 65, no. 4, pp. 3286–3295, 2017.
- [83] S. K. Kollimalla, M. K. Mishra, and N. L. Narasamma, “Design and analysis of novel control strategy for battery and supercapacitor storage system,” *IEEE Trans. Sustain. Energy*, vol. 5, no. 4, pp. 1137–1144, 2014, doi: 10.1109/TSTE.2014.2336896.
- [84] N. R. Tummuru, M. K. Mishra, and S. Srinivas, “Dynamic energy management of renewable grid integrated hybrid energy storage system,” *IEEE Trans. Ind. Electron.*, vol. 62, no. 12, pp. 7728–7737, 2015.
- [85] D. Shin, Y. Kim, J. Seo, N. Chang, Y. Wang, and M. Pedram, “Battery-supercapacitor hybrid system for high-rate pulsed load applications,” in 2011 Design, Automation & Test in Europe, 2011, pp. 1–4.
- [86] A. Lahyani, A. Sari, I. Lahbib, and P. Venet, “Optimal hybridization and amortized cost study of battery/supercapacitors system under pulsed loads,” *J. Energy Storage*, vol. 6, pp. 222–231, 2016.
- [87] C. R. Lashway, A. T. Elsayed, and O. A. Mohammed, “Hybrid energy storage management in ship power systems with multiple pulsed loads,” *Electr. Power Syst. Res.*, vol. 141, pp. 50–62, 2016.
- [88] M. Farhadi and O. A. Mohammed, “Real-time operation and harmonic analysis of isolated and non-isolated hybrid DC microgrid,” *IEEE Trans. Ind. Appl.*, vol. 50, no. 4, pp. 2900–2909, 2014.
- [89] M. Farhadi and O. A. Mohammed, “Performance enhancement of actively controlled hybrid DC microgrid incorporating pulsed load,” *IEEE Trans. Ind. Appl.*, vol. 51, no. 5, pp. 3570–3578, 2015.
- [90] M. Farhadi and O. Mohammed, “Adaptive energy management in redundant hybrid DC microgrid for pulse load mitigation,” *IEEE Trans. Smart Grid*, vol. 6, no. 1, pp. 54–62, 2014.
- [91] A. Lahyani, P. Venet, A. Guermazi, and A. Troudi, “Battery/supercapacitors combination in uninterruptible power supply (UPS),” *IEEE Trans. Power Electron.*, vol. 28, no. 4, pp. 1509–1522, 2012.
- [92] Z. Shuai et al., “Microgrid stability: Classification and a review,” *Renew. Sustain. Energy Rev.*, vol. 58, pp. 167–179, 2016.
- [93] A. Cansiz, C. Faydaci, M. T. Qureshi, O. Usta, and D. T. McGuinness, “Integration of a SMES–battery-based hybrid energy storage system into microgrids,” *J. Supercond. Nov. Magn.*, vol. 31, no. 5, pp. 1449–1457, 2018.
- [94] H. Alafnan et al., “Stability improvement of DC power systems in an all-electric ship using hybrid SMES/battery,” *IEEE Trans. Appl. Supercond.*, vol. 28, no. 3, pp. 1–6, 2018.
- [95] J. Li, A. M. Gee, M. Zhang, and W. Yuan, “Analysis of battery lifetime extension in a SMES-battery hybrid energy storage system using a novel battery lifetime model,” *Energy*, vol. 86, pp. 175–185, 2015, doi: 10.1016/j.energy.2015.03.132.
- [96] T. Weitzel, M. Schneider, C. H. Glock, F. Löber, and S. Rinderknecht, “Operating a storage-augmented hybrid microgrid considering battery aging costs,” *J. Clean. Prod.*, vol. 188, pp. 638–654, 2018.
- [97] J. Li et al., “Design and real-time test of a hybrid energy storage system in the microgrid with the benefit of improving the battery lifetime,” *Appl. Energy*, vol. 218, pp. 470–478, 2018.
- [98] S. Mane, M. Mejari, F. Kazi, and N. Singh, “Improving lifetime of fuel cell in hybrid energy management system by lure–lyapunov-based control formulation,” *IEEE Trans. Ind. Electron.*, vol. 64, no. 8, pp. 6671–6679, 2017.
- [99] H. Aouzellag, K. Ghedamsi, and D. Aouzellag,

- “Energy management and fault tolerant control strategies for fuel cell/ultra-capacitor hybrid electric vehicles to enhance autonomy, efficiency and life time of the fuel cell system,” *Int. J. Hydrogen Energy*, vol. 40, no. 22, pp. 7204–7213, 2015.
- [100] Y. Yang, S. Bremner, C. Menictas, and M. Kay, “Battery energy storage system size determination in renewable energy systems: A review,” *Renew. Sustain. Energy Rev.*, vol. 91, pp. 109–125, 2018.
- [101] A. Abbassi, M. A. Dami, and M. Jemli, “A statistical approach for hybrid energy storage system sizing based on capacity distributions in an autonomous PV/Wind power generation system,” *Renew. Energy*, vol. 103, pp. 81–93, 2017, doi: 10.1016/j.renene.2016.11.024.
- [102] I. San Martín et al., “Integration of fuel cells and supercapacitors in electrical microgrids: Analysis, modelling and experimental validation,” *Int. J. Hydrogen Energy*, vol. 38, no. 27, pp. 11655–11671, 2013, doi: 10.1016/j.ijhydene.2013.06.098.
- [103] Y. Liu, W. Du, L. Xiao, H. Wang, S. Bu, and J. Cao, “Sizing a Hybrid Energy Storage System for Maintaining Power Balance of an Isolated System with High Penetration of Wind Generation,” *IEEE Trans. Power Syst.*, vol. 31, no. 4, pp. 3267–3275, 2016, doi: 10.1109/TPWRS.2015.2482983.
- [104] H. Jia, Y. Mu, and Y. Qi, “A statistical model to determine the capacity of battery–supercapacitor hybrid energy storage system in autonomous microgrid,” *Int. J. Electr. Power Energy Syst.*, vol. 54, pp. 516–524, 2014.
- [105] T. Zhou and W. Sun, “Optimization of battery–supercapacitor hybrid energy storage station in wind/solar generation system,” *IEEE Trans. Sustain. energy*, vol. 5, no. 2, pp. 408–415, 2014.
- [106] M. Masih-Tehrani, M.-R. Ha’iri-Yazdi, V. Esfahanian, and A. Safaei, “Optimum sizing and optimum energy management of a hybrid energy storage system for lithium battery life improvement,” *J. Power Sources*, vol. 244, pp. 2–10, 2013.
- [107] A. S. Jacob, R. Banerjee, and P. C. Ghosh, “Sizing of hybrid energy storage system for a PV based microgrid through design space approach,” *Appl. Energy*, vol. 212, pp. 640–653, 2018.
- [108] I. Janghorban Esfahani, P. Ifaei, J. Kim, and C. K. Yoo, “Design of Hybrid Renewable Energy Systems with Battery/Hydrogen storage considering practical power losses: A MEPoPA (Modified Extended-Power Pinch Analysis),” *Energy*, vol. 100, pp. 40–50, 2016, doi: 10.1016/j.energy.2016.01.074.
- [109] I. Janghorban Esfahani, S. C. Lee, and C. K. Yoo, “Extended-power pinch analysis (EPoPA) for integration of renewable energy systems with battery/hydrogen storages,” *Renew. Energy*, vol. 80, pp. 1–14, 2015, doi: 10.1016/j.renene.2015.01.040.
- [110] Y. Zhang, X. Tang, Z. Qi, and Z. Liu, “The Ragone plots guided sizing of hybrid storage system for taming the wind power,” *Int. J. Electr. POWER ENERGY Syst.*, vol. 65, pp. 246–253, 2015, doi: 10.1016/j.ijepes.2014.10.006.
- [111] M. A. Tankari, M. B. Camara, B. Dakyo, and G. Lefebvre, “Use of ultracapacitors and batteries for efficient energy management in wind–diesel hybrid system,” *IEEE Trans. Sustain. energy*, vol. 4, no. 2, pp. 414–424, 2012.
- [112] A. Wangsupphaphol, N. R. Nik Idris, A. Jusoh, N. D. Muhamad, and S. Chamchuen, “Acceleration-based Control Strategy and Design for Hybrid Electric Vehicle Auxiliary Energy Source,” *ECTI Trans. Comput. Inf. Technol.*, vol. 9, no. 1, pp. 83–92, 1970, doi: 10.37936/ecti-cit.201591.54407.
- [113] A. Wangsupphaphol and N. R. Nik Idris, “Acceleration-based design of electric vehicle auxiliary energy source,” *IEEE Aerosp. Electron. Syst. Mag.*, vol. 31, no. 1, pp. 32–35, 2016, doi: 10.1109/TAES.2016.140011.
- [114] F. Ju, Q. Zhang, W. Deng, and J. Li, “Review of structures and control of battery-supercapacitor hybrid energy storage system for electric vehicles,” in 2014 IEEE International Conference on Automation Science and Engineering (CASE), 2014, pp. 143–148.
- [115] V. F. Pires, E. Romero-Cadaval, D. Vinnikov, I. Roasto, and J. F. Martins, “Power converter interfaces for electrochemical energy storage systems—A review,” *Energy Convers. Manag.*, vol. 86, pp. 453–475, 2014.
- [116] J. Li, S. Zhou, and Y. Han, “REVIEW OF STRUCTURES AND CONTROL OF BATTERY - SUPERCAPACITOR HYBRID ENERGY STORAGE SYSTEM FOR ELECTRIC VEHICLES,” pp. 303–317, 2017.
- [117] J. P. Zheng, T. R. Jow, and M. S. Ding, “Hybrid power sources for pulsed current applications,” *IEEE Trans. Aerosp. Electron. Syst.*, vol. 37, no. 1, pp. 288–292, 2001.
- [118] R. A. Dougal, S. Liu, and R. E. White, “Power and life extension of battery-ultracapacitor hybrids,” *IEEE Trans. components Packag. Technol.*, vol. 25, no. 1, pp. 120–131, 2002.
- [119] H. A. Catherino, J. F. Burgel, P. L. Shi, A. Rusek, and X. Zou, “Hybrid power supplies: A capacitor-assisted battery,” *J. Power Sources*, vol. 162, no. 2, pp. 965–970, 2006.
- [120] X. Zhang, Z. Dong, and C. Crawford, “Hybrid Energy Storage System for Hybrid and Electric Vehicles: review and a new control strategy,” in ASME International Mechanical Engineering Congress and Exposition, 2011, vol. 54907, pp. 91–101.
- [121] Z. Song, H. Hofmann, J. Li, X. Han, X. Zhang, and M. Ouyang, “A comparison study of different semi-active hybrid energy storage system topologies for electric vehicles,” *J. Power Sources*, vol. 274, pp. 400–411, 2015.
- [122] J. Cao and A. Emadi, “A new battery/ultracapacitor

- hybrid energy storage system for electric, hybrid, and plug-in hybrid electric vehicles,” *IEEE Trans. Power Electron.*, vol. 27, no. 1, pp. 122–132, 2011.
- [123] M. Momayyezani, D. B. W. Abeywardana, B. Hredzak, and V. G. Agelidis, “Integrated reconfigurable configuration for battery/ultracapacitor hybrid energy storage systems,” *IEEE Trans. Energy Convers.*, vol. 31, no. 4, pp. 1583–1590, 2016.
- [124] R. Mo and H. Li, “Hybrid energy storage system with active filter function for shipboard MVDC system applications based on isolated modular multilevel DC/DC converter,” *IEEE J. Emerg. Sel. Top. Power Electron.*, vol. 5, no. 1, pp. 79–87, 2016.
- [125] C. A. Bharadwaj and S. Maiti, “Modular multilevel converter based hybrid energy storage system,” in *2017 IEEE PES Asia-Pacific Power and Energy Engineering Conference (APPEEC)*, 2017, pp. 1–6.
- [126] L. Zhang, Y. Tang, S. Yang, and F. Gao, “A modular multilevel converter-based grid-tied battery-supercapacitor hybrid energy storage system with decoupled power control,” in *2016 IEEE 8th International Power Electronics and Motion Control Conference (IPEMC-ECCE Asia)*, 2016, pp. 2964–2971.
- [127] W. Jiang et al., “Flexible power distribution control in an asymmetrical-cascaded-multilevel-converter-based hybrid energy storage system,” *IEEE Trans. Ind. Electron.*, vol. 65, no. 8, pp. 6150–6159, 2017.
- [128] S. Khosrogorji, M. Ahmadian, H. Torkaman, and S. Soori, “Multi-input DC/DC converters in connection with distributed generation units—A review,” *Renew. Sustain. Energy Rev.*, vol. 66, pp. 360–379, 2016.
- [129] T. Anno and H. Koizumi, “Double-input bidirectional DC/DC converter using cell-voltage equalizer with flyback transformer,” *IEEE Trans. Power Electron.*, vol. 30, no. 6, pp. 2923–2934, 2014.
- [130] N. Zhang, D. Sutanto, and K. M. Muttaqi, “A review of topologies of three-port DC–DC converters for the integration of renewable energy and energy storage system,” *Renew. Sustain. Energy Rev.*, vol. 56, pp. 388–401, 2016.
- [131] A. M. Gee, F. V. P. Robinson, and R. W. Dunn, “Analysis of battery lifetime extension in a small-scale wind-energy system using supercapacitors,” *IEEE Trans. Energy Convers.*, vol. 28, no. 1, pp. 24–33, 2013.
- [132] I. J. Cohen, D. A. Wetz, J. M. Heinzl, and Q. Dong, “Design and characterization of an actively controlled hybrid energy storage module for high-rate directed energy applications,” *IEEE Trans. Plasma Sci.*, vol. 43, no. 5, pp. 1427–1433, 2014.
- [133] S. K. Kollimalla, M. K. Mishra, A. Ukil, and H. B. Gooi, “DC grid voltage regulation using new HESS control strategy,” *IEEE Trans. Sustain. Energy*, vol. 8, no. 2, pp. 772–781, 2016.
- [134] J. Hou, Y. Shao, M. W. Ellis, R. B. Moore, and B. Yi, “Graphene-based electrochemical energy conversion and storage: Fuel cells, supercapacitors and lithium ion batteries,” *Phys. Chem. Chem. Phys.*, vol. 13, no. 34, pp. 15384–15402, 2011, doi: 10.1039/c1cp21915d.
- [135] Y. Zhang, Y. Xu, H. Guo, X. Zhang, C. Guo, and H. Chen, “A hybrid energy storage system with optimized operating strategy for mitigating wind power fluctuations,” *Renew. Energy*, vol. 125, pp. 121–132, 2018, doi: 10.1016/j.renene.2018.02.058.
- [136] A. Mohamed, V. Salehi, and O. Mohammed, “Real-time energy management algorithm for mitigation of pulse loads in hybrid microgrids,” *IEEE Trans. Smart Grid*, vol. 3, no. 4, pp. 1911–1922, 2012, doi: 10.1109/TSG.2012.2200702.
- [137] L. Barelli et al., “Dynamic Analysis of a Hybrid Energy Storage System (H-ESS) Coupled to a Photovoltaic (PV) Plant,” *Energies*, vol. 11, no. 2, 2018, doi: 10.3390/en11020396.
- [138] L. Kong, J. Yu, and G. Cai, “Modeling, control and simulation of a photovoltaic /hydrogen/ supercapacitor hybrid power generation system for grid-connected applications,” *Int. J. Hydrogen Energy*, vol. 44, no. 46, pp. 25129–25144, 2019, doi: 10.1016/j.ijhydene.2019.05.097.
- [139] S. Bae, S. U. Jeon, and J. W. Park, “A Study on Optimal Sizing and Control for Hybrid Energy Storage System with SMES and Battery,” *IFAC-PapersOnLine*, vol. 48, no. 30, pp. 507–511, 2015, doi: 10.1016/j.ifacol.2015.12.430.
- [140] B. Liu, F. Zhuo, and X. Bao, “Fuzzy control for hybrid energy storage system based on battery and Ultra-capacitor in Micro-grid,” *Conf. Proc. - 2012 IEEE 7th Int. Power Electron. Motion Control Conf. - ECCE Asia, IPEMC 2012*, vol. 2, pp. 778–782, 2012, doi: 10.1109/IPEMC.2012.6258934.
- [141] W. Jing, C. H. Lai, W. S. H. H. Wong, and M. L. D. Wong, “Dynamic power allocation of battery-supercapacitor hybrid energy storage for standalone PV microgrid applications,” *Sustain. Energy Technol. Assessments*, vol. 22, pp. 55–64, 2017, doi: 10.1016/j.seta.2017.07.001.
- [142] C. M. M. R. S. Silva et al., “Integrated Control Strategy for Grid Connected Photovoltaic Array, Battery Storage and Supercapacitors,” *2018 2nd Int. Conf. Electr. Eng. EEECon 2018*, pp. 51–57, 2018, doi: 10.1109/EECon.2018.8541009.
- [143] F. Ongaro, S. Saggini, and P. Mattavelli, “Li-Ion battery-supercapacitor hybrid storage system for a long lifetime, photovoltaic-based wireless sensor network,” *IEEE Trans. Power Electron.*, vol. 27, no. 9, pp. 3944–3952, 2012, doi: 10.1109/TPEL.2012.2189022.
- [144] P. K. S. Roy, H. B. Karayaka, Y. Yan, and Y. Alqudah, “Size optimization of battery-supercapacitor hybrid energy storage system for 1MW grid connected PV array,” *2017 North Am. Power Symp. NAPS* 2017, 2017, doi:

10.1109/NAPS.2017.8107181.

- [145] G. Sikha and B. N. Popov, "Performance optimization of a battery–capacitor hybrid system," *J. Power Sources*, vol. 134, no. 1, pp. 130–138, 2004.
- [146] A. Kuperman and I. Aharon, "Battery–ultracapacitor hybrids for pulsed current loads: A review," *Renew. Sustain. Energy Rev.*, vol. 15, no. 2, pp. 981–992, 2011.



**ANTON YUDHANA** received B. Eng. and M. Eng. in electrical engineering from Institut Teknologi sepuluh November and Universitas Gajah Mada, Indonesia, in 2001 and 2005, respectively, and the Ph.D. degree from Universiti Teknologi Malaysia in 2010. He is a Lecturer with the Electrical Engineering Department, Universitas Ahmad Dahlan, Indonesia. His current research interests include communication-multimedia, signal processing, and wireless communication.



**TOLE SUTIKNO** received B. Eng. and M. Eng. in electrical engineering from Universitas Diponegoro and Universitas Gajah Mada, Indonesia, in 1999 and 2004, respectively, and the Ph.D. degree from Universiti Teknologi Malaysia in 2016. He is an Associate Professor with the Electrical Engineering Department, Universitas Ahmad Dahlan, Indonesia, and the leader of Embedded Systems & Power Electronics Research Group (ESPERG). His current research interests include power electronics, motor drives, renewable energy, FPGA, and intelligent control systems.



**MOCHAMMAD FACTA** received the B.S. degree in electrical engineering from the Universitas Hasanuddin, Makassar, Malaysia, the M.Eng. degree from the Institut Teknologi Sepuluh Nopember Surabaya, Indonesia, and the Ph.D. degree in electrical engineering from the Universiti Teknologi Malaysia, Johor Bahru, Malaysia, in 2012. His current research interests include Electrical Power Engineering.



**WATRA ARSADIADNO** received B. Eng. in electrical engineering from Universitas Ahmad Dahlan, Indonesia, in 2017. He is a member of the Embedded Systems & Power Electronics Research Group (ESPERG). His current research interests include renewable energy, robotics, and digital control system.



**AREE WANGSUPPHAPHOL** received a Degree in Engineering and a Masters in Engineering in electrical engineering from King Mongkut's Institute of Technology, Ladkrabang, Thailand, in 1999 and 2007, respectively. He is currently supported by the Ph.D. Merit Scholarship of Islamic Development Bank (IDB) for conducting researches at the UTM-PROTON Future Drives Laboratory. His research interests are mainly in energy management system, electric vehicle applications, and control of power electronics systems.



---

# A New FL-MPPT High Voltage DC-DC Converter for PV Solar Application

---

Tole Sutikno<sup>1,2</sup>, Arsyad Cahya Subrata<sup>1,2</sup>, Awang Jusoh<sup>3</sup>  
and Sanjeevikumar Padmanaban<sup>4</sup>

<sup>1</sup>*Department of Electrical Engineering, Universitas Ahmad Dahlan, Yogyakarta, Indonesia; tole@ee.uad.ac.id; arsyadcahya@gmail.com*

<sup>2</sup>*Embedded Systems & Power Electronics Research Group, Yogyakarta, Indonesia; tole@ee.uad.ac.id; arsyadcahya@gmail.com*

<sup>3</sup>*Department of Electrical Power Engineering, Universiti Teknologi Malaysia, Johor, Malaysia; awang@fke.utm.my*

<sup>4</sup>*CTiF Global Capsule, Department of Business Development and Technology, Aarhus University, Herning 7400, Denmark; sanjeev@btech.au.dk*

## Abstract.

To reduce the effects of global warming, there is an increasing need for renewable energy sources. Several studies have been carried out on photovoltaic (PV) systems to maximize their potential as an alternative electricity generator. However, various power converters for high voltage ratio applications have multiple drawbacks. This research was carried out to develop a power converter topology connected between the PV and the load for the need. In this research, the high step-up DC-DC converter for high-voltage gain conversion ratio and high efficiency is proposed. Furthermore, the fuzzy logic-based Maximum Power Point Tracking (MPPT) technique connected to the power converter was used to maximize the power converted from PV in changing atmospheric conditions. The MPPT control with fuzzy logic controller (FLC) was analysed and compared with the perturb and observe (P&O) algorithm. The results showed that the FLC algorithm could control the HSU DC-DC converter with an output voltage of 29% higher than the P&O algorithm.

**Keywords.** Fuzzy Logic, Maximum Power Point Tracking, DC-DC converter, Photovoltaic, Power Converter, Perturb and Observe algorithm, Renewable Energy

## 1. INTRODUCTION

Photovoltaic (PV) system is one of the fastest-growing technologies in line with the severe energy crisis and environmental issues such as pollution and the effects of global warming. Meanwhile, the energy conversion efficiency generated from PV is relatively small [1]–[5]. Therefore, a lot of research has been carried out to develop PV systems regarding

basic materials that form PV and the power converter side. This research was carried out to maximize the energy conversion results of a PV system and was divided into two main topics [6]. The first topic was related to new, high-efficiency, and low-cost PV cells and modules. In contrast, the second topic was related to the power converter topology and control strategy used.

Various topologies have been developed from the power converter point of view to maximize the energy conversion results obtained from PV. In general, conventional DC-DC converters were used for low-power applications [7]. Meanwhile, for applications requiring high voltage ratios, the development of a power converter topology has also received special attention [8]–[10]. Theoretically, a significant voltage gain in the DC-DC converter is achievable by providing a high duty ratio. Meanwhile, the increase in voltage generated by a high duty ratio is limited due to its electronic components, such as the effect of switches, diodes, equivalent series resistance (ESR) of inductors and capacitors. Therefore, many researchers have developed converters with high step performance, low cost, and high efficiency in power applications requiring high voltage ratios and various topologies.

Furthermore, Afzal et al. [11] and Ebrahimi et al. [12] developed a boost converter with a coupled inductor for high step-up applications due to the simplicity of the structure. However, this topology results in low efficiency at low power levels due to the leakage in coupled inductors, leading to increased conduction loss in semiconductors and copper losses in inductors. This problem is usually resolved with resistor-capacitor-snubber diodes, but it causes additional power loss [13]. The current-fed converter topology uses a transformer based on switched capacitors suitable for low power application systems. This converter produces zero magnetic DC offset and a low input ripple due to its current-fed structure [14]. Also, Sha et al. [15] optimized the current-fed dual active bridge DC-DC converter.

Meanwhile, this converter's problem is poor voltage regulation on the output side, high voltage, and current surges through semiconductor devices caused by the charging and discharging of switched capacitors [16]. The cascaded converter also produces high voltage ratios but working unstably is its major drawback. Li et al. [17] also proposed a stable converter with an approach based on describing its function methods but, its efficiency is low because it requires two processes. Quadratic Boost Converter (QBC) topology connects two converters in series using one switch. Without optimization, the efficiency of QBC is lower than conventional boost converters. Furthermore, Wang et al. [18] proposed a different mode of operation, which yielded an efficiency of 90%.

Meanwhile, Lee [19] used a QBC with the coupled inductor. The passive voltage clamp connected to the power switch makes recycled energy stored in the leakage inductor of the coupled inductor; therefore, the power switch spike was reduced. Also, the resulting voltage ratio was the same as the one in the cascaded converter. The output voltage with high ratio and efficiency produced by the high step-up (HSU) converter was proposed by Dahono [20] and has been used for maximum power point tracking (MPPT) technique for PV systems, but still employed a conventional controller.

To produce high ratio output voltages, DC-DC converter topologies for PV systems should have high-voltage gain and deliver increased efficiency. In this research, the high step-up

DC-DC converter for high-voltage gain conversion ratio and high efficiency is proposed. Modeling and simulation of MPPT technique using the high-voltage gain DC-DC converter based on a simple fuzzy logic controller (FLC) are presented in this paper. The FLC-based converter is compared with the perturb and observe (P&O) algorithm. Section 2 discusses the modeling and characteristic of PV modules using MATLAB/Simulink. Meanwhile, Section 3 describes the basic MPPT. Modeling of the HSU converter used and the MPPT technique based on FLC were discussed in Section 4. Furthermore, the results and discussion are presented in Section 5, followed by conclusions in Section 6.

## 2. MATERIALS AND METHODS

### 2.1. Modeling PV Module

Since the discovery of PV silicone crystalline designed for outdoor use in 1950 by Bell Labs [21], till now, there are two PV cell models still in use single-diode [22]–[24] and double diode [25], [26]. The single-diode model, shown in Figure 2.1, is superior and widely used due to its accuracy and complexity [27]. The output current of a single-diode model of the PV cell is expressed as

$$I_M = N_p I_{phM} - N_p I_{sM} \left[ \exp \left( \frac{q(V_M + I_M R_{sM} - V_{ocM})}{N_s k T A} - 1 \right) \right] \quad (1)$$

where the module is represented in M,  $V_M$ ,  $I_M$  and  $R_{sM}$  are the voltage, current, and series resistance module,  $N_p$  and  $N_s$  is the number of cells connected parallel and in series,  $I_{phM}$  and  $I_{sM}$  are photocurrent and saturation current of the module,  $V_{ocM}$  is the open-circuit voltage module,  $q$  is the electron charge ( $1.6 \times 10^{-19}$ C),  $k$  is Boltzmann constant ( $1.38 \times 10^{-23}$ J/K)  $T$  is the cell working temperature. At the same time,  $A$  is the diode constant ideality of cells depending on PV technology. With equation (1), the  $V - I$  characteristics of the PV module can be formed and developed to obtain the electrical character of the PV module shown in Figure 2.2.

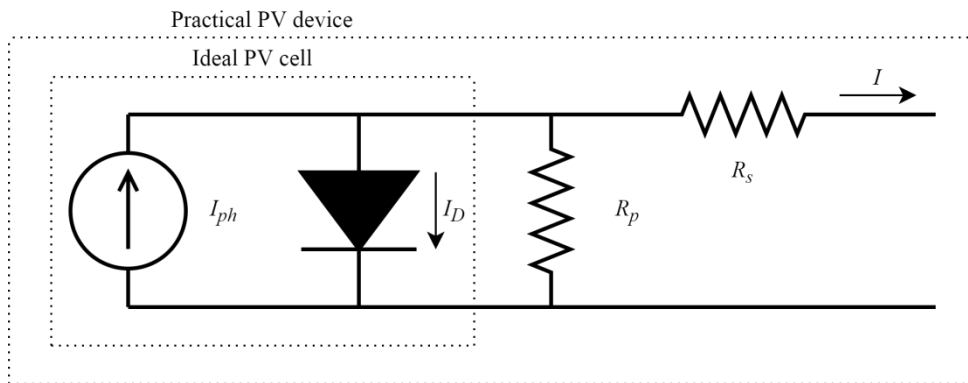


Figure 2. 1. Single-diode model PV cell equivalent circuit.

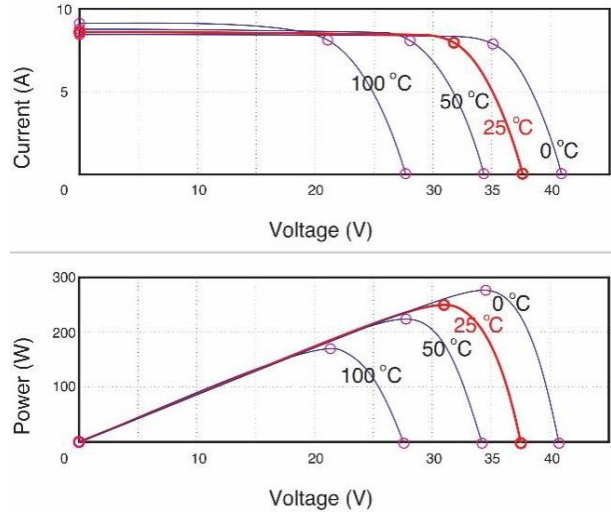


Figure 2. 2. V – I and V – P characteristic

The photocurrent module depends on solar irradiation, and it is also influenced by temperature, as shown in the equation.

$$I_{phM} = [I_{scM} + K_i(T - T_r)]\lambda \quad (2)$$

where  $I_{scM}$  is the short-circuit current of the cell at the temperature of 25°C at 1 kW/m<sup>2</sup>,  $K_i$  is the temperature coefficient of short-circuit cell current,  $T_r$  is the cell reference temperature, meanwhile,  $\lambda$  is the solar irradiance level in kW/m<sup>2</sup>.

The saturation current of the module varies with the cell temperature given by

$$I_{sM} = I_{rsM} \left(\frac{T}{T_r}\right)^3 \exp \left[ qEg \frac{\frac{1}{T_r} - \frac{1}{T}}{kA} \right] \quad (3)$$

where  $I_{rsM}$  reverse saturation current at the reference temperature and solar radiation is the band-gap energy of the semiconductor used in the cell.

The reverse saturation module at the reference temperature is planned as,

$$I_{rsM} = \frac{I_{scM}}{\exp \left[ \frac{qV_{ocM}}{N_s kAT} \right] - 1} \quad (4)$$

where  $V_{ocM}$  the open-circuit voltage at the reference temperature.

## 2.2. Maximum Power Point Tracking

To use energy optimally, PV is installed in an environment where the sun's rays are not obstructed. Meanwhile, irradiation and temperature due to the atmosphere affect the efficiency of the power output [28]. Therefore, many researchers have developed the

MPPT technique to obtain the maximum energy conversion efficiency to solve the efficiency problem in PV systems. MPPT is a method for tracing the Maximum Power Point (MPP), using the parameters such as voltage, current, and/or power as input. At the same time, the output from MPPT is a PWM signal or a change in a duty cycle that controls the power converter used.

MPPT is a technique used to trace the MPP of PV by moving its operating module point to its MPP. The  $V - I$  and  $V - P$  curves of the PV module show that the maximum power is only available under one specific functional condition called MPP. Also, its location varies with changes in irradiation and operating temperature. A simple example can be seen in the  $V - P$  curve shown in Figure 2.3, produced from a PV module with a maximum voltage of 18.6 V (measured at a cell temperature of 25°C, connected to a DC load of 12 V). The output voltage of the PV module varies with the cell temperature.

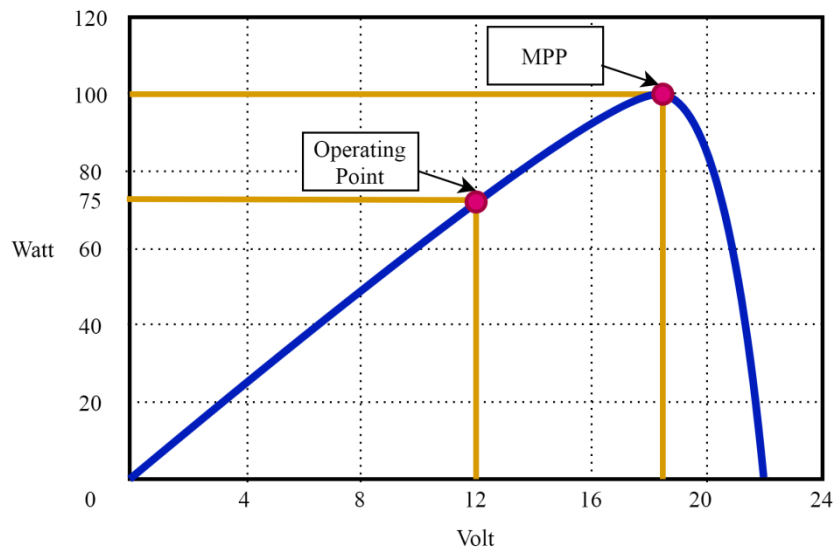


Figure 2. 3. Curve of the  $V - P$  characteristics of the PV module connected to a 12 V load.

The operating point of the PV module is not at its peak when it is directly connected to the load. For example, in Figure 3, the PV output power is 75 W, so the power generated is less than the maximum power available in the PV module. The electrical operation point can be moved to the high-power point by varying the impedance in the PV module. Furthermore, to change the impedance of the PV circuit to the load circuit, a DC-DC converter is used by changing its duty ratio [29].

The algorithm used to discover MPP is the hill-climbing method, namely Perturb and Observe (P&O). The conventional algorithm is easy to build algorithms because it does not require PV characteristics or solar intensity and cell temperature measurements. Meanwhile, the P&O algorithm is more straightforward and flexible, making it useful for commercial applications [30]. Furthermore, P&O works by perturbing the PV operating point to increase or decrease the control parameters in a small step size and measure the output power of the PV array before and after perturbation. If the power increases, the algorithm will perturb the system in the same direction. Also, it will perturb the system in

the opposite direction if the power decreases [31]. P&O techniques use reference voltage and reference current perturbation or direct duty ratio perturbation which are widely used today.

Meanwhile, the P&O algorithm fluctuates in the MPP estimate around the actual reference MPP voltage depending on the perturbation size [32]. The resulting fluctuation becomes high if the step size used is significant. Also, if the step size is too small, the tracking speed to reach MPP will take a long time.

Furthermore, power oscillations also occur in both stable and unstable atmospheric conditions [33]. Due to the potential and advantages of Artificial Intelligent (AI), various AI-based algorithms are widely used in the MPPT technique. Furthermore, FLC, an intelligent control algorithm, is widely used in recent years because of its good performance and structural simplicity [6], [34]. The results reported by these researchers show that the FLC algorithm used for duty cycle control in the MPPT technique performs better than conventional techniques.

### 2.3. High Step-up DC-DC Converter

The system developed in this research is a stand-alone PV system, as shown in the general block diagram in Figure 2.4. The system consists of a PV generator, HSU DC-DC converter with MPPT based on fuzzy logic to adjust the converter's duty ratio and resistive loads.

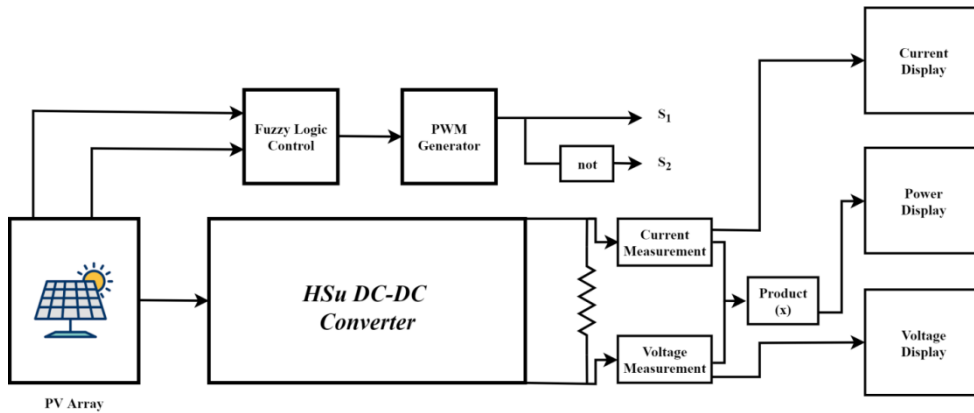


Figure 2. 4. General block diagram of the system.

The converter used in this research was DC-DC buck-boost converter, producing a high voltage gain. This converter modification combines a derived boost and buck DC-DC converter, Dahono [20]. The conventional DC-DC boosts converter is shown in Figure 2.5a.

The voltage gain of the conventional DC-DC boost converter is

$$\frac{V_o}{E_d} = \frac{1}{1 - \alpha} \quad (5)$$

where  $\alpha$  is the duty factor of the transistor Q. While the output voltage is given by

$$\bar{v}_o = E_d \frac{1}{1 - \alpha} - \frac{R_L + R}{(1 - \alpha)^2} I_o \quad (6)$$

Furthermore, the conventional DC-DC boost converter is differentiated with a parallel-connected input and a series-connected output, as shown in Figure 2.5b. This connection increases the load ratio of the converter. Therefore, the voltage gain is given by

$$\frac{E_o}{E_d} = \frac{1 + \alpha}{1 - \alpha} \quad (7)$$

while the output voltage at steady-state condition is

$$\bar{v}_o = E_d \frac{1 + \alpha}{1 - \alpha} - 2 \frac{R_L + R}{(1 - \alpha)^2} I_o \quad (8)$$

Furthermore, the buck-boost converter is differentiated by the same method. This converter is shown in Figure 2.5c, and it also produces the same voltage ratio (5). However, it has discontinuous input currents with significant ripple content, which reduced PV module performance or load. The total ripple input and output can be reduced by controlling two converters as two-phase converters.

The HSU converter was produced by combining a diversified boost and buck-boost converter. The converter made is shown in Figure 2.6, with the resulting voltage ratio equal to the one given by (10). In addition, the switch in this converter is used to reduce the ripple content of the switching device in a two-phase converter, as shown in Figure 2.5b and Figure 2.5c.

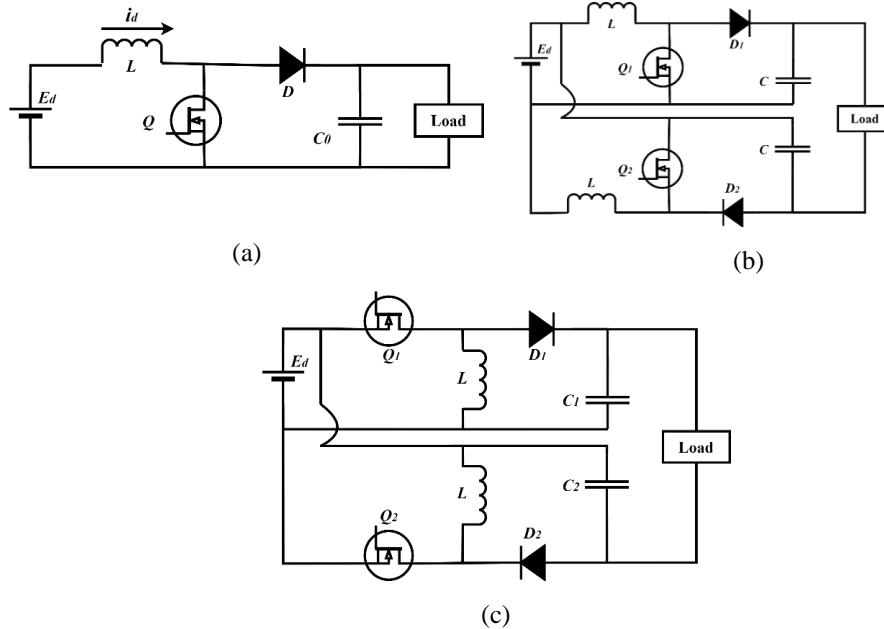


Figure 2. 5. DC-DC converter (a) boost, (b) boost derived converter, and (c) buck-boost derived converter.

The RMS value of the output voltage ripple of this converter is

$$\tilde{V}_o = \frac{\bar{i}_o}{Cf_s} \frac{\alpha(1-2\alpha)}{2\sqrt{3}(1-\alpha)} \quad (9)$$

Meanwhile, the output voltage ripple for duty cycles more than half is

$$\tilde{V}_o = \frac{\bar{i}_o}{Cf_s} \frac{(2\alpha-1)}{2\sqrt{3}} \quad (10)$$

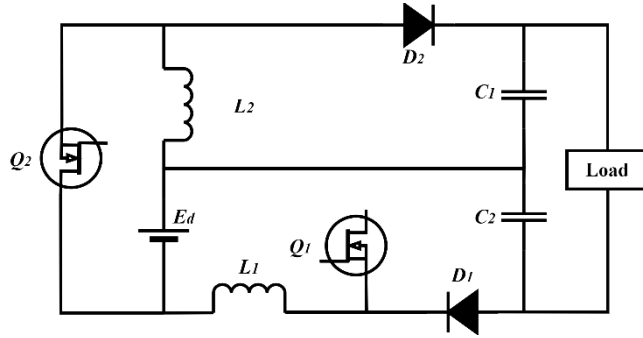


Figure 2. 6. HSU converter.

### 3. FUZZY LOGIC CONTROL FOR MPPT

The control method using the FLC algorithm has been developed for many applications. FLC implementation is rapidly increasing because of its simplicity and does not require mathematical modeling data [34]–[36]. Furthermore, FLC shows good performance in overcoming non-linear systems [29], [33], [37], [38].

The FLC algorithm design has three main stages: fuzzification, rule evaluation, and defuzzification, as shown in Figure 3.1. At the fuzzification stage, there is a membership function that acts as FLC inputs. The number of input membership functions affects the accuracy of the FLC algorithm. Also, in rule evaluation, FLC linguistic rules are used to provide control measures that link logical functions between input and output membership functions. Furthermore, rule evaluation generates fuzzy membership function output for each action of the input membership function. The last stage is defuzzification which predicts the value of MF output obtained as the output of the whole system.

Solar PV has non-linear properties; therefore, the FL implemented in the MPPT technique overcomes this problem. In a solar PV system, the FL input is as Error (E) and Change in Error ( $\Delta E$ ), with the output as a PWM feed, which controls the converter duty cycle. The error signal is obtained from the change in the PV output power divided by the change in output voltage. The two inputs are defined as

$$\text{Error,} \quad E(k) = \frac{\Delta P}{\Delta V} = \frac{P(k) - P(k-1)}{V(k) - V(k-1)} \quad (11)$$

$$\text{Error Change,} \quad \Delta E(k) = E(k) - E(k-1) \quad (12)$$



where  $k$  is the sample time,  $P(k)$  is power,  $V(k)$  the PV voltage,  $P(k - 1)$  and  $V(k - 1)$  is the previous PV power and voltage, respectively.  $E(k)$  shows that the operating load-point is located on the left or right, while  $\Delta E(k)$  the direction of motion of the point.

The FLC evaluates the output power of the PV and determines the change in power relative to voltage ( $\Delta P/\Delta V$ ). If the value is greater than zero, the controller changes the PWM cycle to increase the voltage until it reaches the maximum power ( $\Delta P/\Delta V = 0$ ). Conversely, if the value is less than zero, the controller changes the PWM cycle to reduce the voltage until it reaches the MPP.

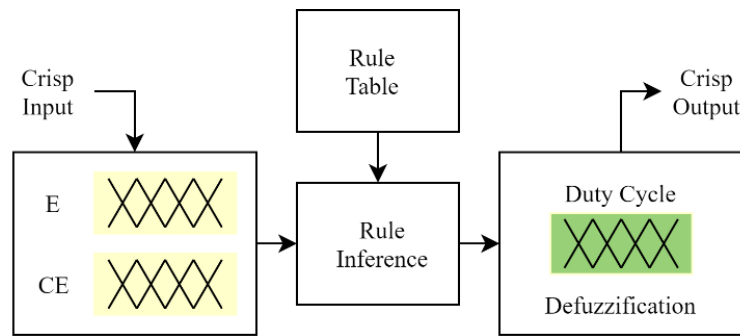


Figure 3. 1. The basic structure of the FLC.

### 3.1. Fuzzification

As shown in Figure 3.2, fuzzification is the initial process with input as crisp numbers. Furthermore, there are two input membership functions in estimating  $E$  and  $\Delta E$  in the proposed FLC algorithm. Each input and output have five triangular subsets, namely NB (negative big), NS (negative small), Z (zero), PS (positive small), and PB (positive big). Also, both input and output use a symmetrical membership function.

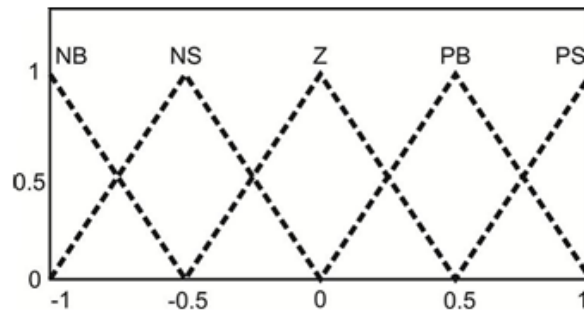


Figure 3. 2. Membership function input and output.

This stage discovers out the value as a fuzzy number based on the membership function. In the input triangle function, the equation for discovering the fuzzy number for the left triangle ( $\mu_{mf1}$ ) which is tangent to the right triangle ( $\mu_{mf2}$ ) is given by

$$\mu_{mf1} = \frac{c_1 - x}{c_1 - b_1} \quad (13)$$

$$\mu_{mf2} = \frac{x - a_2}{b_2 - a_2} \quad (14)$$

where  $a$  is the left end of each triangle,  $b$  is the vertex of the triangle,  $c$  is the right end of the triangle, and  $x$  is the input value.

### 3.2. Rule Evaluation (FIS and Rule Base)

Since each input has five membership functions, there are 25 rules for fuzzy control. The fuzzy numbers are therefore compared in the FIS, based on the created rule base. The rule base is a knowledge base that defines the desired relationship rules between input and output variables. The knowledge base is shown in Table 3.1. In contrast, the results of the rule base are illustrated with a surface in Figure 3.3.

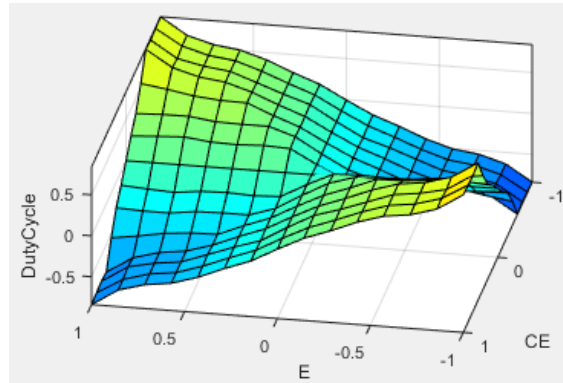


Figure 3. 3. Rule surface of FLC.

Table 3. 1. Knowledge Base.

E/ΔE	NB	NS	Z	PS	PB
NB	NB	NB	Z	PB	PB
NS	NS	NS	Z	PS	PS
Z	Z	Z	Z	Z	Z
PS	PS	PS	Z	NS	NS
PB	PB	PB	Z	NB	NB

This test uses Fuzzy Mamdani, which is based on the Min-Max function. In the first stage, when comparing fuzzy numbers, the value taken is Minimum. In the second stage, the linguistic variable will be handled with the Maximum fuzzy number if there are the same linguistic variables.

### 3.3. Defuzzification

In the third stage, fuzzy numbers are converted into crisp numbers as the output of the FLC. This process is based on the center of gravity. The FLC output is used to control the converter duty cycle. The equation in the defuzzification process is given by

$$D = \frac{\sum x_i \times \mu_i}{\sum \mu_i} \quad (15)$$

where  $D$  is the duty cycle, and  $x$  is the output triangle value.

Error and error changes as FLC inputs are obtained from the PV output as voltage ( $V_{pv}$ ) and current ( $I_{pv}$ ). Figure 3.4 shows an FLC with  $V_{pv}$  and  $I_{pv}$  Inputs are connected to the PWM generator at its output.

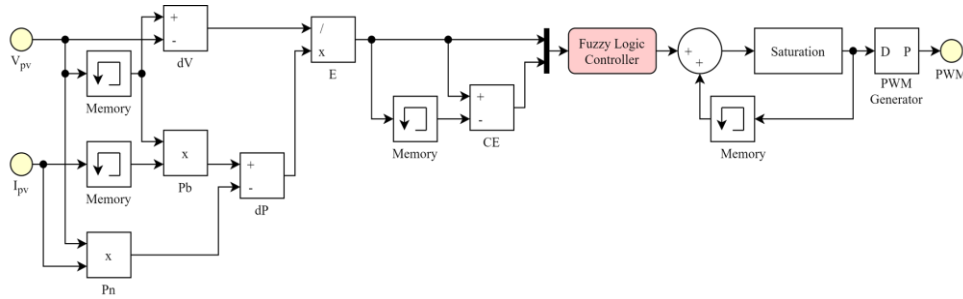


Figure 3. 4. FLC algorithm with input and output in simulation.

## 4. RESULTS AND DISCUSSION

The MATLAB/Simulink PV module model is used to test the MPPT on two converter topologies and two different algorithms. The converter models used are conventional and HSU DC-DC converters. The P&O and FLC algorithms are used in each converter model to control the duty ratio cycle. Furthermore, each converter is connected between the PV module and a resistive load. The first test was carried out by varying the PWM generator frequency, namely 5, 10, 20, and 40 kHz, and it was also carried out to discover the suitable PWM value for the HSU DC-DC converter used.

Figure 4.1a compares the PV generator output voltage simulation results on each converter with the P&O and FLV algorithms at various PWM generator values. It also shows that the oscillations in the HSU converter with P&O have large fluctuations at the PWM generator 5, 10, and 20 kHz. Meanwhile, the fluctuations in other conditions are more minor. Conversely, the output voltage ratio of the HSU-P&O converter has a higher value than the conventional P&O and FLC converters, as well as the HSU-FLC on the PWM generator of 5, 10, and 20 kHz.

At the 40 kHz PWM generator, the oscillation of conventional and HSU converters with P&O and FLC algorithms has the smallest values. Therefore, the fluctuation of the HSU-P&O converter decreased, but the resulting voltage ratio is not greater than that of the HSU-FLC converter. Furthermore, the detailed data of the HSU converter's output voltage

and oscillation values with the P&O and FLC algorithms are shown in Figure 4.1b. The HSU DC-DC converter with the P&O algorithm has a voltage drop on a large PWM generator, but its oscillation decreases. Meanwhile, the HSU DC-DC converter with the FLC algorithm increases the voltage on a large PWM generator, and its fluctuation also decreases.

A further test was carried out to vary the irradiation parameters and temperature, which represent atmospheric changes. The irradiation parameters were run at 700, 800, to 1000 W/m<sup>2</sup> at 25 °C. Figure 12 shows the voltage, current, and output power results when testing with varied irradiation and temperature parameters.

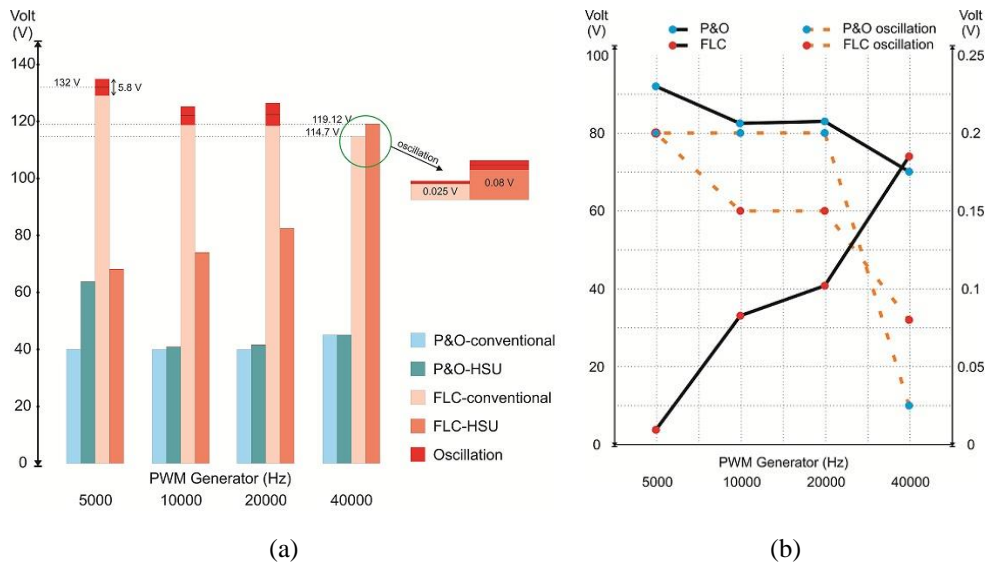


Figure 4. 1. Comparison of voltage and oscillations (a) for each converter model with P&O and FLC, (b) details on HSU-P&O and HSU-FLC.

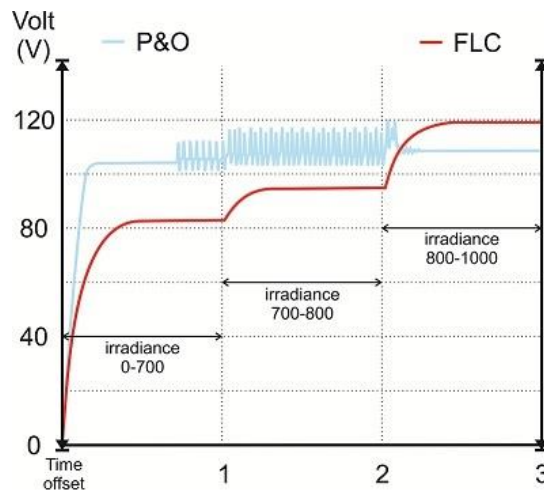


Figure 4. 2. Rule surface of FLC.

As seen in Figure 4.2, the HSU-FLC output voltage at 700 to about 800 W/m<sup>2</sup> irradiation has a lower ratio than HSU-P&O. Meanwhile, the oscillation at HSU-P&O is more prominent in this condition. At 1000 W/m<sup>2</sup> irradiation conditions, the HSU-FLC ratio was higher than HSU-P&O. Meanwhile, the HSU-P&O oscillation decreases in this condition. In addition, HSU-FLC produced lower oscillations than HSU-P&O under all conditions.

## 5. CONCLUSIONS

In this research, the high step-up DC-DC converter for high-voltage gain conversion ratio and high efficiency was proposed. A simple fuzzy logic controller (FLC)-based MPP tracking (MPPT) technique using the DC-DC converter was employed to maximize the power converted from solar photovoltaic. The FLC performance was compared with Perturb and Observe (P&O) algorithm with a similar converter under varying irradiation conditions. Furthermore, the FLC was built as a duty cycle control for the DC-DC converter to track the maximum power available in the PV module. The first test was carried out to obtain a suitable PWM frequency. The results showed that the PWM generator with a frequency input of 40 kHz and the FLC algorithm for the control of the DC-DC converter produces a higher output ratio with lower oscillations than the P&O on the output voltage side. The next test was carried out by changing the irradiation value to determine the performance of the FLC and P&O techniques with the atmospheric changes. The test results of the two methods showed that they have advantages and disadvantages. The P&O algorithm produced a higher voltage ratio than FLC at low irradiation but large oscillations under the same conditions. Meanwhile, the FLC algorithm produced high voltage ratios at maximum irradiation. The resulting oscillations in the FLC algorithm were lower compared to the P&O under all conditions. This shows that the performance of the FLC algorithm applied to the DC-DC converter is better than that of P&O. Therefore, the efficiency of power transferred from PV can be maximum. Because power operation can always be controlled at a point close to MPP.

## 6. ACKNOWLEDGEMENTS

This research was funded by the Directorate of Research and Community Service, Directorate General of Strengthening for Research and Development, Ministry of Research and Technology/National Research and Innovation Agency of Republic Indonesia, for supporting this research under Word Class Research (WCR) grant, contract No: WCR-001/SKPP.ATJ/LPPM UAD/IV/2020.

## 7. REFERENCES

- [1] D. Yousri, T. S. Babu, D. Allam, V. K. Ramachandaramurthy, and M. B. Etiba, "A Novel Chaotic Flower Pollination Algorithm for Global Maximum Power Point Tracking for Photovoltaic System Under Partial Shading Conditions," *IEEE Access*, vol. 7, pp. 121432–121445, 2019.

- [2] A. Jusoh, R. Alik, T. K. Guan, and T. Sutikno, "MPPT for PV system based on variable step size p&o algorithm," *Telkomnika*, vol. 15, no. 1, p. 79, 2017.
- [3] N. Kacimi, S. Grouni, A. Idir, and M. S. Boucherit, "New improved hybrid MPPT based on neural network-model predictive control-Kalman filter for photovoltaic system," *Indones. J. Electr. Eng. Comput. Sci.*, vol. 20, no. 3, 2020.
- [4] K. L. Shenoy, C. G. Nayak, and R. P. Mandi, "Effect of partial shading in grid connected solar pv system with fl controller," *Int. J. Power Electron. Drive Syst.*, vol. 12, no. 1, pp. 431–440, 2021.
- [5] L. Farah, A. Haddouche, and A. Haddouche, "Comparison between proposed fuzzy logic and ANFIS for MPPT control for photovoltaic system," *Int. J. Power Electron. Drive Syst.*, vol. 11, no. 2, p. 1065, 2020.
- [6] S. Ozdemir, N. Altin, and I. Sefa, "Fuzzy logic based MPPT controller for high conversion ratio quadratic boost converter," *Int. J. Hydrogen Energy*, vol. 42, no. 28, pp. 17748–17759, 2017.
- [7] R. Palanisamy, K. Vijayakumar, V. Venkatachalam, R. M. Narayanan, D. Saravanakumar, and K. Saravanan, "Simulation of various DC-DC converters for photovoltaic system," *Int. J. Electr. Comput. Eng.*, vol. 9, no. 2, p. 917, 2019.
- [8] B. Chandrasekar *et al.*, "Non-Isolated High-Gain Triple Port DC-DC Buck-Boost Converter With Positive Output Voltage for Photovoltaic Applications," *IEEE Access*, vol. 8, pp. 113649–113666, 2020.
- [9] A. Pradhan and B. Panda, "A simplified design and modeling of boost converter for photovoltaic sytem," *Int. J. Electr. Comput. Eng.*, vol. 8, no. 1, p. 141, 2018.
- [10] A. C. Subrata, T. Sutikno, S. Padmanaban, and H. S. Purnama, "Maximum power point tracking in pv arrays with high gain Dc-Dc boost converter," in *International Conference on Electrical Engineering, Computer Science and Informatics (EECSI)*, 2019.
- [11] R. Afzal, Y. Tang, H. Tong, and Y. Guo, "A High Step-up Integrated Coupled Inductor-Capacitor DC-DC Converter," *IEEE Access*, vol. 9, pp. 11080–11090, 2021.
- [12] R. Ebrahimi, H. M. Kojabadi, L. Chang, and F. Blaabjerg, "Coupled-inductor-based high step-up DC-DC converter," *IET Power Electron.*, vol. 12, no. 12, pp. 3093–3104, 2019.
- [13] S. Lee and H. Do, "High Step-Up Coupled-Inductor Cascade Boost DC-DC Converter With Lossless Passive Snubber," *IEEE Trans. Ind. Electron.*, vol. 65, no. 10, pp. 7753–7761, 2018.
- [14] S. S. Dobakhshari, J. Milimonfared, M. Taheri, and H. Moradisizkoochi, "A Quasi-Resonant Current-Fed Converter With Minimum Switching Losses," *IEEE Trans. Power Electron.*, vol. 32, no. 1, pp. 353–362, 2017.
- [15] D. Sha, T. Sun, and J. Zhang, "Varying Switching Frequency Control for Current-Fed Dual-Active Bridge DC-DC Converter With Constant Flux Density Change for Transformers," *IEEE Trans. Power Electron.*, vol. 35, no. 4, pp. 3766–3777, 2020.
- [16] A. Ajami, H. Ardi, and A. Farakhor, "A Novel High Step-up DC/DC Converter Based on Integrating Coupled Inductor and Switched-Capacitor Techniques for Renewable Energy Applications," *IEEE Trans. Power Electron.*, vol. 30, no. 8, pp. 4255–4263, 2015.
- [17] H. Li, C. Liu, X. Zhang, Z. Guo, and T. Q. Zheng, "Stability Analysis for Two-Stage Cascaded DC-DC Converters System Based on Describing Function

- Method,” in *2018 IEEE Energy Conversion Congress and Exposition (ECCE)*, 2018, pp. 4141–4147.
- [18] Y. Wang, Y. Qiu, Q. Bian, Y. Guan, and D. Xu, “A Single Switch Quadratic Boost High Step Up DC–DC Converter,” *IEEE Trans. Ind. Electron.*, vol. 66, no. 6, pp. 4387–4397, 2019.
- [19] S. Lee and H. Do, “Quadratic Boost DC–DC Converter With High Voltage Gain and Reduced Voltage Stresses,” *IEEE Trans. Power Electron.*, vol. 34, no. 3, pp. 2397–2404, 2019.
- [20] P. A. Dahono, “New step-up DC-DC converters for PV power generation systems,” in *2017 International Seminar on Intelligent Technology and Its Applications (ISITIA)*, 2017, pp. 187–192.
- [21] M. A. Green, “Silicon photovoltaic modules: a brief history of the first 50 years,” *Prog. Photovoltaics Res. Appl.*, vol. 13, no. 5, pp. 447–455, 2005.
- [22] A. K. Panchal, “I–V Data Operated High-Quality Photovoltaic Solution Through Per-Unit Single-Diode Model,” *IEEE J. Photovoltaics*, vol. 10, no. 4, pp. 1175–1184, 2020.
- [23] I. A. Ibrahim, M. J. Hossain, B. C. Duck, and C. J. Fell, “An Adaptive Wind-Driven Optimization Algorithm for Extracting the Parameters of a Single-Diode PV Cell Model,” *IEEE Trans. Sustain. Energy*, vol. 11, no. 2, pp. 1054–1066, 2020.
- [24] H. K. Mehta, H. Warke, K. Kukadiya, and A. K. Panchal, “Accurate Expressions for Single-Diode-Model Solar Cell Parameterization,” *IEEE J. Photovoltaics*, vol. 9, no. 3, pp. 803–810, 2019.
- [25] F. Bradaschia, M. C. Cavalcanti, A. J. do Nascimento, E. A. da Silva, and G. M. de S. Azevedo, “Parameter Identification for PV Modules Based on an Environment-Dependent Double-Diode Model,” *IEEE J. Photovoltaics*, vol. 9, no. 5, pp. 1388–1397, 2019.
- [26] S. Kumar, H. S. Sahu, and S. K. Nayak, “Estimation of MPP of a Double Diode Model PV Module From Explicit I–V Characteristic,” *IEEE Trans. Ind. Electron.*, vol. 66, no. 9, pp. 7032–7042, 2019.
- [27] Z. Mao, Z. Sunan, M. Peng, S. Yanlong, and Z. Weiping, “Modelling of PV module and its application for partial shading analysis – part I: model and parameter estimation of PV module,” *J. Eng.*, vol. 2017, no. 13, pp. 1295–1298, 2017.
- [28] T. Kamal, M. Karabacak, S. Z. Hassan, H. Li, and L. M. Fernández-Ramírez, “A Robust Online Adaptive B-Spline MPPT Control of Three-Phase Grid-Coupled Photovoltaic Systems Under Real Partial Shading Condition,” *IEEE Trans. Energy Convers.*, vol. 34, no. 1, pp. 202–210, 2019.
- [29] A. S. Samosir and H. Gusmedi, “Modeling and simulation of fuzzy logic based maximum power point tracking (MPPT) for PV application,” *Int. J. Electr. Comput. Eng.*, 2017.
- [30] R. Ahmad, A. F. Murtaza, and H. A. Sher, “Power tracking techniques for efficient operation of photovoltaic array in solar applications—A review,” *Renew. Sustain. Energy Rev.*, vol. 101, pp. 82–102, 2019.
- [31] M. A. Elgendy, B. Zahawi, and D. J. Atkinson, “Operating Characteristics of the P&O Algorithm at High Perturbation Frequencies for Standalone PV Systems,” *IEEE Trans. Energy Convers.*, vol. 30, no. 1, pp. 189–198, 2015.

- [32] B. Subudhi and R. Pradhan, "Adaptive predictive error filter-based maximum power point tracking algorithm for a photovoltaic system," *J. Eng.*, vol. 2016, no. 4, pp. 54–61, 2016.
- [33] A. Hussain, H. A. Sher, A. F. Murtaza, and K. Al-Haddad, "Improved Restricted Control Set Model Predictive Control (iRCS-MPC) Based Maximum Power Point Tracking of Photovoltaic Module," *IEEE Access*, vol. 7, pp. 149422–149432, 2019.
- [34] H. Rezk, M. Aly, M. Al-Dhaifallah, and M. Shoyama, "Design and Hardware Implementation of New Adaptive Fuzzy Logic-Based MPPT Control Method for Photovoltaic Applications," *IEEE Access*, vol. 7, pp. 106427–106438, 2019.
- [35] D. N. Luta and A. K. Raji, "Comparing fuzzy rule-based MPPT techniques for fuel cell stack applications," *Energy Procedia*, vol. 156, pp. 177–182, 2019.
- [36] S. Assahout, H. Elaissaoui, A. El Ougli, B. Tidhaf, and H. Zrouri, "A neural network and fuzzy logic based MPPT algorithm for photovoltaic pumping system," *Int. J. Power Electron. Drive Syst.*, vol. 9, no. 4, pp. 1823–1833, 2018.
- [37] K. Y. Yap, C. R. Sarimuthu, and J. M.-Y. Lim, "Artificial Intelligence Based MPPT Techniques for Solar Power System: A review," *J. Mod. Power Syst. Clean Energy*, vol. 8, no. 6, pp. 1043–1059, 2020.
- [38] H. A. Attia and F. delAma Gonzalo, "Stand-alone PV system with MPPT function based on fuzzy logic control for remote building applications," *Int J Pow Elec Dri Syst ISSN*, vol. 2088, no. 8694, p. 8694, 2019.

## Biographies



**Tole Sutikno** received B. Eng. and M. Eng. in electrical engineering from Universitas Diponegoro and Universitas Gajah Mada, Indonesia, in 1999 and 2004, respectively, and the Ph.D. degree from Universiti Teknologi Malaysia in 2016. He is an Associate Professor with the Electrical Engineering Department, Universitas Ahmad Dahlan, Indonesia, and the leader of Embedded Systems & Power Electronics Research Group (ESPERG). His current research interests include power electronics, motor drives, renewable energy, FPGA, and intelligent control systems.





**Arsyad Cahya Subrata** received B. Eng. and M.Eng. in electrical engineering from Universitas Ahmad Dahlan, Indonesia and Universitas Diponegoro, Indonesia in 2016 and 2020. He is a research assistant in Embedded Systems and Power Electronics Research Group (ESPERG) since 2018. His current research interests include artificial intelligence, digital control systems, renewable energy, and intelligent control systems.



**Awang Jusoh** received B.Eng. in electrical and electronic engineering from Brighton Polytechnic, the UK, in 1985, the M.Sc. and Ph.D. degree in power electronics and electrical engineering from the University of Birmingham, the UK, in 1995 and 2004. He is an Associate Professor with the Department of Electrical Power Engineering, Faculty of Electrical Engineering, Universiti Teknologi Malaysia, Johor, Malaysia. His current research interests include power electronics, energy conversion, and renewable energy.



**P. Sanjeevikumar** received a Ph.D. degree in electrical engineering from the University of Bologna, Bologna, Italy 2012. He was an Associate Professor at VIT University from 2012 to 2013. In 2013, he joined the National Institute of Technology, India, as a Faculty Member. In 2014, he was invited as a Visiting Researcher at the Department of Electrical Engineering, Qatar University, Doha, Qatar, funded by the Qatar National Research Foundation (Government of Qatar). He continued his research activities with the Dublin Institute of Technology, Dublin, Ireland, in 2014.

Further, he served as an Associate Professor with the Department of Electrical and Electronics Engineering, University of Johannesburg, Johannesburg, South Africa, from 2016 to 2018. From March 2018 to February 2021, he has been a Faculty Member with the Department of Energy Technology, Aalborg University, Esbjerg, Denmark. Since March 2021, he has been with the CTIF Global Capsule (CGC) Laboratory, Department of Business Development and Technology, Aarhus University, Herning, Denmark.

S. Padmanaban has authored over 300 scientific papers and received the Best Paper cum Most Excellence Research Paper Award from IET-SEISCON'13, IET-CEAT'16, IEEE-EECSI'19, IEEE-CENCON'19, and five best paper awards from ETAEERE'16 sponsored Lecture Notes in Electrical Engineering, Springer book. He is a Fellow of the Institution of Engineers, India, the Institution of Electronics and Telecommunication Engineers, India, and the Institution of Engineering and Technology, UK. He is an Editor/Associate Editor/Editorial Board for refereed journals, in particular the IEEE SYSTEMS JOURNAL, IEEE Transaction on Industry Applications, IEEE ACCESS, IET Power Electronics, IET Electronics Letters, and Wiley-International Transactions on Electrical Energy Systems, Subject Editorial Board Member—Energy Sources—Energies Journal, MDPI, and the Subject Editor for the IET Renewable Power Generation, IET Generation, Transmission and Distribution, and FACTS journal (Canada).



**SUB KONTRAK PENELITIAN TAHUN TUNGGAL  
PENELITIAN DASAR DAN PENGEMBANGAN/KAPASITAS  
SUMBERDANA KEMENRISTEK/BRIN TAHUN ANGGARAN 2021  
NOMOR: 002/SKP.TT.PD/LPPM/IV/2021**

Pada hari ini **Senin** tanggal **Dua puluh enam** ulan **April** tahun **dua ribu dua puluh satu (26-04-2021)**, kami yang bertandatangan di bawah ini:

- 1. ANTON YUDHANA, M.T., Ph.D.** : Kepala Lembaga Penelitian dan Pengabdian kepada Masyarakat Universitas Ahmad Dahlan (LPPM UAD) dalam hal ini bertindak untuk dan atas nama Universitas Ahmad Dahlan, yang berkedudukan di Kampus UAD 2B Jalan Pramuka 5F, Pandeyan, Umbulharjo Yogyakarta 55161, untuk selanjutnya disebut **PIHAK PERTAMA**;
- 2. TOLE SUTIKNO, M.T., Ph.D.** : Dosen/Peneliti Program Studi Teknik Elektro Universitas Ahmad Dahlan, dalam hal ini bertindak sebagai Ketua Pelaksana Penelitian sumberdana DRPM Kemenristek/BRIN Tahun Anggaran 2020 untuk selanjutnya disebut **PIHAK KEDUA**.

**PIHAK PERTAMA** dan **PIHAK KEDUA**, secara bersama-sama sepakat mengikatkan diri dalam Sub Kontrak Penelitian (SKP) Penelitian Dasar dan Pengembangan/Kapasitas Sumberdana Kemenristek/BRIN Tahun Anggaran 2021 dengan ketentuan dan syarat-syarat sebagai berikut.

**Pasal 1**

**DASAR HUKUM**

Kontrak penelitian ini didasarkan pada:

- a. Keputusan Kuasa Pengguna Anggaran Deputi Bidang Penguatan Riset dan Pengembangan Kementerian Riset dan Teknologi/Badan Riset dan Inovasi Nasional Nomor: 9/E1/KPT/2021 tentang Penetapan Pendanaan Penelitian di Perguruan Tinggi Tahun Anggaran 2021;
- b. Kontrak Penelitian Tahun Anggaran 2020 antara Direktorat Riset dan Pengabdian Masyarakat dengan LLDIKTI Wilayah V Nomor: 066/SP2H/LT/DRPM/2021;
- c. Kontrak Penelitian Tahun Anggaran 2020 antara LLDIKTI Wilayah V DIY dengan Universitas Ahmad Dahlan Nomor: 1804.7/LL5/PG/2021 tanggal 19 April 2021.

**Pasal 2**

**RUANG LINGKUP**

- (1) **PIHAK PERTAMA** memberi pekerjaan kepada **PIHAK KEDUA** dan **PIHAK KEDUA** menerima tugas tersebut dari **PIHAK PERTAMA** berupa pekerjaan penelitian pada skema World Class Research.
- (2) Judul penelitian sebagaimana dimaksud pada ayat (1) di atas adalah: **Pengembangan Metode Maximum Power Point Tracking (MPPT) dan Pengendali DC-DC Boost Converter Berbasis Field Programmable Gate Array (FPGA) pada Sistem Photovoltaic.**

### Pasal 3

#### Personalia Pelaksana Penelitian

Personalia pelaksana penelitian ini terdiri dari:

Ketua Peneliti : Tole Sutikno, M.T., Ph.D.  
Anggota Peneliti 1 : Anton Yudhana, M.T., Ph.D.  
Anggota Peneliti 2 : Mochammad Facta, M.T., Ph.D.

### Pasal 4

#### JANGKA WAKTU PENELITIAN

Jangka waktu pelaksanaan penelitian sebagaimana dimaksud Pasal 1 terhitung sejak subkontrak ini ditandatangani dan berakhir pada tanggal **16 November 2021**.

### Pasal 5

#### KEWAJIBAN DAN HAK

(1) **PIHAK PERTAMA** berkewajiban untuk:

- a. menyalurkan pendanaan penelitian kepada PIHAK KEDUA;
- b. melakukan pemantauan dan evaluasi terhadap pengunggahan: (i) revisi proposal; (ii) laporan kemajuan; (iii) dan/atau laporan akhir; (iv) dan/atau luaran penelitian;

(2) **PIHAK KEDUA** berkewajiban untuk mengunggah ke laman SIMLITABMAS dokumen sebagai berikut:

- a. revisi proposal penelitian
- b. surat pernyataan ksanggupan penyusunan laporan penelitian;
- c. catatan harian pelaksanaan penelitian;
- d. laporan kemajuan pelaksanaan penelitian;
- e. Surat Pernyataan Tanggungjawab Belanja (SPTB) atas dana penelitian yang telah ditetapkan;
- f. laporan akhir penelitian (dilaporkan pada tahun terakhir pelaksanaan penelitian); dan
- g. luaran penelitian.

Batas akhir unggah laporan kemajuan pada tanggal **18 September 2021** dan untuk laporan akhir pada tanggal **16 November 2021**.

(3) **PIHAK PERTAMA** berhak untuk menerima dokumen yang diunggah oleh PIHAK KEDUA pada laman SIMLITABMAS sebagaimana dimaksud pada ayat (2).

(4) **PIHAK KEDUA** berhak menerima dana penelitian sesuai ketentuan dalam kontrak penelitian ini.

### Pasal 6

#### CARA PEMBAYARAN

(1) Biaya pokok penelitian ini sebesar Rp 117.900.000,00 (Seratus Tujuhbelas Juta Sembilanratus Ribu rupiah) yang pendanaannya bersumber pada DIPA Deputi Bidang Penguatan Riset dan Pengembangan Kemenristek/BRIN Tahun Anggaran 2021.

(2) **PIHAK PERTAMA** membayarkan biaya penelitian kepada **PIHAK KEDUA** dengan ketentuan sebagai berikut.

- a. Pembayaran **Tahap I** yaitu sebesar 70% dari nilai kontrak atau *sebesar Rp 82.530.000,00* (Delapanpuluh Dua Juta Limaratus Tigapuluh Ribu rupiah).
- b. Pembayaran **Tahap II** yaitu sebesar 30% dari nilai kontrak atau *sebesar Rp 35.370.000,00* (Tigapuluh Lima Juta Tigaratus Tujuh puluh Ribu rupiah).

- (3) Dana penelitian sebagaimana dimaksud pada ayat (1) dibayarkan oleh **PIHAK PERTAMA** kepada **PIHAK KEDUA** ke rekening atas nama **PIHAK KEDUA**.

Nama Pemegang Rekening : TOLE SUTIKNO, M.T., Ph.D.  
Nama Bank : BPD DIY SYARIAH  
Nomor Rekening : 001.221.007.462

- (4) Dana luaran tambahan dibayarkan, jika luaran tambahan penelitian ini tercapai dan dinyatakan valid oleh Tim Penilai/*Reviewer* Luaran Tambahan..
- (5) Pendanaan penelitian sebagaimana dimaksud pada ayat (2) dapat dibayarkan apabila **PIHAK KEDUA** telah memenuhi kewajiban-kewajibannya sebagaimana dimaksud pada Pasal 4 ayat (2).

#### Pasal 7

##### PENGGANTIAN KEANGGOTAAN

- (1) Apabila **PIHAK KEDUA** tidak dapat menyelesaikan penelitian ini atau mengundurkan diri, maka **PIHAK KEDUA** wajib menunjuk pengganti Ketua Tim Pelaksana yang merupakan salah satu anggota tim pelaksana penelitian yang memenuhi persyaratan kepada Direktur DRPM Kemenristek/BRIN melalui **PIHAK PERTAMA**.
- (2) Apabila Ketua Tim Pelaksana tidak dapat melaksanakan tugas dan tidak ada pengganti ketua sebagaimana dimaksud pada ayat (1), maka **PIHAK KEDUA** harus mengembalikan dana penelitian kepada **PIHAK PERTAMA** yang selanjutnya disetor ke Kas Negara.
- (3) Bukti setor sebagaimana dimaksud pada ayat (2) diserahkan kepada **PIHAK PERTAMA** dan salinanya disimpan oleh **PIHAK KEDUA**.

#### Pasal 8

##### PAJAK DAN PELAPORAN PENGGUNAAN DANA

- (1) **PIHAK KEDUA** bertanggungjawab atas penggunaan dana penelitian yang telah diterima sesuai dengan ketentuan yang berlaku;
- (2) Hal-hal yang berkenaan dengan kewajiban pajak berupa PPN dan/atau PPh menjadi tanggungjawab **PIHAK KEDUA** dan harus dibayarkan oleh **PIHAK KEDUA** ke kantor pelayanan pajak setempat sebagai berikut:
- (a) pembelian barang dan jasa dikenai PPN sebesar 10% dan PPh 22 sebesar 1,5%;
  - (b) pajak-pajak lain sesuai ketentuan yang berlaku.
- (2) **PIHAK KEDUA** wajib menyusun dan laporan penggunaan dana yang dilampiri dengan bukti pengeluaran yang sah termasuk bukti setor pajak dan menyimpan untuk keperluan pemeriksaan jika diminta untuk keperluan tersebut.

#### Pasal 9

##### KEKAYAAN INTELEKTUAL DAN PUBLIKASI ILMIAH

- (1) Hak atas Kekayaan Intelektual yang dihasilkan dari pelaksanaan penelitian diatur dan dikelola sesuai dengan peraturan dan perundang-undangan yang berlaku.
- (2) Setiap publikasi, makalah dan/atau ekspos dalam bentuk apapun yang berkaitan dengan hasil penelitian ini wajib mencantumkan nama pemberi dana penelitian yaitu Direktorat Riset dan Pengabdian Masyarakat, Deputi Bidang Penguatan Riset dan Pengembangan, Kementerian Riset dan Teknologi/Badan Riset dan Inovasi Nasional.
- (3) Pencantuman nama sebagaimana dimaksud pada ayat (2), paling sedikit mencantumkan nama Kementerian Riset dan Teknologi/Badan Riset dan Inovasi Nasional.

**Pasal 10**  
**INTEGRITAS AKADEMIK**

- (1) Pelaksana penelitian wajib menjunjung tinggi integritas akademik yaitu komitmen dalam bentuk perbuatan yang berdasarkan pada nilai kejujuran, kredibilitas, kewajaran, kehormatan, dan tanggung jawab dalam kegiatan penelitian yang dilaksanakan.
- (2) Penelitian dilakukan sesuai dengan kerangka etika, hukum dan profesionalitas, serta kewajiban sesuai dengan peraturan yang berlaku.
- (3) Penelitian dilakukan dengan menjunjung tinggi standar ketelitian dan integritas tertinggi dalam semua aspek penelitian.

**Pasal 11**  
**KEADAAN MEMAKSA**

- (1) PARA PIHAK dibebaskan dari tanggung jawab atas keterlambatan atau kegagalan dalam memenuhi kewajiban yang dimaksud dalam kontrak Penelitian disebabkan atau diakibatkan oleh peristiwa atau kejadian di luar kekuasaan PARA PIHAK yang dapat digolongkan sebagai keadaan memaksa (*force majeure*).
- (2) Peristiwa atau kejadian yang dapat digolongkan keadaan memaksa (*force majeure*) dalam Kontrak Penelitian ini adalah bencana alam, wabah penyakit, kebakaran, perang, blokade, sabotase, revolusi, pemberontakan, huru-hara, serta adanya tindakan pemerintah dalam bidang ekonomi dan moneter yang secara nyata berpengaruh terhadap pelaksanaan Kontrak Penelitian ini.
- (3) Apabila terjadi keadaan memaksa (*force majeure*), maka pihak yang mengalami wajib memberitahukan kepada pihak lainnya secara tertulis, selambat-lambatnya 7 (tujuh) hari kerja sejak terjadinya keadaan memaksa (*force majeure*), disertai dengan bukti-bukti yang sah dari pihak yang berwajib, dan PARA PIHAK dengan i'tikad baik akan segera membicarakan penyelesaiannya.

**Pasal 12**  
**PENYELESAIAN SENGKETA**

Apabila terjadi perselisihan antara **PIHAK PERTAMA** dan **PIHAK KEDUA** dalam pelaksanaan perjanjian ini akan dilakukan penyelesaian secara musyawarah dan mufakat, dan apabila tidak tercapai penyelesaian secara musyawarah dan mufakat, maka penyelesaian dilakukan melalui proses hukum.

**Pasal 13**  
**AMANDEMEN KONTRAK**

Apabila terdapat hal lain yang belum diatur atau terjadi perubahan dalam Kontrak Penelitian ini, maka akan dilakukan amandemen Kontrak Penelitian.

**Pasal 14**  
**SANKSI**

- (1) Apabila sampai dengan batas waktu yang telah ditetapkan untuk melaksanakan penelitian ini telah berakhir, **PIHAK KEDUA** tidak melaksanakan kewajiban sebagaimana dimaksud pada Pasal 4 ayat (2), maka **PIHAK KEDUA** dikenakan sanksi administratif.
- (2) Saksi administratif sebagaimana dimaksud pada ayat (1) dapat berupa: penghentian pembayaran dan/atau Ketua Tim Pelaksana Penelitian tidak dapat mengajukan proposal penelitian dalam waktu dua tahun berturut-turut.
- (3) Mengembalikan dana penelitian yang telah diterimakan kepada Kas Negara, jika diminta oleh pihak pemberi dana.

**Pasal 15**

**KETENTUAN LAIN-LAIN**

- (1) Dalam hal PIHAK PERTAMA berhenti dari jabatannya sebagai Kepala LPPM sebelum Kontrak Penelitian ini selesai, maka PIHAK PERTAMA wajib melakukan serah terima tanggung jawabnya kepada pejabat baru yang menggantikannya.
- (2) Dalam hal PIHAK KEDUA berhalangan tetap atau tidak dapat melaksanakan tugas sebagai Ketua Tim Pelaksana sebelum Kontrak Penelitian ini selesai, maka PIHAK KEDUA wajib melakukan pergantian dengan anggota peneliti yang memenuhi persyaratan.

**Pasal 16**

**PENUTUP**

Perjanjian ini dibuat dan ditandatangani oleh **PARA PIHAK** pada hari dan tanggal tersebut di atas, dibuat dalam rangkap 2 (dua) dan bermeterai cukup sesuai dengan ketentuan yang berlaku, yang masing-masing mempunyai kekuatan hukum yang sama.

PIHAK PERTAMA,  
  
  
**ANTON YUDHANA, M.T., Ph.D.**  
NIY: 60010383

PIHAK KEDUA,  
  
  
**TOLE SUTIKNO, M.T., Ph.D.**  
NIY: 60010310

**Pasal 15**



**KETENTUAN LAIN-LAIN**

- (1) Dalam hal PIHAK PERTAMA berhenti dari jabatannya sebagai Kepala LPPM sebelum Kontrak Penelitian ini selesai, maka PIHAK PERTAMA wajib melakukan serah terima tanggung jawabnya kepada pejabat baru yang menggantikannya.
- (2) Dalam hal PIHAK KEDUA berhalangan tetap atau tidak dapat melaksanakan tugas sebagai Ketua Tim Pelaksana sebelum Kontrak Penelitian ini selesai, maka PIHAK KEDUA wajib melakukan pergantian dengan anggota peneliti yang memenuhi persyaratan.

**Pasal 16**

**PENUTUP**

Perjanjian ini dibuat dan ditandatangani oleh **PARA PIHAK** pada hari dan tanggal tersebut di atas, dibuat dalam rangkap 2 (dua) dan bermeterai cukup sesuai dengan ketentuan yang berlaku, yang masing-masing mempunyai kekuatan hukum yang sama.

PIHAK PERTAMA,  
  
  
ANISA SUDIANA, M.T., Ph.D.  
NIY: 60010383

PIHAK KEDUA,

  
TOLE SUTIKNO, M.T., Ph.D.  
NIY: 60010310